AD 291 712

63-1-6

ARL 62-467

NOX

THEORETICAL AND EXPERIMENTAL INVESTIGATION OF SUPERSONIC COMBUSTION

Antonio Ferri, Paul A. Libby and Victor Zakkay

POLYTECHNIC INSTITUTE OF BROOKLYN
Department of Aerospace Engineering
and Applied Mechanics

SEPTEMBER 1962

AERONAUTICAL RESEARCH LABORATORIES
OFFICE OF AEROSPACE RESEARCH
UNITED STATES AIR FORCE

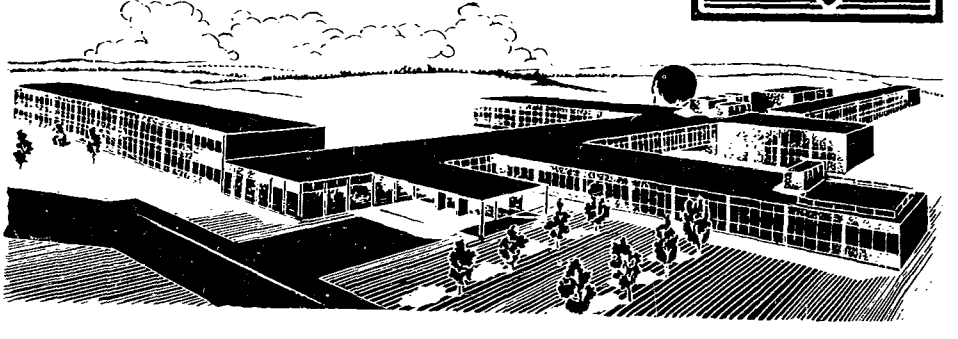

NOTICES

When Government drawings, specifications, or other data are used for any purpose other than in connection with a definitely related Government procurement operation, the United States Government thereby incurs no responsibility nor any obligation whatsoever; the fact that the Government may have formulated, furnished, or in any way supplied the said drawings, specifications, or other data, is not to be regarded by implication or otherwise as in any manner licensing the holder or any other person or corporation, or conveying any rights or permission to manufacture, use, or sell any patented invention that may in any way be related thereto.

The information furnished herewith is made available for study upon the understanding that Polytechnic Institute of Brooklyn proprietary interest in and relating thereto shall not be impaired.

Qualified requesters may obtain copies of this report from the Armed Services Technical Information Agency, (ASTIA), Arlington Hall Station, Arlington 12, Virginia.

This report has been released to the Office of Technical Services, U.S. Department of Commerce, Washington 25, D.C. for sale to the general public.

Copies of ARL Technical Reports and Technical Notes should not be returned to the Aeronautical Research Laboratory unless return is required by security considerations, contractual obligations, or notices on a specific document.

ARL 62-467

THEORETICAL AND EXPERIMENTAL INVESTIGATION OF SUPERSONIC COMBUSTION

ANTONIO FERRI
PAUL A. LIBBY
VICTOR ZAKKAY

POLYTECHNIC INSTITUTE OF BROOKLYN

SEPTEMBER 1962

CONTRACT AF 33(616)-7661
PROJECT 7064
TASK 7064-01

AERONAUTICAL RESEARCH LABORATORIES
OFFICE OF AEROSPACE RESEARCH
UNITED STATES AIR FORCE
WRIGHT-PATTERSON AIR FORCE BASE OHIO

FOREWORD

This interim report was prepared by Dr. Antonio Ferri, Professor of Aerospace Engineering, Dr. Paul A. Libby, Professor of Aerospace Engineering, and Dr. Victor Zakkay, Research Associate Professor of Aerospace Engineering. The work presented herein has been carried out with the sponsorship of the Department of the Air Force under the following contracts: at PIBAL the experimental research involving the hypersonic facility has been performed under Contract No. AF 33(616)-7661, "Research on Thermal and Aerodynamic Effects at Hypersonic Mach Numbers in High Speed Flow," Project No. 7064, "Aerothermodynamic Investigations," Task No. 7064-01, "Research on Hypersonic Flow Phenomena." This contract is administered by the Aeronautical Research Laboratories, Office of Aerospace Research, United States Air Force, and is partially supported by the Ballistic Systems Division. Colonel Andrew Boreske, Jr. of the Hypersonic Research Laboratory, ARL, is the contract monitor. The mixing research as PIBAL was supported by the Office of Scientific Research under Contract No. AF 49(638)-217 with Mr. Joseph E. Long serving as project monitor. Finally, the research on the chemical kinetics of the hydrogen-air system was carried out by General Applied Science Laboratories, Inc. for the Office of Scientific Research under Contract No. AF 49(638)-991. Dr. M. M. Slawsky is the technical monitor thereof. The authors gratefully acknowledge the support and cooperation of these Air Force organizations and the efforts of Mr. Samuel Lederman, Mr. Louis Alpinieri, Mr. Gdalia Kleinstein, and Mr. Herbert Fox, and of Mr. Harold Pergament. In addition, the authors acknowledge with thanks helpful discussions with Professors Manlio Abele and Lu Ting.

ABSTRACT

A theoretical and experimental investigation of mixing and supersonic combustion is presented. A review of the problem under investigation is given in Section I. Then an analysis of inviscid flow fields with a finite rate chemistry for a hydrogen-air reaction is presented in Section II. In Section III, an analysis of a turbulent mixing for flows with large density gradients with no chemical reaction is presented. The analysis is compared with the experimental results. In Section IV, the results of the experiments in supersonic combustion are presented.

TABLE OF CONTENTS

LIST OF ILLUSTRATIONS

LIST OF ILLUSTRATIONS (Contd)

LIST OF ILLUSTRATIONS (Contd)

LIST OF ILLUSTRATIONS (Contd)

LIST OF SYMBOLS

a	radius of the jet
a_e	effective area
A	area
A_o	arbitrary flow area at $x = 0$
c_p	specific heat
D	turbulent diffusion coefficient
G_k	quantity defined by Eq. (II-2.7)
H	total enthalpy
k	constant given by Prandtl as 0.025 for (III-4.2); mass concentration
K_c	mass concentration at the center line
$K_{c,j}$	equilibrium constant based on molar concentration
K_j	specific rate constant
L	number of elements
M_i	chemical formula of the species i
M_j	Mach number of jet
n	coordinate normal to streamline
N	number of species
p	pressure
r	radial coordinate of jet
$(r_{\frac{1}{2}})_i$	width of the mixing wave in the incompressible plane wherein the velocity change for u_{max} to $(u_{max} + u_c)\frac{1}{2}$
R_o	universal gas constant
s	coordinate along streamline

LIST OF SYMBOLS (Contd)

S_t	Schmidt number
T	temperature
U	$= u/u_j$
v	velocity
$\dot{w}_i$	rate of formation of species i
W	mean molecular weight of the mixture
W_i	molecular weight of i^{th} species
x	coordinate along the axis of the jet
Y_1	mass fraction of O_2
Y_2	mass fraction of H_2
Y_3	mass fraction of H_2O
Y_4	mass fraction of N_2
Y_5	mass fraction of O
Y_6	mass fraction of H
Y_7	mass fraction of HO
Y_i	mass fraction of i^{th} element
$\tilde{Y}_i$	element mass fraction of i^{th} element
ϵ	compressible eddy viscosity
θ	flow deflection
μ	kinematic viscosity; Mach angle
ν_{ij}	number of atoms j in chemical species i
ν_{ij}	stoichiometric coefficients for the j^{th} section
ξ	coordinate in transformed plane

ρ	density
τ_D	characteristic time associated with diffusion
τ_c	characteristic time associated with chemical reaction
τ_i	the time at which the computed temperature starts to rise significantly (μ_{sec})
$\tilde{\psi}$	stream function

Subscripts

c	center
e	external flow
inc	incompressible
j	for the jet
^oK	degree Kelvin
s	stagnation

SECTION I

INTRODUCTION

In recent years the problem of combustion in a stream which moves at supersonic velocity has attracted the attention of several groups of investigators. One of the practical motivations for research on this problem is the hypersonic ramjet employing supersonic combustion. In the studies of the detailed processes involved in the release of chemical energy in a supersonic stream two modes of combustion have been considered: detonations which are controlled by a wave mechanism and supersonic diffusion flames which are controlled by mixing of the fuel and oxidizer.

Consider briefly these two modes; in detonation the oxidizer and fuel are completely premixed upstream of the combustor in a region of the flow wherein the static pressure and temperature are sufficiently low so that essentially no chemical reaction takes place. When the stream of premixed gases arrives at the combustor, it encounters waves which produce an increase in pressure and temperature and which initiate chemical reaction. Initially the waves are generated by the geometry of the combustor; however, the wave pattern is directly influenced by the heat release so that under steady operating conditions the geometry, upstream flow conditions and heat release are intimately related. Indeed, after steady combustion is established the geometry of the combustion could possibly be altered so that a self-sustaining wave pattern is achieved.

This detonation mode of combustion in supersonic flows has been studied by Gross and Chinitz[I-1], Nicholls[I-2], and more recently by Rhodes and co-workers[I-3, -4]. It is related from a fundamental point of view to detonation waves which have been studied for roughly 80 years (cf. reference I-5 for a recent, excellent review of the research pertaining thereto). While this mode of combustion is of considerable interest for the investigation of the fundamentals of chemically reacting

Manuscript released 23 November 1962 by the authors for publication as an ARL Technical Documentary Report.

flows in general and of chemical kinetics in particular, it seems from the available experimental results that it will be difficult to apply in an operating engine system primarily because of the aforementioned interdependence of combustor geometry and of aerodynamic and heat release effects. Indeed operating limits associated with combustion instability may be expected in an engine system employing this mode.

The second mode of combustion, the supersonic diffusion flame, involves a fuel jet in a supersonic oxidizing stream, as shown schematically in Figure I-1. The processes of mixing and chemical reaction are in general intimately connected, the reactants at first mixing and then combining so as to release chemical energy. It will be recognized that this mode is analogous to the fuel jet in low speed flow, apparently first treated in 1928 by Burke and Schumann[I-6] (or see reference I-7). As in all viscous flows involving chemical reaction it is instructive to consider two characteristic times, one associated with diffusion τ_D and one with the chemical reaction, τ_c. The diffusion time can be associated with the time required by a fluid element with the external stream velocity u_e to travel the distance in which the velocity at the axis is close to that in the external stream. The chemical time can be estimated from the kinetic rates under the assumption of infinitely fast mixing. In the treatment of low speed fuel jets it is implicitly assumed that $\tau_D >> \tau_c$ so that effectively equilibrium chemistry prevails, i.e., so that diffusion is rate controlling. In a practical supersonic diffusion flame τ_D and τ_c can be of the same order for some flow conditions; therefore, in the analysis of the combustion process the interplay of chemical and fluid dynamic effects must be considered.

There are a variety of fluid mechanical and chemical problems which must be considered in achieving an understanding of the basic features of this mode of combustion. There has been under way for several years research on these problems at the Aerodynamics Laboratory of the Polytechnic Institute of Brooklyn (PIBAL) and at the General Applied Science Laboratories (GASL). It is the scope and

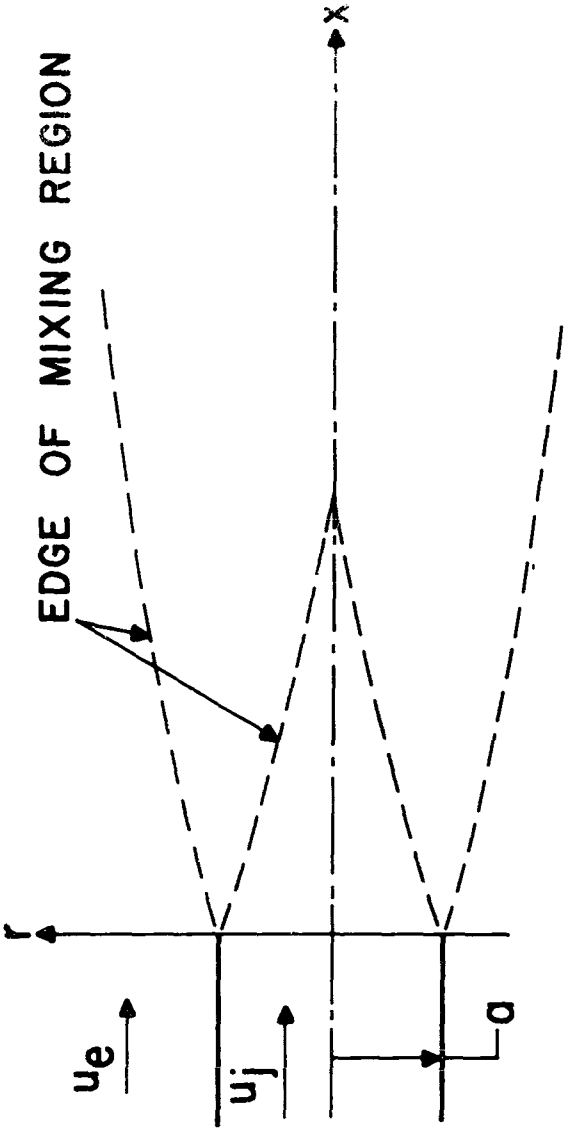

FIG. I-1. Schematic Representation of Flame Showing Coordinate System.

purpose of this paper to review some of the fundamental aspects of this research effort including the progress to date, and to indicate problem areas requiring additional research.

For purposes of orientation it may be instructive to consider some of the overall aspects connected with the hypersonic ramjet employing supersonic combustion. In the discussion of reference I-8 at the First ICAS, the first author suggested for the first time the use of deflagration or diffusion flame in a supersonic combustor. This idea was developed further in reference I-9 where the first author presented a detailed discussion of a hypersonic ramjet employing hydrogen as a fuel with this mode of combustion. It was shown therein that such a ramjet can produce a large thrust per unit frontal area and can operate at a high specific impulse even at hypersonic speeds. Figure I-2 is taken from reference I-9 and provides the results significant for present purposes. Other studies of various aspects of hypersonic ramjets employing supersonic combustion are discussed in references I-10 and -11.

It is fundamental to the operation of such a ramjet to decelerate the flow in an inlet from the flight Mach number to a supersonic value such that at the entrance to the mixing region the static temperatures are in the range of 1000 to 2000°K. The hydrogen fuel is injected parallel to, and in the downstream direction with respect to, the air flow. Mixing and heat release occur in the combustor; by controlling the mixing and by changing the cross-sectional area available to the flow, the pressure distribution in the mixing region can be controlled so as to avoid shock formation. A nozzle connected to the combustor expands the combustion products to obtain gross thrust from the engine. In view of the specific impulse which can be realized with hydrogen as a fuel, research at PIBAL and GASL has been confined to the hydrogen-air system; only this system will be discussed explicitly herein although many aspects of the discussion would apply to other fuels.

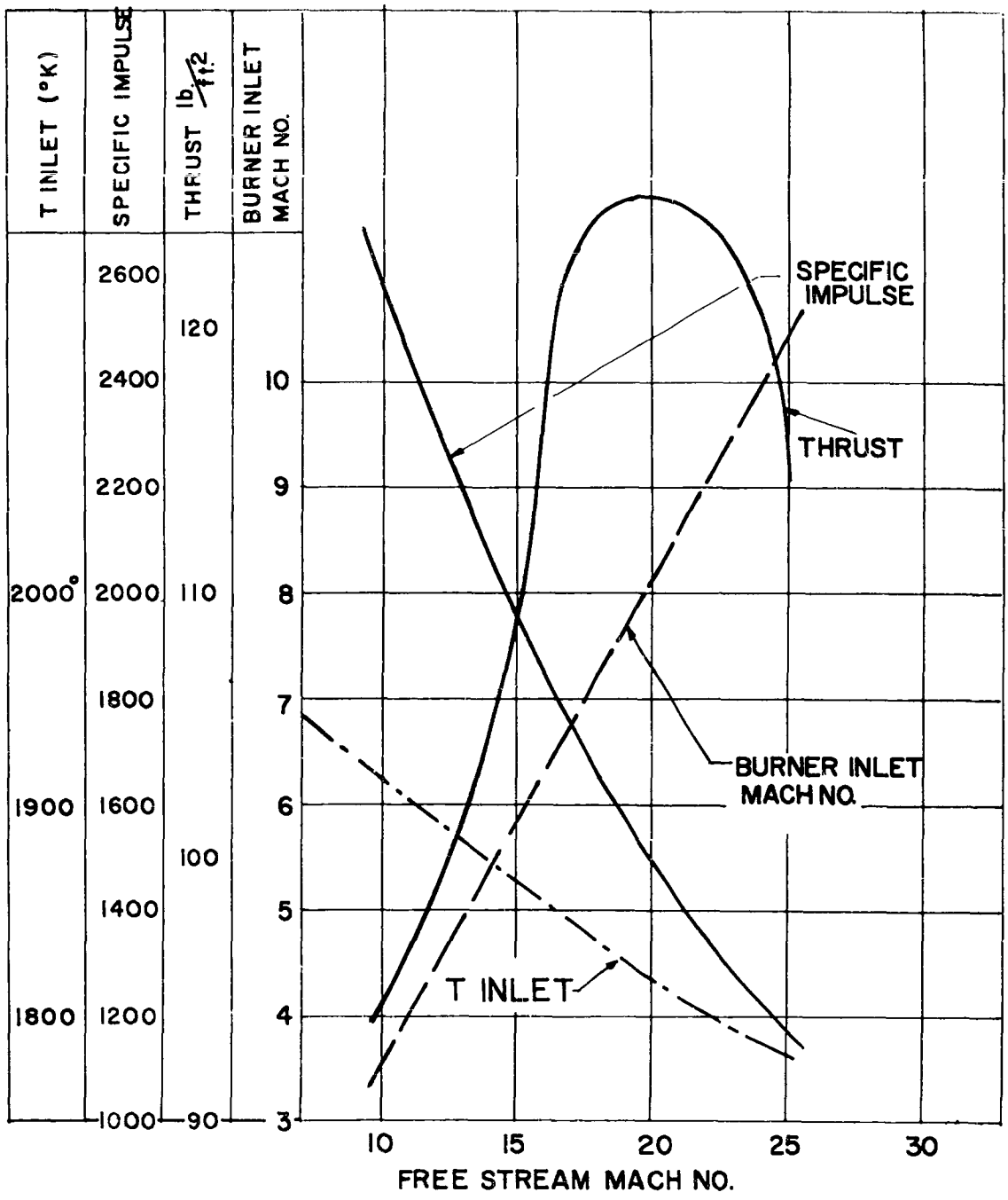

FIG. 1-2. Ramjet. Inlet Static Temperatures, Thrust, and Specific Impulse, for Various Free Stream Mach Numbers (Hydrogen Fuel). Altitude 150,000 ft.

The investigation of supersonic diffusion flames is complicated by the simultaneous occurrence of fluid mechanical and chemical effects. After mixing of fuel and oxidizer, reaction occurs with large heat release and, therefore, produces large changes of density and pressure. In a supersonic combustion process the pressure variation propagates in the flow through a wave mechanism in a diffused medium. A complete analysis of such processes is complex and, therefore, many simplifications are required to increase the understanding of the phenomena. For a large range of static pressure and temperatures important for practical applications, the reaction process is much faster than the diffusion process. In this case the effect of transport properties during the time in which the chemical process takes place can be neglected in the first approximation, and the concentration of all elements along a given streamline can be assumed to be constant, unaffected by the diffusion process. Then the chemical behavior along the streamlines can be considered an inviscid phenomenon. Pressure and density can change along the streamline; therefore, chemical reaction with variable pressure must be analyzed. The results of this type of analysis will indicate for what range of problems this assumption can be accepted. If this assumption is sufficiently accurate, the mixing process can also be analyzed in a simplified form by assuming that the chemical reaction is infinitely fast with respect to the mixing process. Then the flow everywhere is in chemical equilibrium; however, the mixing may occur with pressure gradients in all directions. The combustion process that is of practical interest is one which avoids formation of shock waves in the flow; therefore, the analysis of heterogeneous mixing, i.e., of fuel and oxidizer, with constant pressure is of great importance. However, the mixing rate and heat release must be controlled and related to the shape of the combustor in order to achieve constant pressure.

Following this line of investigation this paper is organized as follows: Section II is devoted to the analysis of inviscid flows with finite rate chemistry, to a discussion of the mechanisms in the

hydrogen-air reaction, and to the description of the relation between combustor shape and mixing process required to avoid shock formation. Section III is concerned with turbulent mixing in flows with large density gradients due to large differences in temperature and in concentration of light gases but with either no chemical reaction or with equilibrium chemical behavior. Finally, the results of experiments, which employ the hypersonic facility of PIBAL to investigate the combustion of hydrogen in a supersonic stream, are discussed in Section IV.

The authors gratefully acknowledge the support and cooperation of the Air Force organizations and the efforts of Mr. Samuel Lederman, Mr. Louis Alpinieri, Mr. Gdalia Kleinstein, and Mr. Herbert Fox, and of Mr. Harold Pergament. In addition, the authors acknowledge with thanks helpful discussions with Professors Manlio Abele and Lu Ting.

SECTION II
INVISCID FLOWS WITH CHEMICAL REACTION

As part of the investigation of supersonic diffusion flames with the hydrogen-air system, there is considered herein the mechanisms and kinetics involved when mixing and diffusive effects are absent. These considerations correspond to the assumption, either of premixed fuel and oxidizer, or to the other limit wherein chemical reaction is so fast with respect to the diffusion process, so that the diffusive effects taking place during the combustion process can be neglected.

The problem of inviscid gas flows with non-equilibrium chemical behavior has been studied intensively in the past several years. Primary attention has been devoted to non-equilibrium air flows around bodies in hypersonic flight and through nozzles of hypersonic test facilities. Recently, nozzle flows involving combustion products of interest in high-performance propulsion devices have been considered because of the practically important differences in gross-thrust associated with the limiting cases of frozen and equilibrium flow. Olson[II-1] provides a recent review of these latter flows.

In all of the analyses of non-equilibrium behavior for propulsion the flow fields and the thermodynamic behavior of the gases have been

idealized. The flow is treated either as one-dimensional with the area-distribution of the nozzle specified or is considered along streamlines with the pressure distribution specified. As will be discussed in detail below, the latter idealization appears to have several advantages. With respect to the thermodynamic behavior of the combustion products, there will be assumed thermodynamic equilibrium, i.e., full rotational and vibrational equilibration of all molecules at a local translational temperature which is the same for all species. In addition, the forward and reverse rate constants are assumed to be related by the appropriate equilibrium constant. It is generally considered that these assumptions are satisfactory in view of the inaccuracy with which the mechanisms and rates associated with practical fuel-oxidizer systems are known.

1. REVIEW OF RECENT RESEARCH

Consider now the available results of theoretical calculations applicable to the hydrogen-air system. The fundamental paper is that of Duff[II-2] who carried out calculations of the reaction profile behind a detonation wave satisfying the Chapman-Jouget condition in a hydrogen-oxygen mixture. Duff attributes the individual reaction steps and the relevant rate data to N. Davidson. This research was continued at Los Alamos by Schott, et al.[II-3, -4]; experimental research confirmed in general the overall accuracy of the chemistry. In reference II-5, Libby, Pergament, and Bloom presented the results of reaction histories for hydrogen-air mixtures at constant pressure using the chemistry of Duff and nitrogen treated as an inert diluent.* Recently, Westenberg and Favin[II-6] carried out one-dimensional nozzle calculations for the hydrogen-air system and for a second mixture corresponding to rocket exhaust gases. A range of pressures in the settling chamber, a single stagnation temperature of 3000°K and two equivalence ratios were

*Some of the results of these and similar calculations will be discussed in detail below.

assumed There was obtained the expected effect of pressure, namely, that the flow tends to remain near equilibrium when the pressure is high and to depart from equilibrium, indeed to freeze effectively at some point downstream of the throat, when the pressure is low. Also of interest was a result, found independently by Westenberg and Favin and by the present authors as discussed below, concerning the behavior of the intermediates atomic hydrogen and the hydroxyl radical under essentially frozen conditions. It is found that in an expanding flow at sufficiently low pressures so that the three-body reactions are frozen, the intermediates do not necessarily have concentrations between their frozen and equilibrium values.

Finally, Momtchiloff, et al.[II-7] carried out calculations for constant area combustion of hydrogen and air. A range of initial conditions of pressure, temperature, velocity and equivalence ratio were covered although to reduce computing time, the reaction profiles were not carried to equilibrium. In this work several nitrogen-oxygen reactions leading to the formation of nitric oxide (NO) were included in the reaction steps but were found to be unimportant below 2200°K, justifying in part the assumption employed herein of nitrogen as a diluent.

As discussed in more detail below, the reaction steps and the rate constants for the above references are essentially the same as those given by reference II-2. The rate constants differ somewhat but probably only within the accuracy to which such data are known.*

*After completion of this manuscript the attention of the authors was called to the recent paper by Fowler, R. G., "A Theoretical Study of the Hydrogen-Air Reaction for Application to the Field of Supersonic Combustion," Proceedings of the 1962 Heat Transfer and Fluid Mechanics Institute, Stanford University Press. There is presented constant density calculations employing chemical mechanisms and rates similar to those described therein.

2. ANALYSIS ALONG STREAMLINES - GENERAL CONSIDERATIONS

To indicate in more detail the characteristics of the hydrogen-air reaction in a flowing system and the methods of analysis for inviscid flows, the pertinent gas dynamical equations, the reaction steps, the rate constants, and some numerical results will be discussed. Consider the inviscid, steady flow along streamlines of a chemical reacting gas involving N species and L elements. The conservation of momentum, energy, species and elements can be stated as follows:

Momentum

$$\rho V \frac{dV}{ds} = - \frac{dp}{ds} \tag{II-2.1}$$

Energy

$$\frac{dH}{ds} = 0, \qquad H \equiv (V^2/2) + \sum_{i}^{N} Y_i h_i \tag{II-2.2}$$

Species

$$\rho V \frac{dY_i}{ds} = \dot{w}_i, \qquad i = 1, 2, \cdots N-L \tag{II-2.3}$$

Elements

$$\frac{d\tilde{Y}_j}{ds} = 0, \qquad j = N-L+1, \cdots N$$

$$\tilde{Y}_j \equiv \sum_{i=1}^{N} \mu_{ij} W_j Y_i / W_i \tag{II-2.4}$$

These equations are supplemented by algebraic equations: An equation of state

$$p = \rho R_o T \sum_{i=1}^{N} Y_i/W_i = \rho R_o T/W ; \tag{II-2.5}$$

the creation terms as functions of composition and state; and the species enthalpy-temperature relations $h_i = h_i(T)$.*

The form of the creation terms is

$$\dot{w}_i = W_i \sum_{j=1}^{K} (\nu''_{ij} - \nu'_{ij}) k_j \rho^{n_j} \prod_{i=1}^{N} (Y_i/W_i)^{\nu'_{ij}} G_j \qquad \text{(II-2.6)}$$

where

$$G_j \equiv 1 - \rho^{m_j} K_{c,j}^{-1} \prod_{i=1}^{N} (Y_i/W_i)^{\nu''_{ij} - \nu'_{ij}} \qquad \text{(II-2.7)}$$

$$m_j = \sum_{i=1}^{N} (\nu''_{ij} - \nu'_{ij})$$

and where k_j is the specific rate constant, $K_{c,j}$ is the equilibrium constant based on molar concentrations, and ν''_{ij} and ν'_{ij} are the stoichiometric coefficients for the j^{th} reaction

$$\sum_{i=1}^{N} \nu'_{ij} M_i \xrightarrow{k_j} \sum_{i=1}^{N} \nu''_{ij} M_i ; \qquad j = 1, \cdots K \qquad \text{(II-2.8)}$$

Basically, these equations have been employed to date in all inviscid calculations with non-equilibrium chemical behavior. In nozzle flows, the system of equations is usually completed by the assumption of one-dimensional flow so that $\rho VA \equiv m$ with the area distribution prescribed.

*In the calculations reported here linear relations between h_i and T have been assumed. This corresponds to taking an average $c_{p,i}$ for the temperature range of interest and leads through Eq. (II-2.2) to a convenient, explicit relation for temperature $T = T(Y_i, V^2)$.

This approach does not permit generalization to more complex flow field calculations, for example, performed in connection with the method of characteristics. In such analyses the physical properties such as pressure and density are determined along any given streamline, and not streamtube area. For these reasons herein the pressure distribution is specified along the streamline under consideration, as suggested by Bloom and Steiger[II-8] in connection with non-equilibrium dissociation and recombination in external, hypersonic flows. This also completes specification of the problem, i.e., given initial conditions at a generic point ($s = 0$) the distribution of flow composition and state variables with respect to s can be found by integration.

It is perhaps worth while at this point to make some remarks about several numerical problems which arise in the treatment of the above equations. The number of differential equations which must be integrated with respect to the space variable s can be reduced by employing the element conservation equations [Eqs. (II-2.4)]. These can be integrated immediately and provide L algebraic equations among the N species, so that only N-L equations involving creation terms need be considered. However, in many calculations the mass fractions of the intermediates can be many orders of magnitudes less than the mass fractions of the major constituents. As a result the solution of the algebraic equations can involve a loss of accuracy due to the practical problem of small differences in relatively large numbers. Similar difficulties can be encountered when the flow is near-equilibrium; the creation term in Eqs. (II-2.3) represents in general the sum of differences between the forward and backward rates associated with a series of reaction steps. At equilibrium in a flowing system with pressure and temperature changes, the net result of the sum is non-zero but can involve small differences and thus a loss in accuracy. Another numerical problem is related to starting the integration in some cases; in nozzle calculations the combustion products in the settling chamber or combustor are usually assumed to be in equilibrium; but at equilibrium the creation terms must be considered indeterminant in that

a large reaction rate multiplies a quantity which is the equilibrium condition, i.e., a quantity which is essentially zero. The product yields a value of $\dot{w}_i$ maintaining the species concentration at its equilibrium value at each point in the flow. Thus integration from an equilibrium state involves a singular perturbation such as has been discussed by Bloom and Ting[II-9], Hall and Russo[II-10] and Vincenti[II-11]. However, it has been found possible in actual calculations as per the present report and in references II-6 and -12 to start the integration from a nominal equilibrium state with an initial step-size which is smaller than that usually required by integration accuracy. After a few integration steps, the effect of the numerically uncontrolled start is found to disappear and the solution of the differential equations becomes a well-behaved approximation to equilibrium flow, which is, of course, described by a solution to a set of algebraic equations. Finally, it is remarked that computing time with standard accuracy requirements for the selection of step-size can become excessive even for high speed computing equipment when the flow is near-equilibrium. This is due to a tendency for the solution to oscillate about the equilibrium solution.*

3. THE REACTION STEPS AND REACTION RATES

The reaction steps and rate constants used here are derived from the work of Duff and co-workers[II-2 to -4]. The same chemical reactions suggested by Duff have been used independently by the several investigators cited above; thus it currently appears to represent the best available set of reactions for the hydrogen-oxygen system. Here and in reference II-6 nitrogen is treated as an inert diluent; this assumption as shown in reference II-7 is considered valid for temperatures below roughly 2500°K. It is worth mentioning at this point that the temperature range of interest in supersonic combustion appears to

*A detailed discussion of numerical difficulties associated with calculations of non-equilibrium nozzle flows is given by Emanuel and Vincenti[II-12]. The current state of development for air calculations is indicated in reference II-13.

be below roughly 3000°K; this is within the range covered by the shock tube experiments of Schott et al.[II-3, -4] and only somewhat above the temperature obtained in detonation experiments, e.g., Nicholls[II-14] and in laminar flame experiments, e.g., Fine[II-15]. These experiments do not verify and establish the individual reaction steps and reaction rates but have verified partially the overall consistency of the ensemble required for practical analysis.

The reaction rates considered here are as follows:

			k_f
1	$H + O_2$	$\rightarrow OH + O$	$3(10^{14})e^{-8810/T}$
2	$O + H_2$	$\rightarrow OH + H$	$3(10^{14})e^{-4030/T}$
3	$OH + H_2$	$\rightarrow H_2O + H$	$3(10^{14})e^{-3020/T}$
4	$2OH$	$\rightarrow H_2O + O$	$3(10^{14})e^{-3020/T}$

			RR No. 1	No. 2	No. 3
5	$2H + M$	$\rightarrow H_2 + M$	10^{15}	$5(10^{15})$	$1(10^{16})$
6	$H + OH + M$	$\rightarrow H_2O + M$	10^{16}	10^{17}	$3(10^{17})$
7	$H + O + M$	$\rightarrow OH + M$	10^{15}	10^{16}	$3(10^{16})$
8	$2O + M$	$\rightarrow O_2 + M$	$3(10^{14})$		

(II-3.1)

The temperatures are in °K; the forward rate constants, i.e., for the reaction proceeding to the right are given in $(\text{mole/cc})^{-1}\ \text{sec}^{-1}$ for second order reactions (1-4) and in $(\text{mole/cc})^{-2}\ \text{sec}^{-1}$ for third order reactions (5-8); the symbol M is used to denote any molecule or atom serving as a third body. As will be discussed in detail below, the rate constants for reaction steps 5 and 6 play an important role at low pressures in determining the chemical history of the flow; therefore,

several values thereof have been selected. Those denoted RR No. 1 and RR No. 2 represent the range of probable values estimated by Schott[II-3] while RR No. 3 are values considered possible on the basis of more recent combustion results. The rate constants for the reverse reactions are obtained from the equilibrium constants approximated as functions of the temperature in the form $Be^{A/T}$.

To indicate the range of values of the reaction rate constants employed in related theoretical studies there are compared in Table II-1 the rate constants for reaction 5 employed therein; this reaction is selected as being an important but typical one in the array of reaction steps. It will be noted that in references II-3, -6, and -7 a different relation between the temperature and k_5 has been assumed. However in the temperature range of 1000 to 3000°K the numerical values given by the different expressions are within an order of magnitude; this is indicative of the accuracy with which these physical-chemical data are known.

TABLE II-1

Reaction Rates for Hydrogen Recombination

$$2H + M \rightarrow H_2 + M$$

	k_5 (moles/cc)$^{-2}$ sec^{-1}
Present Report RR No. 1	10^{15}
RR No. 2	$5(10^{15})$
RR No. 3	$1.2(10^{16})$
Reference II-3	10^{15} to $5(10^{15})$
Reference II-6	$2(10^{18})T^{-1}$
Reference II-7	$5(10^{16})T^{-\frac{1}{2}}$

The reaction steps described by Eqs. (II-3.1) can be separated into two groups: the second-order or "shuffling" reactions (1-4) which

proceeding to the right deplete the population of molecular oxygen and hydrogen and lead to the formation of water and of the intermediates, atomic oxygen and hydrogen and the hydorxyl radical; and the third order reactions (5-8) which proceeding to the right deplete the intermediates and lead to the formation of water and molecular species. This complex array of forward and reverse reactions makes difficult, if not impossible, a priori estimates of chemical behavior in general and of chemical times in particular.

4. NUMERICAL RESULTS FOR CONSTANT PRESSURE

It is instructive for an understanding of the kinetics involved in the supersonic combustion of hydrogen to consider the reaction history of the following flow model: a mixture of hydrogen and air at time zero at an initial temperature of 1000°K or higher. The pressure is assumed constant with time.

In the calculations presented here, some of these results are taken from reference II-5; the additional calculations have been performed by H. Pergament and will be reported "in extenso" elsewhere, the initial state of the gas is assumed to correspond to a partial equilibrium between the atomic and molecular species of oxygen and between the atomic and molecular species of hydrogen. The results are not significantly altered if the initial concentrations of the atomic species are changed somewhat; relatively large concentrations of atomic hydrogen would of course change the early phases of the reaction histories.

Consider the temperature histories for some typical cases based on this model as shown in Figures II-1a-c and as computed by a standard integration program on an IBM 7090 computer. Presented are the results for three pressures, for several equivalence ratios* and for the three rates of reactions 5 and 6 as discussed in Section II-3 above.

*The equivalence ratio, denoted as η, is defined by the chemical equation for the reactants; namely, $O_2 + 2\eta H_2 + 3.76 N_2 \rightarrow$ products.

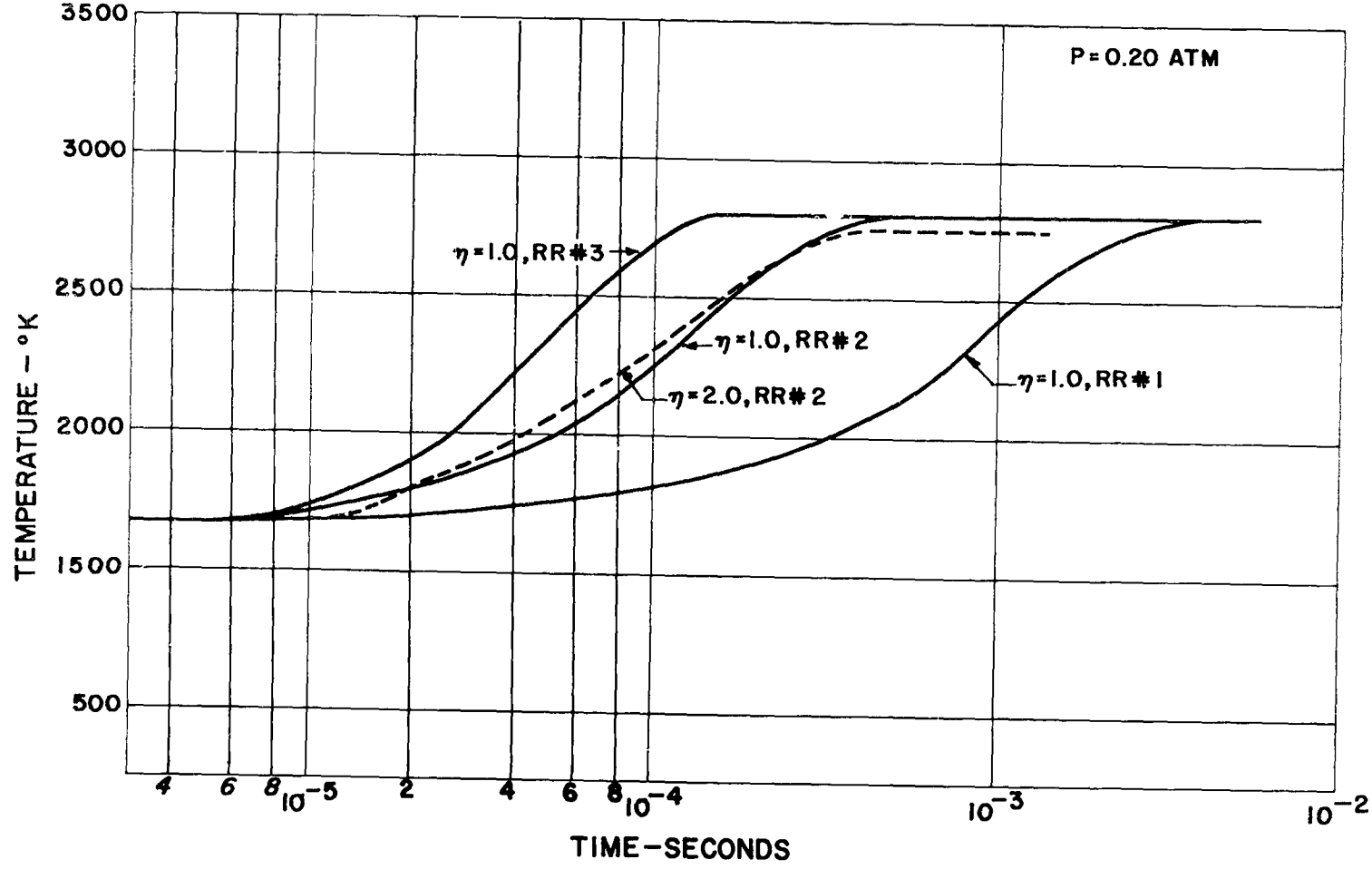

FIG. II-1a. Temperature-time Histories of Hydrogen-Air Mixtures at Constant Pressure.

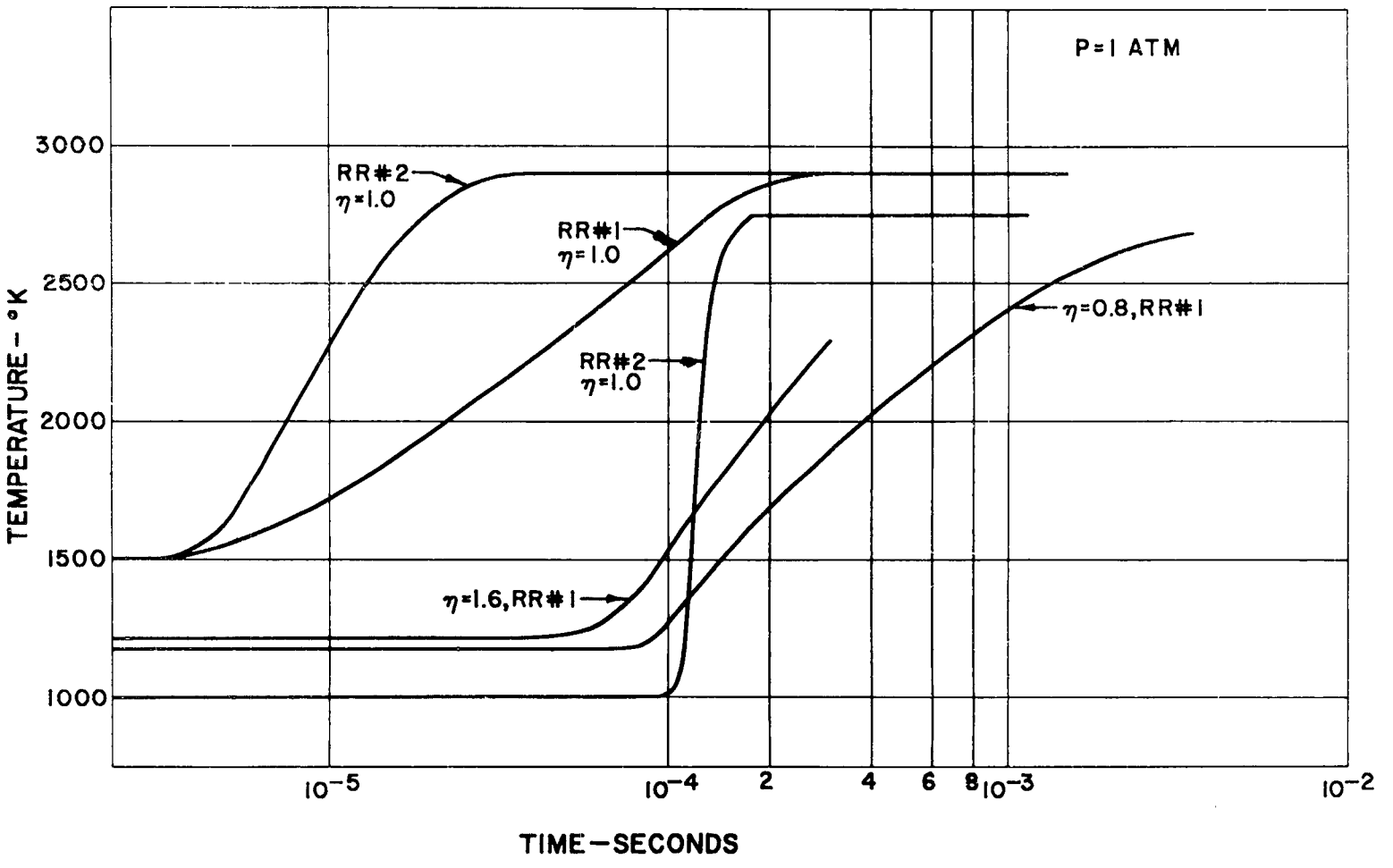

FIG. II-1b. Temperature-Time Histories of Hydrogen-Air Mixtures at Constant Pressure.

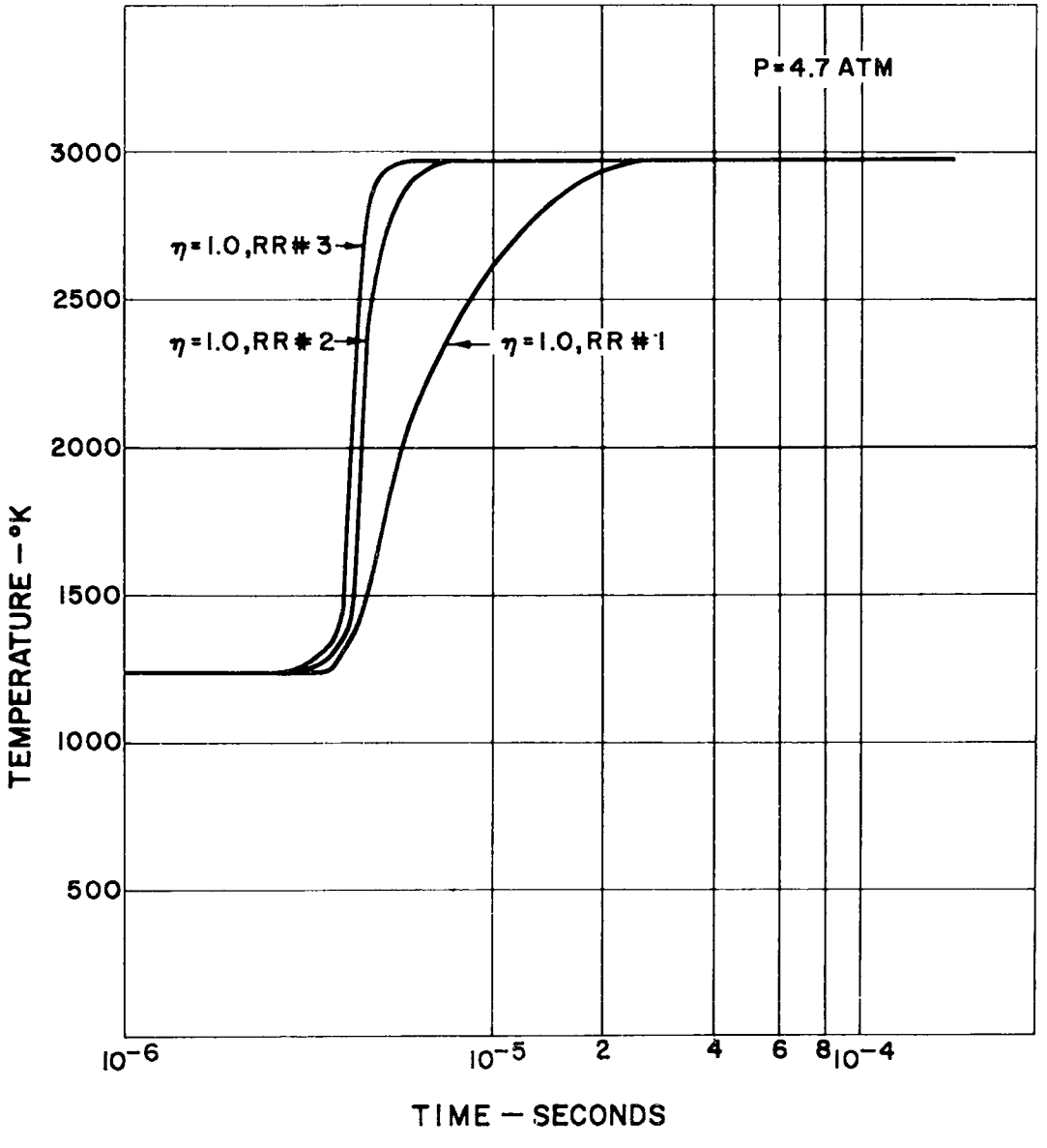

FIG. II-1c. Temperature-Time Histories of Hydrogen-Air Mixtures at Constant Pressure.

These temperature histories are characterized by two time periods; there is an initial time interval, usually termed the induction time and denoted τ_i, during which the temperature remains sensibly constant, and a later phase, during which the temperature increases from its initial value T_i to the final temperature T_f; the latter corresponds in this model to the adiabatic flame temperature (reference II-17). The time associated with the second phase is termed here the energy release time and is denoted τ_r; thus $\tau_c = \tau_i + \tau_r$. Under conditions of high initial temperature and low pressure the second time interval dominates while under conditions of relatively low initial temperature (1000°K) and high pressure (4 atmospheres) the two time intervals are of roughly equal duration. This last result appears not to have been observed previously.

The changes in composition during these periods are shown in representative cases in Figures II-2a-f. Of greatest thermodynamic significance because of its high species enthalpy per unit mass is the behavior of the atomic hydrogen; during the induction phase the concentration of H and the other intermediates O and OH increases rapidly and reaches a maximum corresponding to mass fractions of the order of several percent or less. At the same time the molecular species, O_2 and H_2 are depleted and water is formed. However, the chemical energy released by the formation of water is effectively absorbed by the atomic hydrogen so that no significant change in temperature occurs. During the second time period the intermediates decay to their appropriate equilibrium values releasing chemical energy and leading to the temperature rise seen in Figures II-1a-c. It should be noted that at the end of the induction period the major constituents are close to their equilibrium values; during the second period the decay of the intermediates leads to only secondary adjustments in the concentrations of the major constituents.

This behavior is explicable in terms of the reaction steps given by Eqs (II-3.1). During the induction phase the two-body or "shuffling"

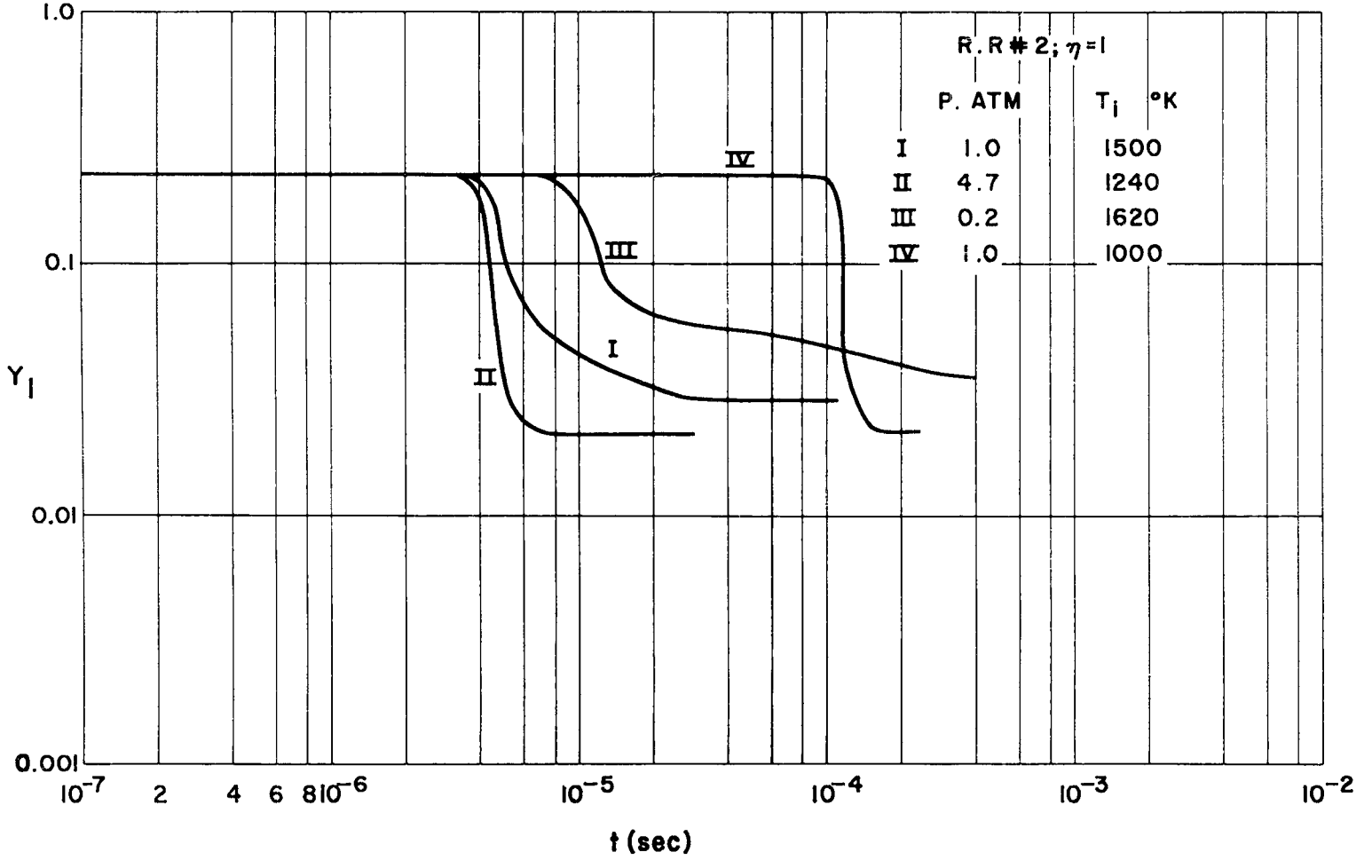

FIG. II-2a. Composition-Time Histories of Hydrogen-Air Mixtures at Constant Pressure, O_2.

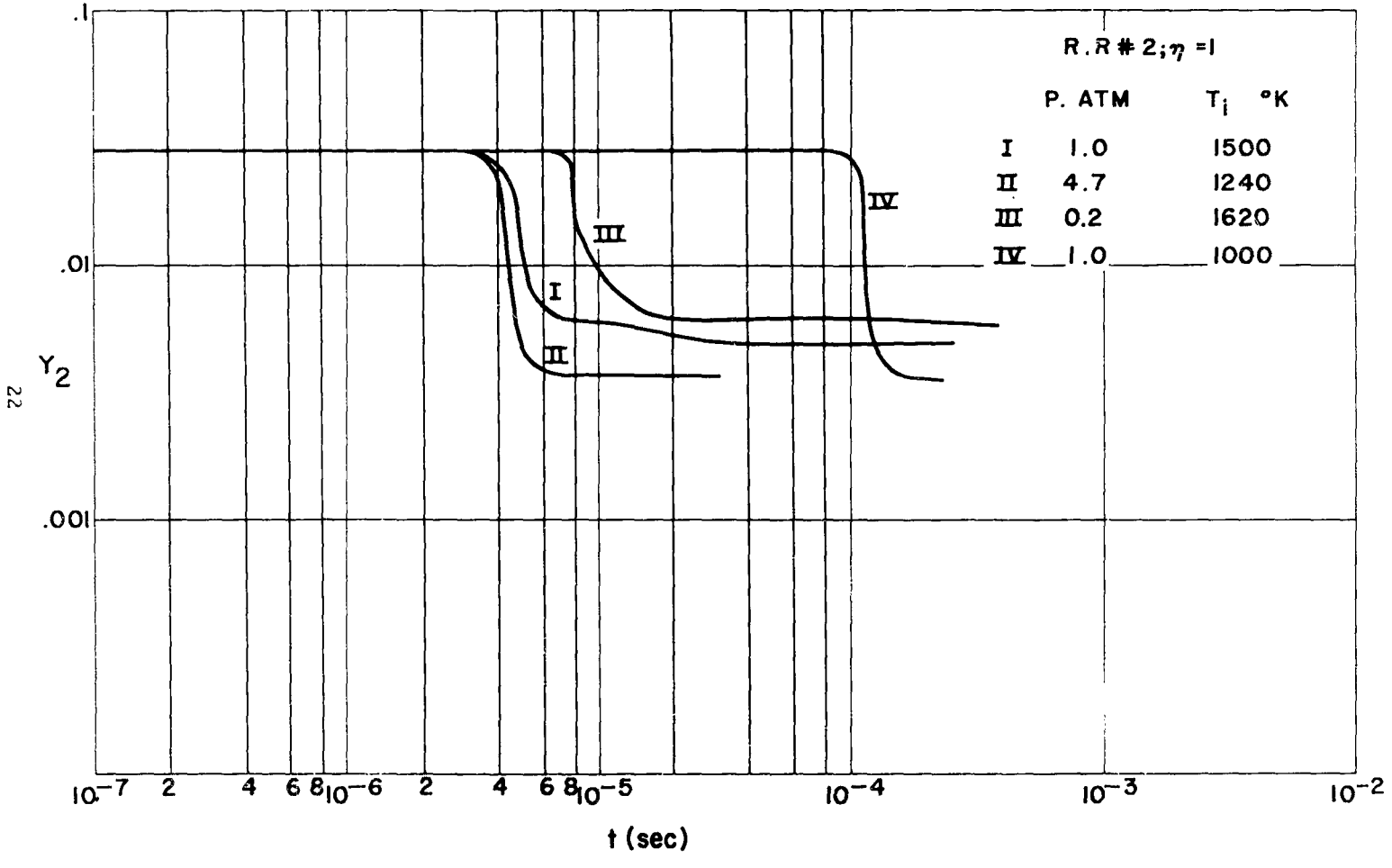

FIG. II-2b. Composition-Time Histories of Hydrogen-Air Mixtures at Constant Pressure, H_2.

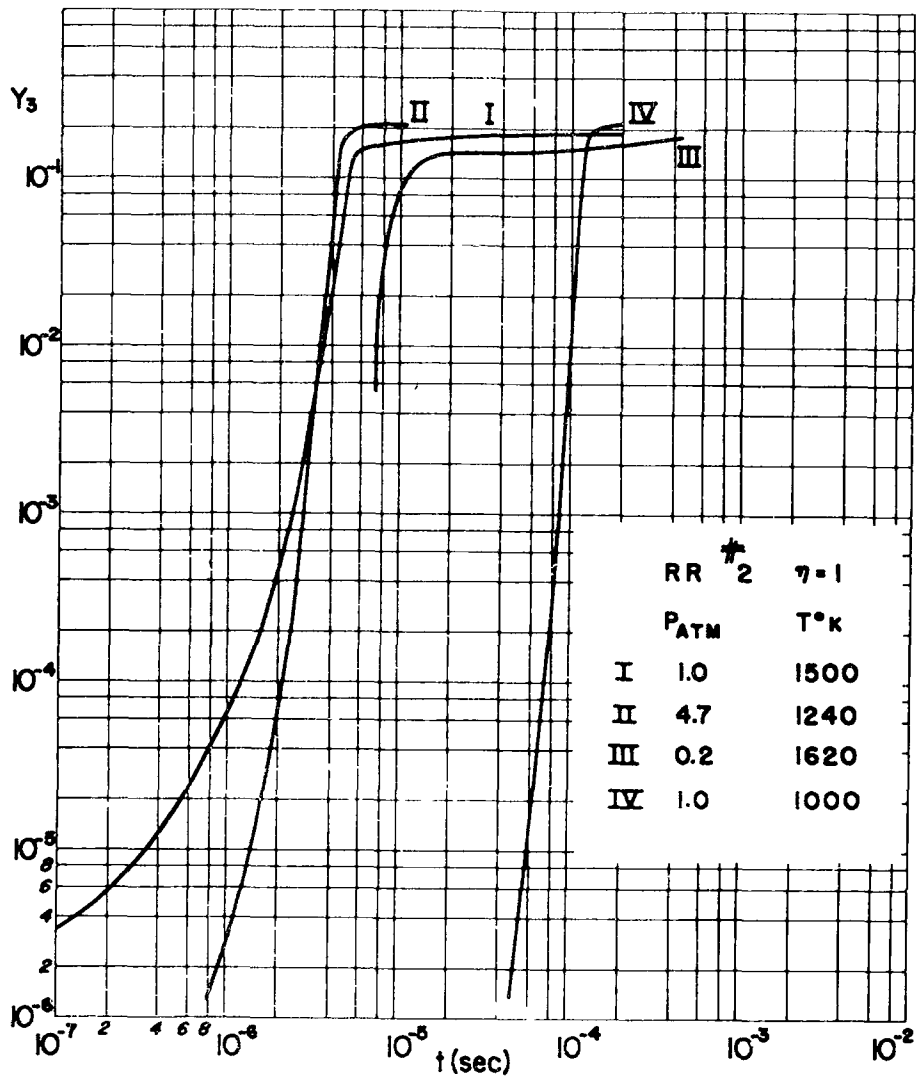

FIG. II-2c. Composition-Time Histories of Hydrogen-Air Mixtures at Constant Pressure, H_2O.

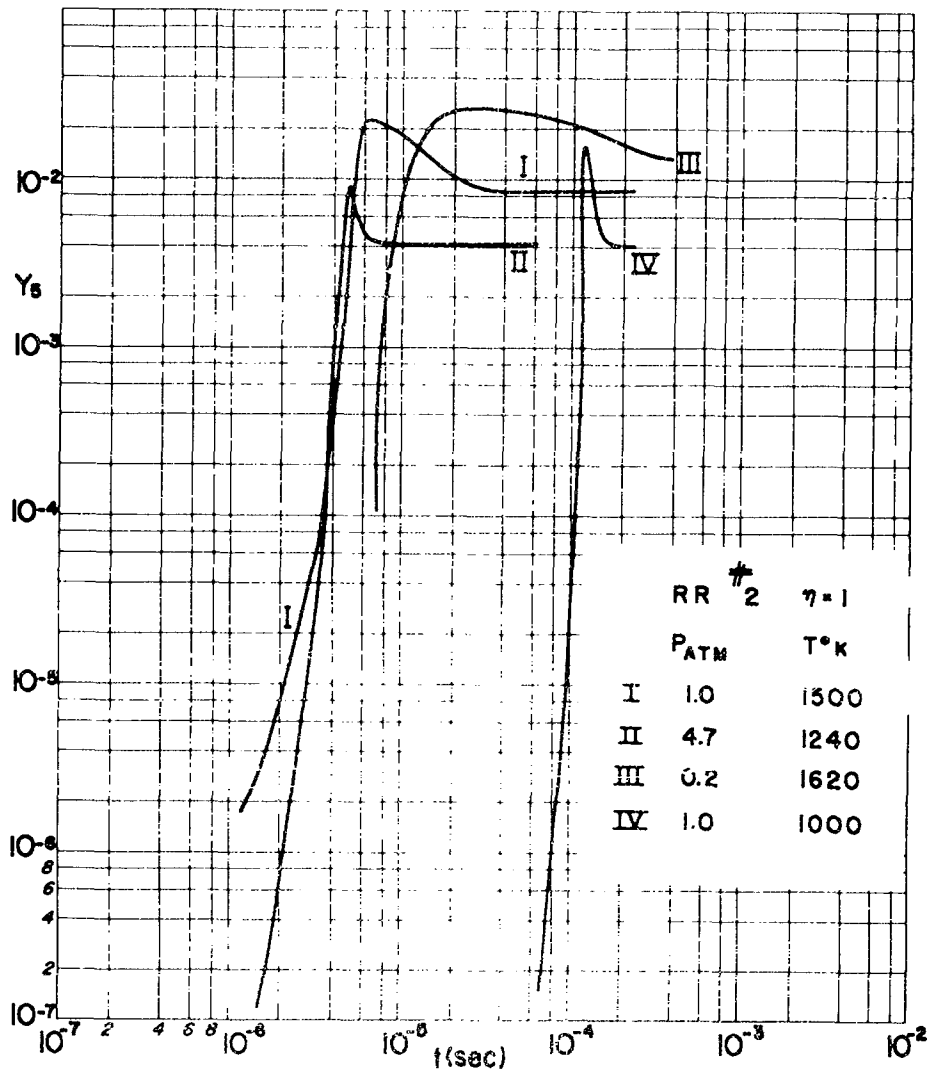

FIG. II-2d. Composition-Time Histories of Hydrogen-Air Mixtures at Constant Pressure, O.

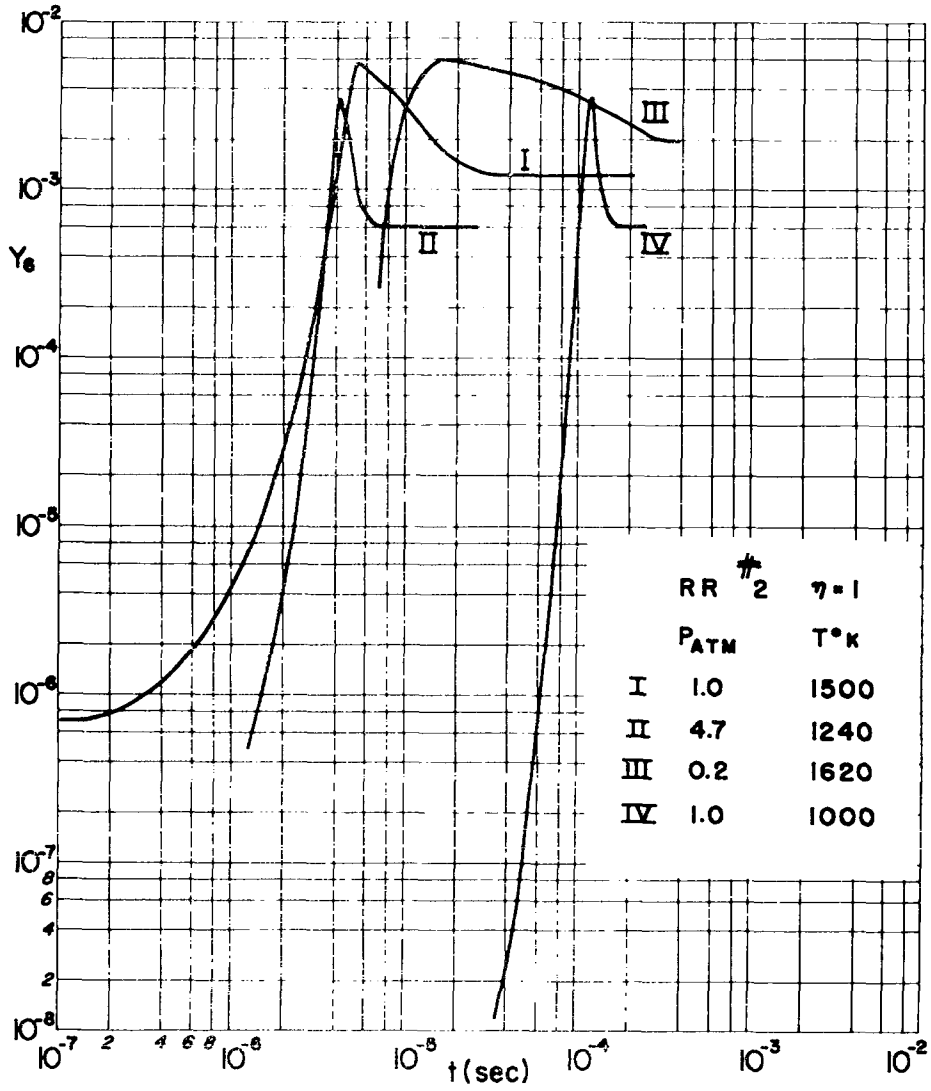

FIG. II-2e. Composition-Time Histories of Hydrogen-Air Mixtures at Constant Pressure, H.

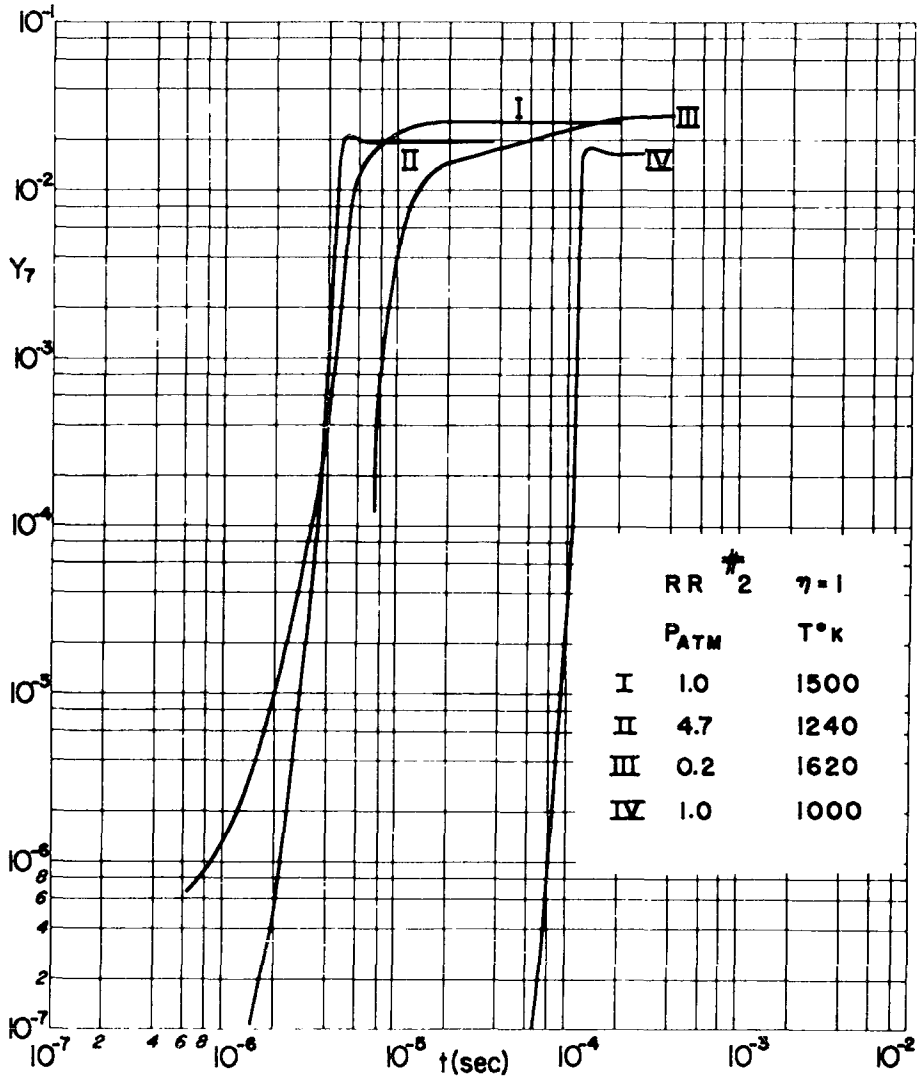

FIG. II-2f. Composition-Time Histories of Hydrogen-Air Mixtures at Constant Pressure, HO.

reactions are relatively fast and lead to an overproduction of the intermediates; during the second period, the third-order reactions lead to recombination and depletion of the intermediates with the accompanying energy release. This characteristics of the hydrogen-oxygen reaction was apparently published first by Duff[II-2]. The results presented here confirm this behavior over a variety of initial conditions.

It is of interest to note that at low pressures the overall reaction time is sensitive to the recombination reaction rate, e.g., for $p = 0.2$ atmospheres the overall reaction time is 15 times less for RR No. 3 than for RR No. 1. On the contrary, for $p = 4.7$ atmospheres these times differ by only a factor of three. It must also be noted that for static pressure of the order of one atmosphere or higher, the energy release time is short; therefore the difference between the results for different reaction rates is not important for practical applications. However, this is not the case at low pressures.

5. THE INDUCTION PERIOD

In the past considerable attention has been devoted to the time associated with the induction period; for example, Schott and Kinsey[II-4] and Nicholls[II-14] present the results of experiments, employing respectively techniques associated with the shock tube and standing detonation waves, to show the dependence of τ_i on pressure, temperature and composition; in both reference theoretical considerations based on the reaction steps were employed to facilitate correlation of the data.

A convenient formula which can be used for estimating τ_i within a factor of two or three for mixtures with equivalence ratios on the order of unity can be obtained by simplifying the functional form suggested by Nicholls and by employing coefficients selected from the present numerical results. With τ_i defined as the time at which the computed temperature starts to rise significantly, there is obtained

$$p\tau_i \simeq 45(10^{-4})e^{10^4/T_i} \qquad \text{(II-5.1)}$$

where τ_i is in μ sec, p in atmospheres and T_i in ^{o}K. In Figure II-3 the numerical results are compared with the predictions of Eq. (II-5.1); it will be seen that within the cited factor of two or three the correlation is satisfactory.

From Figures II-1a-c and from II-3 it will be noted that the induction time is not greatly altered by changes in the equivalence ratio nor in the reaction rates for recombination. By assuming the third order reactions to have a negligible role and the temperature to be constant during the induction period, it is possible to make estimates of the composition at the end of the induction period. Such estimates were made by Schott[II-3] and were shown to be in good agreement with more complete calculations and with shock tube experiments. The calculation assumes that at the end of the induction phase there exists a partial equilibrium state corresponding to equilibrium of any three of the two-body reactions (1-4). In addition, since these dominant reactions involve no change in moles of gas, and since the temperature is approximately constant, it can be assumed that the molecular weight of the mixture remains constant during the induction period. The resulting three equilibrium conditions, the statement concerning molecular weight, and element conservation determine the mass fractions of all species. The parameters involved in such a calculation are η and T_i; the pressure does not enter.

In Figure II-4 the mass fractions of atomic hydrogen at the end of the induction period as computed by this scheme are shown for a range of initial temperatures. The calculations were carried out on a Bendix G-15 computer and involved solution by a combination of iteration and Newton-Raphson methods of a set of algebraic, nonlinear equations. Mr. H. Fox carried out these calculations. Also shown are the maximum values of Y_e obtained from the computer program. The satisfactory agreement will be noted; similar agreement is found for the remaining constituent.

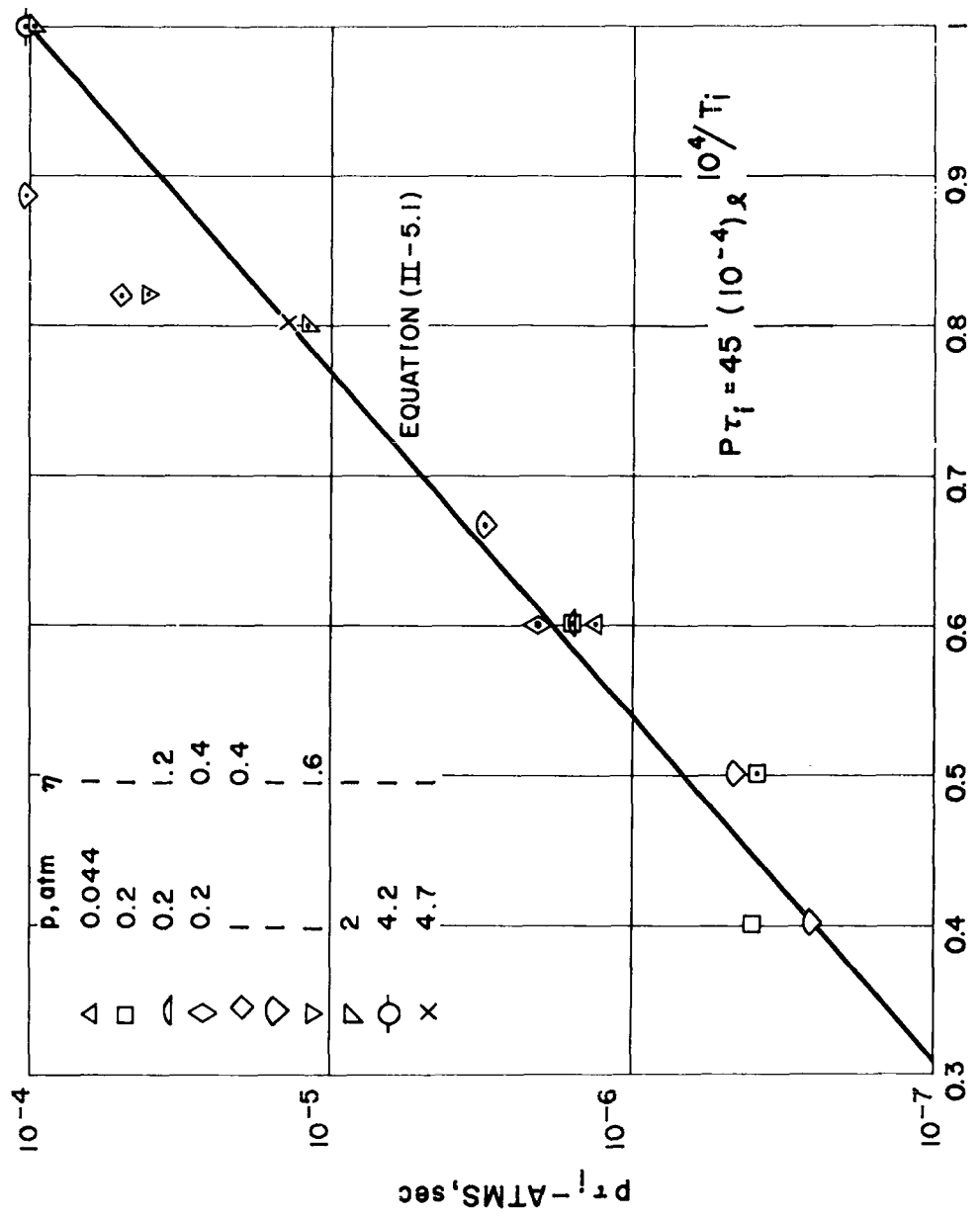

FIG. II-3. Correlation of Compiled Induction Times.

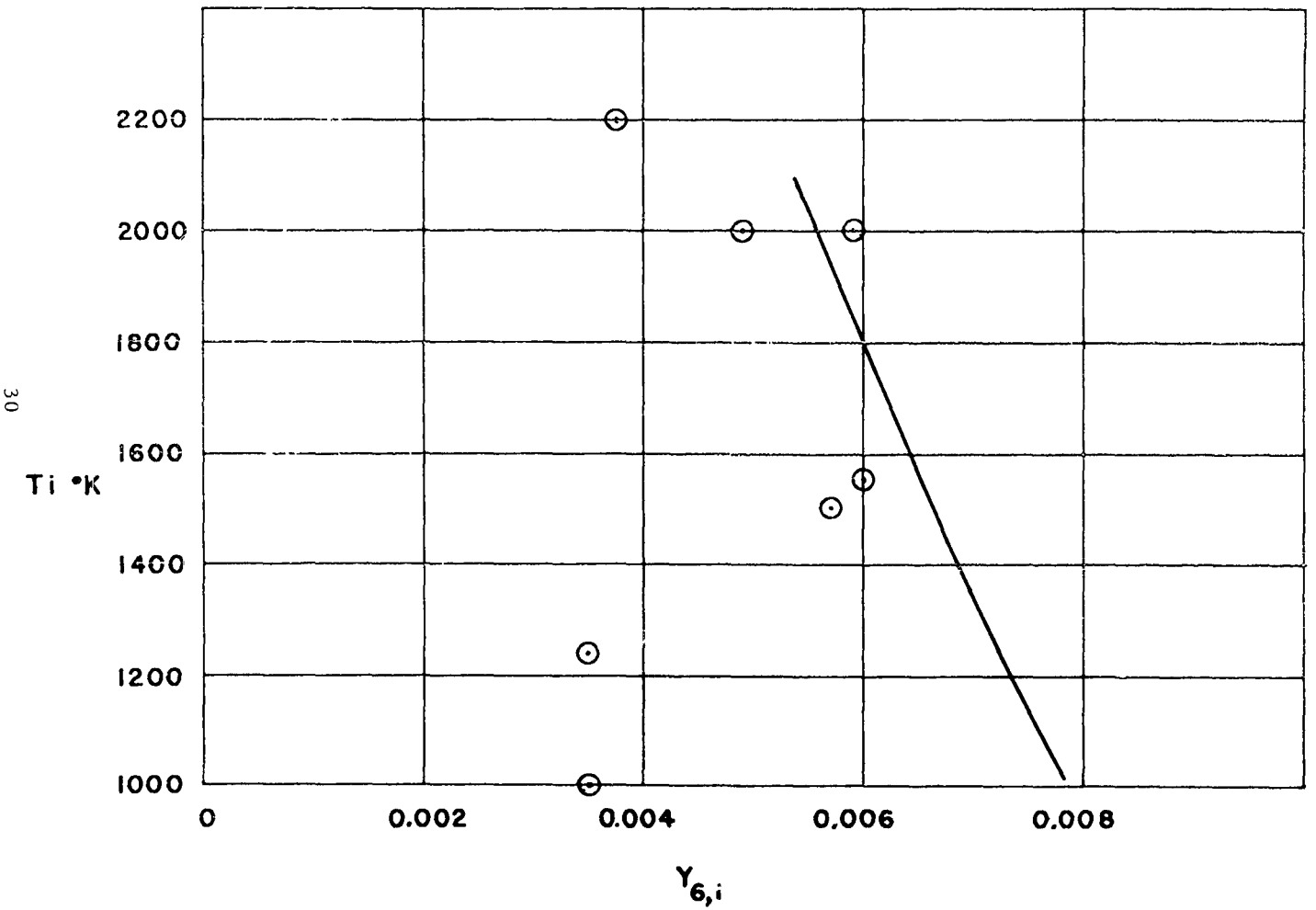

FIG. II-4. Dependence of Mass Fraction of Atomic Hydrogen at the End of the Induction Period on Initial Temperature.

6. APPLICATION OF PARTIAL EQUILIBRIUM FOR ESTIMATES OF THE ENERGY RELEASE PERIOD

As a result of the estimates of the induction time and of the scheme described above for approximating the composition at the end of the reaction period, it is possible to consider a further approximation applicable to the energy release period. The basis for the approximation resides in the coexistence during this period of second and third order reactions, i.e., those corresponding to reactions 1-4 and to 5-8, respectively; if it is assumed that the former are sufficiently fast relative to the latter so as to maintain during the entire second period a partial equilibrium state, an approximate description of the reaction history can be obtained by a single quadrature. It is noted that the concept of partial equilibrium can be applied only when the pressure is sufficiently high so that the assumed equilibration of the two-body reactions can occur. Analyses of this type have been carried out by Westenberg and Favin[II-6] and by Zinman and Romano[II-18]. Care must be exercised in connection with the treatment of partial equilibrium in flowing systems in that there are introduced indeterminacies which correspond to an infinite reaction rate multiplying a zero corresponding to the equilibrium condition for the fast reaction step. The second author discussed this difficulty in general in reference II-19 and showed how it may be overcome.

Consider the analysis of the second period according to a partial equilibrium concept. Take for the three independent, two-body reactions those denoted 1, 2, and 3 in Eqs. (II-3.1) and take reactions 5 and 6 to be the most important three-body reactions.* Now the assumption that the former are relatively fast implies from Eq. (II-2.7)

$$G_1 \equiv 1 - (W_6 W_1 / W_7 W_5) K_{C,1}^{-} (Y_7 Y_5 / Y_6 Y_1) \simeq 0 \qquad \text{(II-6.1)}$$

*The analysis is not complicated in principle by the inclusion of more three-body reactions although numerically the complexity is increased thereby.

$$G_2 \equiv 1 - (W_5 W_2 / W_7 W_6) K_{c,2}^{-1} (Y_7 Y_6 / Y_5 Y_2) \simeq 0 \qquad \text{(II-6.2)}$$

$$G_3 \equiv 1 - (W_7 W_2 / W_3 W_6) K_{c,3}^{-1} (Y_3 Y_6 / Y_7 Y_2) \simeq 0 \qquad \text{(II-6.3)}$$

The element mass fractions for the oxygen-hydrogen system with nitrogen treated as a diluent are from Eqs. (II-2.4)

$$\tilde{Y}_1 = Y_1 + (W_1 / 2W_3) Y_3 + Y_5 + (W_1 / 2W_7) Y_7 = \text{constant} \qquad \text{(II-6.4)}$$

$$\tilde{Y}_2 = Y_2 + (W_2 / W_3) Y_3 + Y_6 + (W_2 / 2W_7) Y_7 = \text{constant} \qquad \text{(II-6.5)}$$

$$Y_4 = \text{constant} \qquad \text{(II-6.6)}$$

Thus Eqs. (II-6.1)-(II-6.6) represent six equations in seven mass fractions and in the temperature and must be supplemented by a single reaction equation and by an energy equation. Since the atomic hydrogen is thermodynamically the most important intermediate, consider the species conservation thereof; prior to making the assumption of partial equilibrium, i.e., that $G_k \simeq 0$, $k = 1, 2, 3$, Eqs. (II-2.3), (II-2.6) and (II-2.7) for $i = 6$, give

$$\frac{dY_6}{dt} = \frac{\dot{w}_6}{\rho W_6} (W_6) = \frac{W_6}{\rho} [-k_1 (Y_6 / W_6)(Y_1 / W_1) \rho^2 G_1 + k_2 (Y_5 / W_5)(Y_2 / W_2) \rho^2 G_2 +$$

$$+ k_3 (Y_7 / W_7)(Y_2 / W_2) \rho^2 G_3 - 2k_5 (Y_6 / W_6)^2 (\rho^3 / W) G_5$$

$$- k_6 (Y_6 / W_6)(Y_7 / W_7)(\rho^3 / W) G_6] \equiv F^{-1} \qquad \text{(II-6.7)}$$

Now with partial equilibrium assumed, the products $k_j \rho^{n_j} \prod_{i=1}^{N} (Y_i / W_i)^{\nu'_{ij}} G_j$ must be interpreted as an infinite rate k_j multiplied by zero, namely G_j, such that partial equilibrium prevails. Accordingly, let σ_j denote these terms and consider σ_j, $j = 1, 2, 3$ as unknowns but σ_5 and σ_6 as

determinant values. If $G_k \simeq 0$, $k = 1, 2, 3$ then Eqs. (II-6.1)-(II-6.3) upon total differentiation imply

$$\left(\rho \frac{dT}{dt}\right) \frac{\partial G_k}{\partial T} = - \sum_{i=1}^{7} \frac{\partial G_k}{\partial Y_i} \dot{w}_i , \quad k = 1, 2, 3$$

$$= \rho \frac{dT}{dt} \left(\frac{d}{dT} \ell n K_{c,k}\right) \tag{II-6.8}$$

At this point it is necessary to consider the energy equation; for constant pressure flow the energy equation is simply $h = \text{constant}$ so that

$$\rho \frac{dT}{dt} = - \left(\sum_{i=1}^{7} h_i \dot{w}_i \right) / c_p \tag{II-6.9}$$

In Eqs. (II-6.8) and (II-6.9), $\dot{w}_i$ can be expressed in terms of the σ_i's according to

$$\dot{w}_i = W_i \sum_{j} (\nu''_{ij} - \nu'_{ij}) \sigma_j , \quad j = 1, 2, 3, 5, 6 \tag{II-6.10}$$

so that Eqs. (II-6.8) and (II-6.9) yield

$$\sum_{i=1}^{7} \sum_{j} \left(\frac{\partial G_k}{\partial Y_i} - \frac{h_i}{c_p} \frac{d}{dT} \ell n K_{c,k} \right) (\nu''_{ij} - \nu'_{ij}) \sigma_j W_i = 0, \qquad \begin{matrix} j = 1, 2, 3, 5, 6 \\ k = 1, 2, 3 \end{matrix} \tag{II-6.11}$$

Eqs. (II-6.11) permit σ_j, $j = 1, 2, 3$ to be expressed in terms of σ_5 and σ_6 so that the right-hand side of Eq. (II-6.7) involves only determinant values. Moreover, Eq. (II-6.7) can be integrated to yield

$$t = \tau_i + \int_{Y_{6,i}}^{Y_6} F dY'_6 \tag{II-6.12}$$

where the constant of integration is selected so that when $t = \tau_i$, Y_e is equal to that given by the analysis of the induction period, namely $Y_{e,i}$.

The calculations involved in applying this analysis can be carried out on a small scale computer; e.g., the results reported here were obtained on a Bendix G-15 computer. The procedure is as follows: The value of Y_e varies from the maximum computed according to partial equilibrium applied to the induction period to that prevailing at equilibrium at the final temperature T_f. This latter value can be estimated by an equilibrium calculation or from available tables of the combustion products of hydrogen and air. This range of values is divided into a number of intervals appropriate to the integration of Eq. (II-6.12). With a generic value of Y_e selected Eqs. (II-6.1)-(II-6.6) and the energy equation $h = \text{constant}$ are employed to determine, e.g., by a combined iteration and Newton-Raphson method, the temperature T and the mass fractions Y_i, $i = 1, 2, 3, 5$, and 7 corresponding thereto. Then Eqs. (II-6.11) are solved by matrix inversion to obtain σ_j, $j = 1, 2, 3$; the integral F in Eq. (II-6.12) can then be evaluated and the integration for the time t carried out. Note that when Y_e equals the equilibrium value $F \to \infty$ so that in reality this final value does not have to be known a priori.

In Figure II-5 there is presented a comparison of the approximate and exact reaction history for one case; shown are the distributions of Y_3, Y_e and T and the initial conditions. It will be seen that in general the agreement is satisfactory. As a result of these considerations it can be concluded that a reasonable understanding of the interaction of the complex mechanisms involved in the hydrogen-oxygen reaction is available; of course, the characterization of the reaction history into two time periods and the approximations employed in the simplified treatment of each have been deduced from more accurate calculations. It is noted that the extension of the analysis of this section to nozzle flows according to either the streamline or one-dimensional point of view is straightforward.

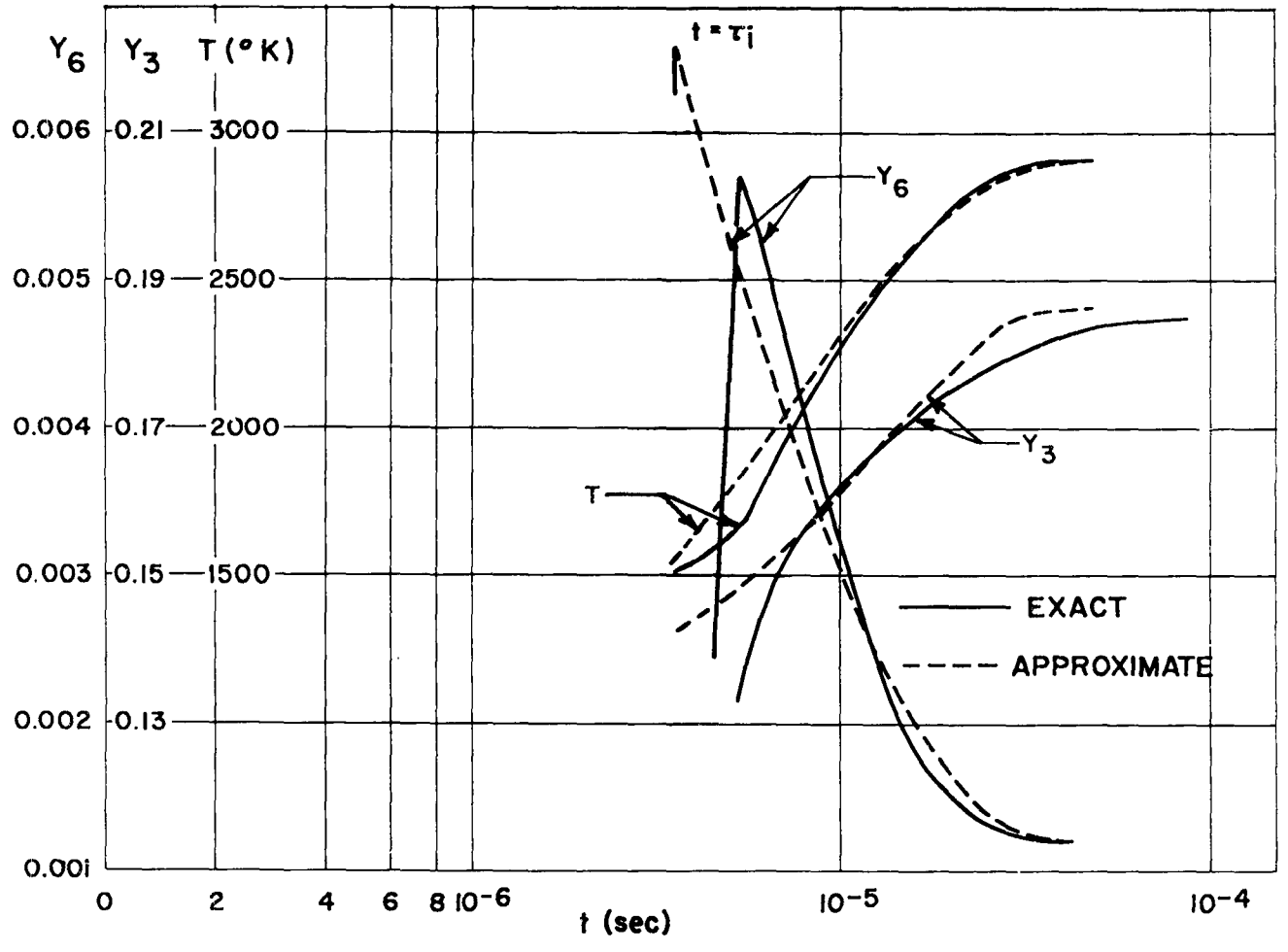

FIG. II-5. Comparison of Approximate and Exact Composition and Temperature Histories.

7. COMPARISON WITH EXPERIMENT FOR NOZZLE EXPANSION

As mentioned previously there are available limited experimental results which can be used to verify the overall reaction mechanism and reaction rates employed in this and similar studies of the hydrogen-oxygen system. In addition to the cited experimental research of Schott et al. [II-3, -4] there are available the tests of nozzle flows of the combustion products of hydrogen and air carried out by Lezberg and Lancashire[II-16]. Of particular interest herein are the measurements of the temperature along the axis of the nozzle. In order to carry out a comparison between experiment and theory the pressure distribution along the axis of the nozzle had to be estimated; the approximate transonic theory for the flow in the throat of a nozzle and the measured pressure distribution along the nozzle wall were employed to obtain the estimated pressure distribution shown in Figure II-6. The composition in the settling chamber of the nozzle was taken to be close to equilibrium at the specified stagnation pressure and temperature and with the specified equivalence ratio. The equations of Section II-2, with the reaction mechanism of Eqs. (II-3.1) with RR No. 2 selected were integrated from upstream of the throat. The composition, velocity and temperature distributions along the axis were computed. Mr. H. Pergament performed these calculations. Shown on Figure II-6 are the temperature distributions corresponding to equilibrium and frozen chemical behavior taken from reference II-16 and corresponding to finite rate chemistry computed here. Also shown are the two experimentally determined temperatures from reference II-16. In view of the approximations attendant upon the estimation of the pressure distribution and in view of the possible inaccuracies in measurement, the agreement with respect to computed and measured temperatures is considered satisfactory. Clearly additional experimental data would be valuable in validating the reaction mechanism and rates.

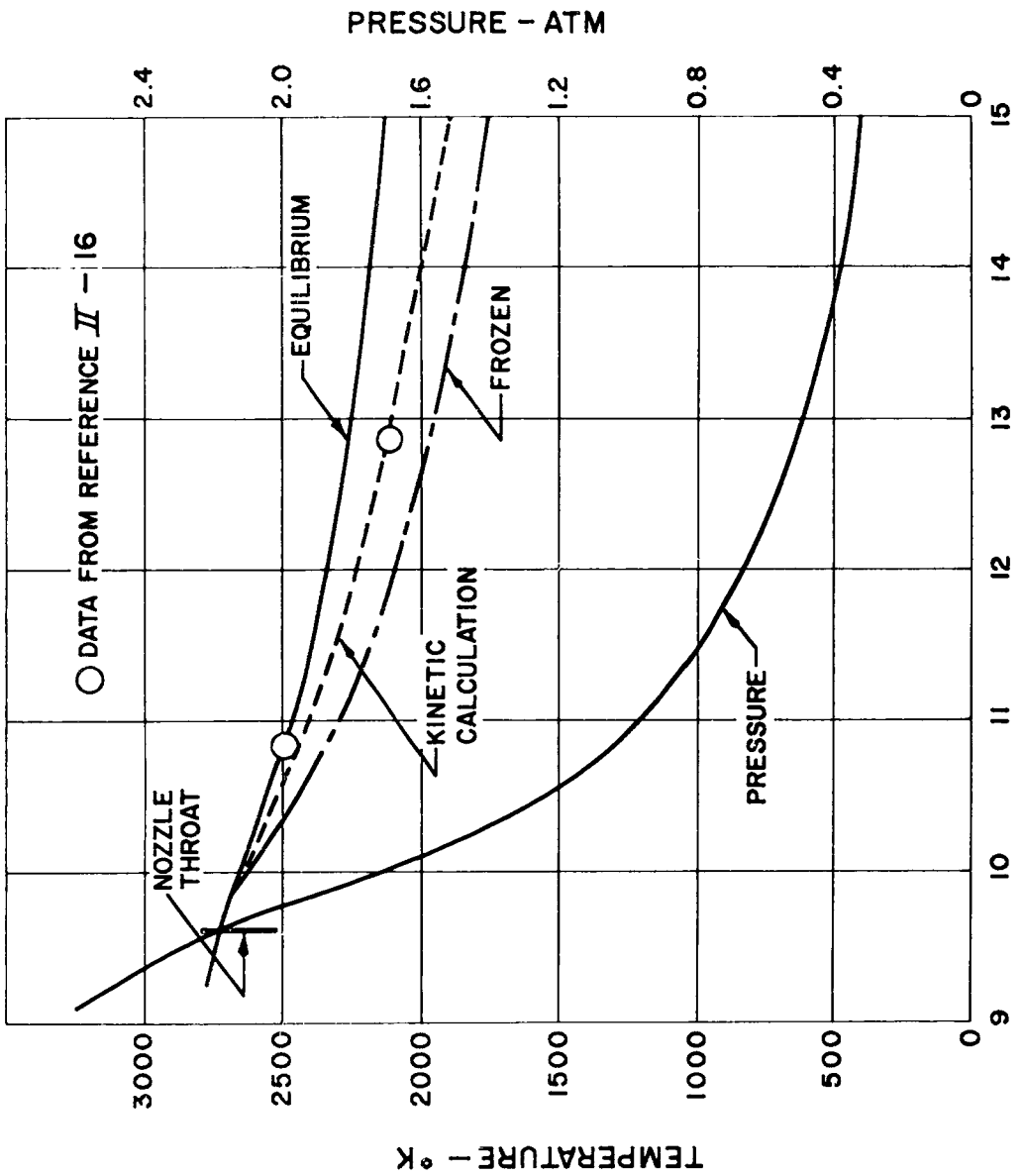

FIG. II-6. Pressure and Temperature Distribution Along the Axis of Nozzle

An interesting result concerning the concentrations of the intermediates in a non-equilibrium flow of combustion products is shown in Figure II-7a-c. Shown there are the distributions of the mass fractions of the species along the axis of the nozzle from the aforementioned calculation. It will be noted that recombination of H and O takes place in the initial part of the expansion, however, downstream of the point where the temperature deviates from the equilibrium distribution and where the mass fraction of the major constituents is frozen, the mass fractions of intermediates continues to change; of particular interest is the increase in H and the descrease in OH. This is somewhat unexpected; in the extensive studies of the expansion of dissociated air through nozzles and around bodies in hypersonic flight it was always found that the concentrations of all species were between those for complete equilibrium and complete frozen flow. The behavior here for the hydrogen-air system appears to be due to the relatively fast two-body reactions (1-4) which can maintain a partial equilibrium of the intermediates while the major constituents are essentially frozen. This indicates that perhaps the partial equilibrium analysis discussed above may provide reasonable estimates of the behavior of combustion products during nozzle expansion. As noted above, this behavior of H and OH was found independently by Westenberg and Favin[II-6].

8. PRELIMINARY CONCLUSIONS OF THE ANALYSIS FOR CONSTANT PRESSURE CHEMICAL REACTION

The results of the analysis described above for constant pressure show that the induction time decreases rapidly when static temperature and pressure increase. Such times of the order of 10^{-5} sec can be easily obtained for high Mach number flight conditions even at high altitudes. As a consequence, in a practical combustor, the ignition zone will be limited to a few inches after mixing and the energy release zone will be of the same order for pressures between 0.5 and 1 atm. On this basis the assumption of inviscid flow for the combustion region, where large variations of pressure may occur, represents a good approximation.

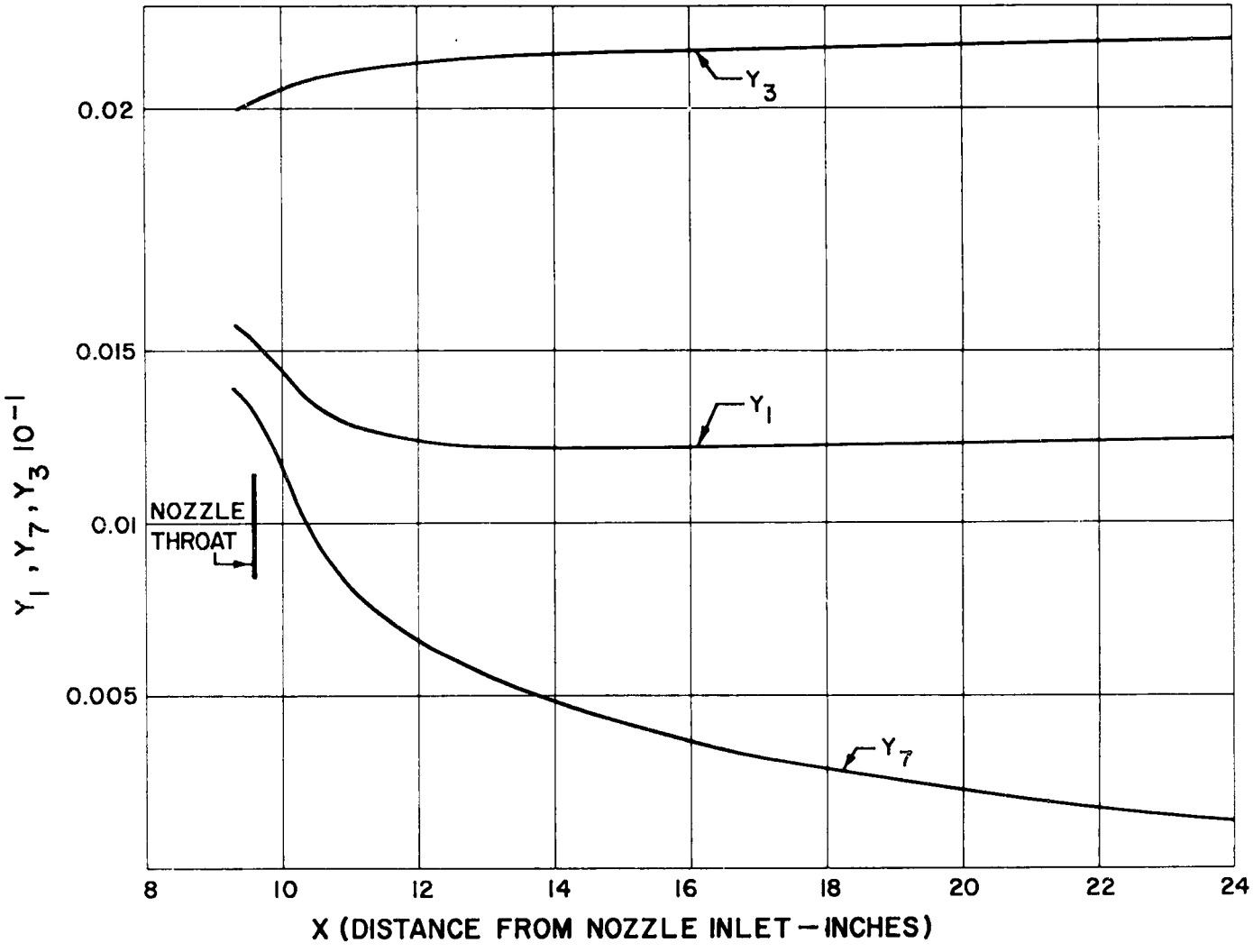

FIG. II-7a. Distribution of Mass Fraction Along the Axis in Nozzle Flow.

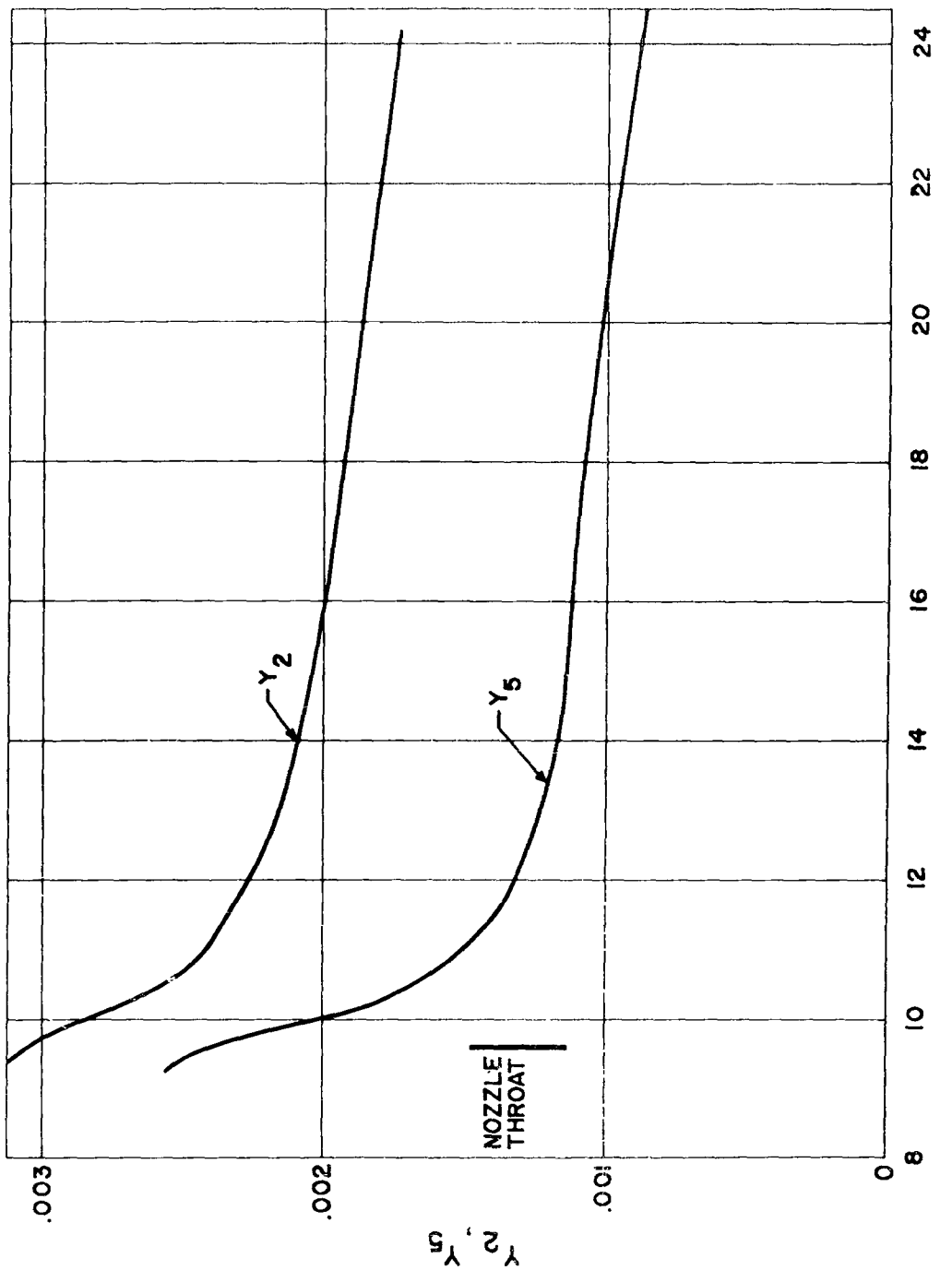

FIG. II-7b. Distribution of Mass Fraction Along the Axis in Nozzle Flow.

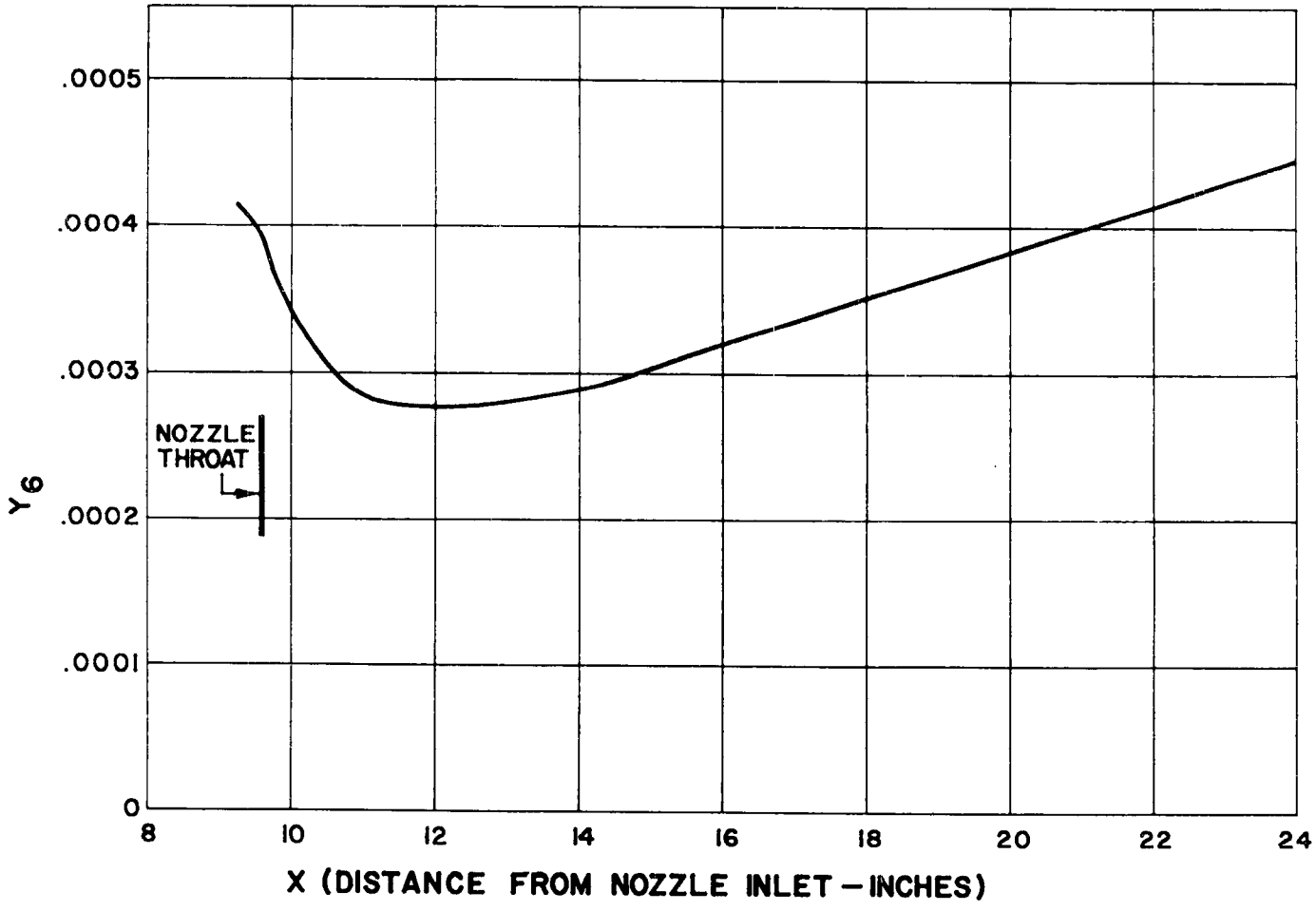

FIG. II-7c. Distribution of Mass Fraction Along the Axis in Nozzle Flow.

For such conditions the analysis of the diffusion and combustion process along a given streamline can be divided into two parts: a mixing region where transport properties are important, and a combustion region where large variation of state occurs, but where viscous effects can be neglected. In general, both processes occur with pressure variations.

9. APPLICATION OF INVISCID ANALYSIS TO COMBUSTOR DESIGN

It is of interest to consider the application of the streamline analysis discussed above to actual combustor design. The objective herein is to indicate how shock waves, which could be associated with heat release, can be avoided by proper design of the combustor, i.e., by expanding the flow area in a manner compatible with the progress of combustion. For this purpose a constant pressure flow will be discussed although similar considerations apply to the more general case of pressure varying along the streamline.

Consider a premixed hydrogen-air mixture corresponding to an equivalence ratio of unity, with a constant pressure of 4.7 atmospheres, a uniform velocity of 11,000 ft/sec., and an initial temperature of 1240°K. Then the numerical integration for the reaction history as discussed above can be employed to compute inter alia the spatial distribution of mass density which can be used to compute the distribution of the area ratio ($A \sim \rho^{-1}$) required to maintain constant pressure flow. The area ratio A/A_o where A_o is an arbitrary flow area at $x = 0$ is shown in Figure II-8; it will be seen that there is a relatively small region in which the density decreases rapidly and in which the flow area must increase if constant pressure is to be maintained. The total increase in cross sectional area is 2.15 Note that if a different analysis, one based on constant a ea were employed, a significant pressure rise and velocity decrease would occur in the region of rapid heat release; this is hown e g . in reference II-7.

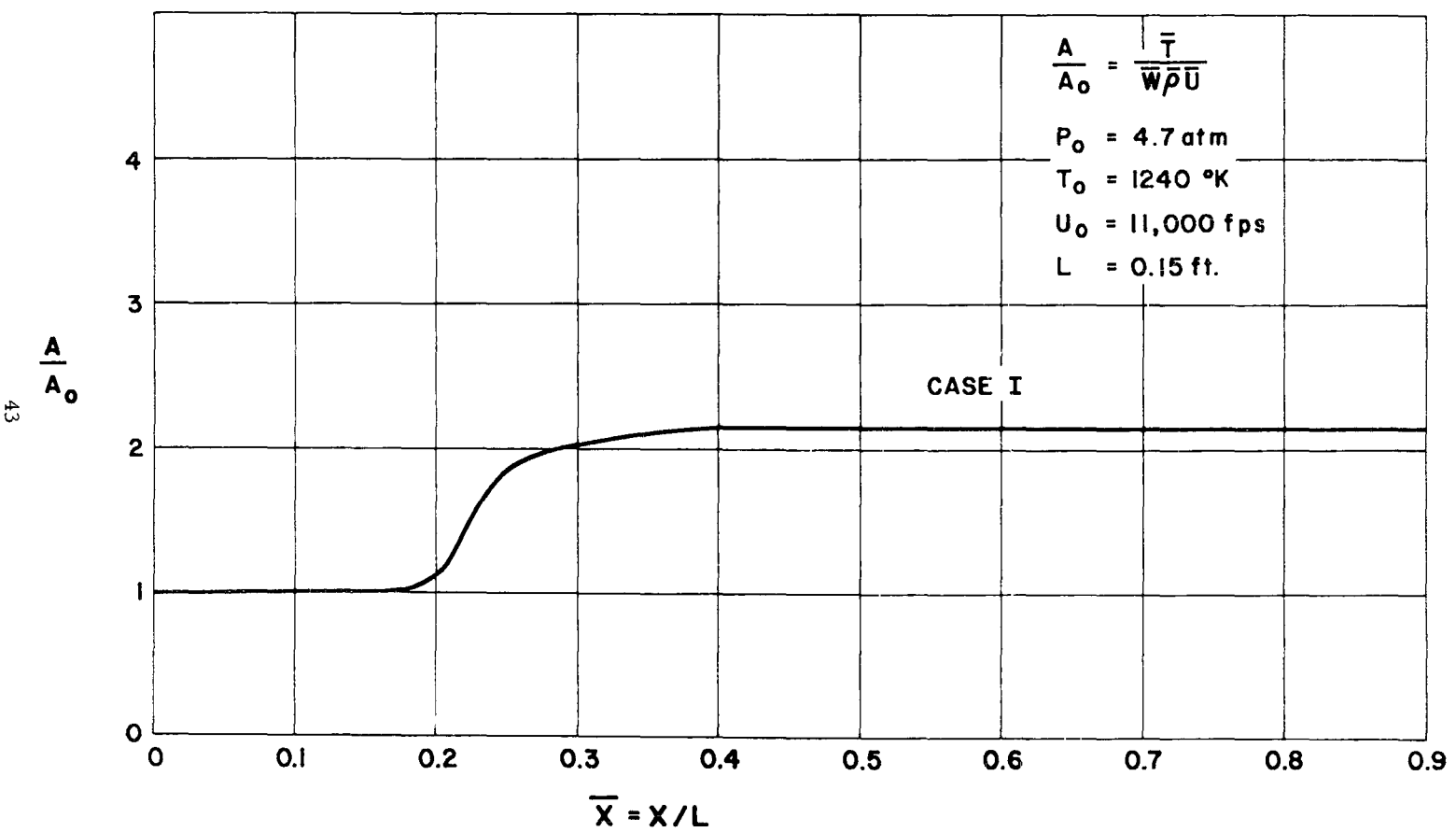

FIG. II-8. Distribution of Flow Area for Constant Pressure Combustion.

Now consider Figure II-9 which indicates how this result can be employed qualitatively in the design of a practical two-dimensional combustor. Assume that the total inlet flow area is divided into streamtubes and that the mixing between hydrogen and air is controlled; in particular, assume that the hydrogen can be distributed by mixing non-uniformly across the inlet to the combustor as would be the case if a "swept" injector were provided. Now select the length AB to correspond to the length in which no significant change in area ratio is required; at B turn the flow by an angle α so that at C the original streamtube has increased in area by a factor of 2.15, where the length AC corresponds to the length obtained from Figure II-8, beyond which the area is again essentially constant. Note that $\alpha \simeq 1.15\ (d/\Delta_x)$ where d is the original streamtube height and Δ_x is the length over which the change in cross-sectional area is effectively required. Now for the second streamtube assume that the origin for the chemical history is shifted by the amount BC so that its required increase in cross-sectional area occurs downstream of point C and is complete in the length $\Delta_x = B'C' = BC$. If this process is carried out for each streamtube, there will be obtained the duct configuration which is shown in Figure II-9 and which involves a final cross-sectional area 2.15 times greater than the original one. It will be recognized that this treatment corresponds to a rough streamtube analysis for a combustor. This analysis can be improved and refined by a two-dimensional treatment of the flow field with finite rate chemistry. An analysis thereof is discussed in the following subsection.

10. METHOD OF CHARACTERISTICS FOR TWO-DIMENSIONAL FLOWS

Consider now the analysis by the method of characteristics of two-dimensional supersonic flows with finite rate chemistry.* It will

*The method of characteristics for non-equilibrium gas flows corresponding to either dissociation or vibrational relaxation has been treated in references II-20 to II-23. The analysis here is more general.

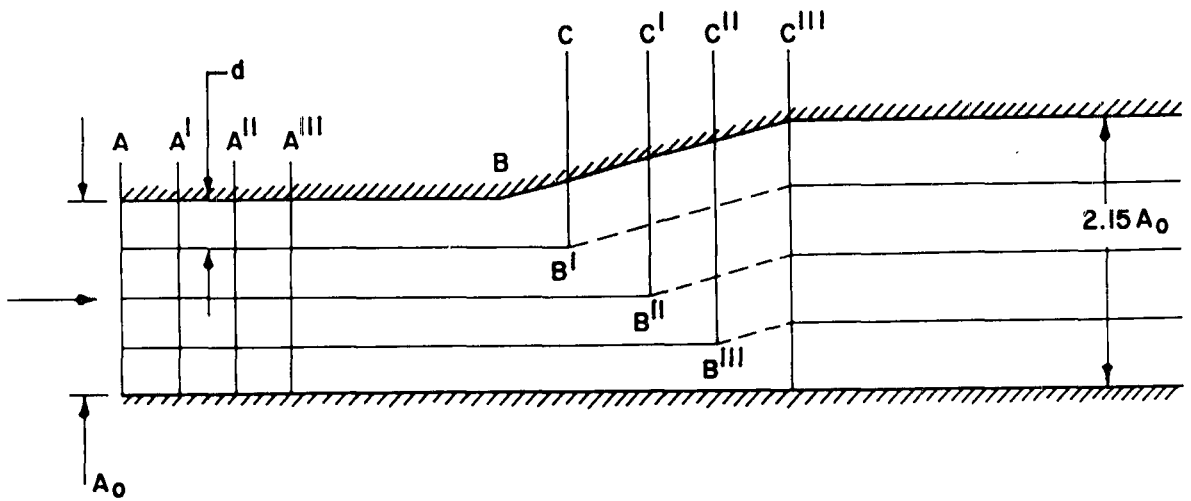

FIG. II-9. Schematic Representation of a Constant Pressure Combustion.

be shown that the streamline analysis forms an integral part of such a method. Although for practical reasons, two-dimensional flow is considered explicitly herein, the extension to the axisymmetric case is straightforward. For completeness some of the equations of Section II-2 are repeated here.

The equations of motion in coordinates along a streamline s and in the normal direction n are

$$\rho V \frac{\partial V}{\partial x} + \frac{\partial p}{\partial s} = 0 \qquad \text{(II-10.1)}$$

$$\rho V^2 \frac{\partial \theta}{\partial s} + \frac{\partial p}{\partial n} = 0 \qquad \text{(II-10.2)}$$

The equations of species conservation are

$$\rho V \frac{\partial Y_i}{\partial s} = \dot{w}_i \qquad \text{(II-10.3)}$$

and the overall continuity equation for two-dimensional flows is

$$\frac{\partial}{\partial s}(\rho V) + \rho V \frac{\partial \theta}{\partial n} = 0 \qquad \text{(II-10.4)}$$

These equations are supplemented by the requirements of energy conservation [Eq. (II-2.2)]; by the equation of state [Eq. (II-2.5)]; by the description of the creation terms [Eqs. (II-2.6) and (II-2.7)]; and finally by the enthalpy-temperature relation for the species.

Now following the usual procedure in the method of characteristics (cf. e.g., references II-24 and -25), Eqs. (II-2.2) and (II-2.5) are differentiated with respect to s; the resulting equations and Eqs. (II-10.1) and (II-10.4) can be used to obtain

$$\frac{1}{p}\frac{\partial p}{\partial s}\left[\left(1-\frac{R_o}{c_p W}\right)-\frac{R_o T}{V^2 W}\right]+\frac{\partial\theta}{\partial n}=\frac{W}{\rho V}\sum_{i=1}^{N}\frac{\dot{w}_i}{W_i}\left(1-\frac{h_i W_i}{c_p T W}\right)\equiv F \tag{II-10.5}$$

which involves only the partial derivatives $\partial p/\partial s$ and $\partial\theta/\partial n$ and finite quantities. As usual there are considered the total differentials

$$\frac{1}{p}\frac{dp}{ds}=\frac{1}{p}\frac{\partial p}{\partial s}+\frac{1}{p}\frac{\partial p}{\partial n}\left(\frac{dn}{ds}\right) \tag{II-10.6}$$

$$\frac{d\theta}{ds}=\frac{\partial\theta}{\partial s}+\frac{\partial\theta}{\partial n}\left(\frac{dn}{ds}\right) \tag{II-10.7}$$

The Eqs. (II-10.2) and (II-10.5)-(II-10.7) are formally considered to yield the four partial derivatives in terms of finite quantities and of $d \ln p/ds$, $d\theta/ds$ and dn/ds. Select dn/ds so that the determinant of these equations vanishes; there are obtained two values of dn/ds; namely,

$$\frac{dn}{ds}=\pm\left[\frac{V^2}{T}\frac{W}{R_o}\left(1-\frac{R_o}{W c_p}\right)-1\right]^{-\frac{1}{2}} \tag{II-10.8}$$

The condition for dn/ds to be real is evident. Moreover, the degeneration of this relation to the special case usually treated in gas dynamics, i.e., constant composition and constant specific heats is also evident. Finally, it is interesting to note that the speed of sound, which arises quite naturally from the analysis, is associated with frozen composition and frozen vibrational energy; namely,

$$a_f^2=(RT/W)\left[1-(R/c_p W)\right] \tag{II-10.9}$$

Additional restrictive assumptions must be made a priori in order that there enter the analysis other limiting speeds of sound, i.e., those associated with equilibrium behavior in some sense.

Denote the values of dn/ds corresponding to the plus and minus signs by $(dn/ds)_I$ and $(dn/ds)_{II}$, respectively; introduce μ_I and μ_{II} where

$$\tan \mu_I = (dn/ds)_I$$
$$\tan \mu_{II} = (dn/ds)_{II} \qquad \text{(II-10.10)}$$

The vanishing of the determinant leading to the special values of dn/ds implies along the line $(dn/ds)_I$ that

$$\frac{1}{p}\frac{dp}{d\xi} + \left[\frac{V^2W}{RT}\left(\frac{dn}{ds}_I\right)\right]\frac{d\theta}{d\xi} = \left(\frac{V^2W}{RT}\right)\left[\left(\frac{dn}{ds}\right)_I\right]^2\left\{1+\left[\left(\frac{dn}{ds}\right)_I\right]^2\right\}^{-\frac{1}{2}} F$$
$$= \left(\frac{V^2W}{RT}\right) F \frac{\sin^2\mu_I}{\cos^3\mu_I} \qquad \text{(II-10.11)}$$

and along the line $(dn/ds)_{II}$ that

$$\frac{1}{p}\frac{dp}{dn} + \left[\frac{V^2W}{RT}\left(\frac{dn}{ds}_{II}\right)\right]\frac{d\theta}{dn} = \left(\frac{V^2W}{RT}\right)\left[\left(\frac{dn}{ds}\right)_{II}\right]^2\left\{1+\left[\left(\frac{dn}{ds}\right)_{II}\right]^2\right\}^{-\frac{1}{2}}$$
$$= \frac{V^2W}{RT} F \frac{\sin^2\mu_{II}}{\cos^3\mu_{II}} \qquad \text{(II-10.12)}$$

where $d\xi$ and dn are differential elements along each characteristic line. In the nonreactive case $F \equiv 0$ so that Eq. (II-10.11) and (II-10.12) reduce to those usually prevailing in gas dynamics. The right-hand sides of Eqs. (II-10.11) and (II-10.12) are equivalent to the terms which arise due to rotationality. In addition to the two characteristic lines related to μ_I and μ_{II} the streamlines are also characteristics along which the reaction equations must be applied.

The application of these equations to a unit problem within the flow field as shown in Figure II-10 follows the chemical numerical procedure. Assume that at two adjacent points 1 and 2 all the flow and state variables are known. Then from Eqs. (II-10.11) and (II-10.12) in the usual way two finite difference equations for p_3 and θ_3 can be established provided the finite quantities in these equations are evaluated from conditions at points 2 and 1 respectively. Thus the location of, and the values of p and θ at point 3 can be found to a first approximation. Now construct point 4 on the streamline inclined at θ_3 passing through point 3 and at θ_4 passing through 4 where linear interpolation between θ_2 and θ_1 is assumed; further, by linear interpolation estimate V, p and Y_i, $i = 1, 2 \ldots N-1$ at point 4. Thus, if the pressure is assumed to vary linearly from points 4 to point 3, these estimates plus the energy equation permits the conservation Eqs. (II-10.1) and (II-10.3), and the supplemental equations relative to the state, kinetics and species enthalpy-temperature to be integrated along s to yield the composition at point 3 in the same fashion as in the usual streamline calculations described above. Iteration can also be used if required.

It is pointed out that the procedure outlined here assumes that requirements for accuracy in integration for the species conservation equations along the streamline are more severe than the requirements for accuracy in the flow variables p, θ, V, etc. If this is not the case, then finite difference approximations for integration along the streamline from point 4 can be readily employed.

In addition to the unit problem for the flow field, special unit problems for points involving shock wave and for boundary points must be established. For the flow across shock fronts use of the von Newman-Doring-Zeldovitch jump conditions would be consistent with the inviscid flow assumption. No special difficulty with respect to these special unit problems would appear likely in principle but as in the method of characteristics for classical gas dynamics, difficulties associated with secondary shocks, numerical accuracy, programming logic, etc. are

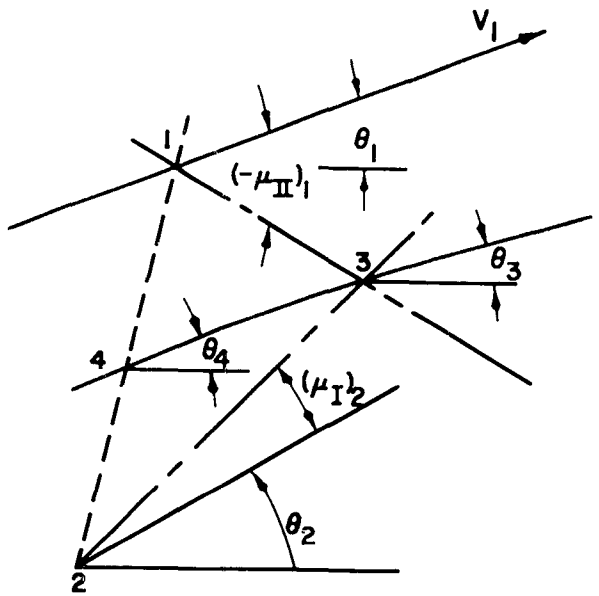

FIG. II-10. Unit Problem for Method of Characteristics.

certain to arise and to require solution. An analysis employing the method of characteristics with finite rate chemistry along the lines described here will be valuable in combustor and exhaust nozzle design and analysis.

It is interesting to note that the effects of viscosity, diffusion and heat conduction normal to the streamlines can be incorporated in the above analysis in an approximate manner, if these effects are slowly varying with respect to combustion processes. For example, in the species conservation equations the effect of diffusion normal to the streamlines is to add an additional term $\partial/\partial n(\rho D \partial Y_i/\partial n)$; an average value thereof for the increment along the streamline from point 4 to point 3 can be evaluated in finite difference form from a knowledge of the state at points 1, 2, and 4. Similarly, the energy equation, which in this case must be treated in differential form, will have an additional term arising from energy transport due to conduction and to diffusion and a dissipation term due to viscosity; again a finite difference representation can be employed. Finally, the viscosity contribution to the streamwise momentum equation can be taken into account. For laminar flow the transport coefficients are clearly defined while as is well-known for turbulent flow effective exchange coefficients must be introduced.

SECTION III

HETEROGENEOUS TURBULENT MIXING

It appears that under flight conditions for hypersonic vehicles of practical sizes, the mixing process between the fuel jet and the air stream will be predominantly turbulent. Accordingly, the present discussion of the mixing problems connected with supersonic diffusion flames will be exclusively devoted to turbulent flows. It will be realized

that at the origin of mixing there will always exist on the fuel injector, boundary layers, one in air and one in the hydrogen fuel; in considering only turbulent processes, it is assumed that either one of these boundary layers is turbulent at the origin of mixing or that transition from laminar to turbulent flow occurs in a negligibly short distance downstream from the origin of mixing.

1. GENERAL REMARKS

The mixing processes in supersonic diffusion flames play an important role in determining the characteristics of a combustor, since the fuel and oxidizer must be brought together by mixing prior to chemical reaction. As mentioned in the Introduction the relative rates of the mixing and of the chemical processes taking place simultaneously in the fuel jet determine the characteristics of the flow; if the chemical reactions are relatively fast, i.e., for the hydrogen-air system of interest herein, if the initial static temperatures and the static pressures are high, then diffusion will be rate controlling. In a limiting sense under these conditions the behavior corresponds to local chemical equilibrium and heat release occurs close to the exit of the fuel injector. If on the contrary, the chemical reaction is relatively slow, the mixing of the fuel and air close to the exit will correspond to a heterogeneous, non-reactive jet; far downstream the fuel and oxidizer will be completely mixed and if conditions are suitable will react in an essentially inviscid manner. This second case in a limiting sense corresponds to "frozen" mixing.

The two limiting cases of equilibrium and frozen chemical behavior are the easiest to treat analytically so that most analyses of viscous reacting flows have considered only such cases. However, for combustor design it is necessary to determine quantitatively the conditions under which the two limiting cases prevail and the characteristics of flows intermediate to the limiting cases, i.e., of flows with finite rate chemistry. In the analysis of mixing with chemical reactions the

interaction between mixing, combustion and boundary conditions introduces severe complications. The combustion process locally effects temperature density and pressure of the flow. If the flow is supersonic pressure variations propagate in the flow through a wave mechanism, and local changes of static pressure can influence reaction rates and mixing rates elsewhere in the flow. These coupling effects can be important in practical applications. In the case of supersonic diffusion flames the mixing process is the controlling mechanism and a strong increase in pressure must be avoided by careful selection of the boundary conditions. Therefore it appears logical to analyze in the first step mixing problems where the pressure can be assumed to be practically constant through the entire flow field.

Even in the case of a constant pressure process complications are introduced by several effects; e.g., by the details of the flow at the origin of mixing; in the boundary layer on the air side of the fuel injector there will exist regions of low velocity and high static temperature because of aerodynamic heating. Now it is known from analyses such as those presented in the previous section that the reaction history for hydrogen-air mixtures is sensitive to initial temperature as well as to static pressure. Thus the chemical times and lengths associated with the static temperatures and velocities near the exit of the fuel jet may actually be several orders of magnitude smaller than those based on the static temperatures and velocities in the streams external to the viscous region. If this is the case, reaction may initiate close to the fuel jet and spread rapidly so as to cause extensive amounts of heat release in flow distances shorter than those expected on the basis of the usual overall considerations of diffusion and chemical times for idealized conditions.

In addition to the effect of initial boundary layers the conditions under which limiting chemical behavior can be expected, are complicated by the wide range of flow velocities which can occur in supersonic diffusion flames of practical interest. For example, consider the

case wherein the fuel jet has a small velocity compared to that in the external stream. In this case chemical reaction may first appear near the axis of symmetry, where the lowest velocities occur, and may spread rapidly outward in constrast to the previous discussion.

The problem of treating analytically the simultaneous effects of turbulent mixing and finite rate chemistry is formidable if some realism is desired. The preliminary research reported here considers first the turbulent mixing of heterogeneous gas streams. Both theoretical and experimental research will be described. In addition some remarks concerning the chemical kinetics of turbulent reacting flows will be made to indicate an essential difficulty in proceeding to the analysis of practically interesting cases wherein the effects of finite rate chemistry are important; clearly these cases are the intermediate ones cited above.

The problem of describing quantitatively turbulent shear flows has occupied the attention of fluid mechanicians for many years. It is generally agreed that even for the simplest case of incompressible flow the available knowledge is incomplete. With respect to turbulent shear flows involving significant gradients of density the present state of knowledge is poor. In view of this situation research directed toward establishing some of the engineering fundamentals of turbulent mixing of heterogeneous gases has been undertaken at PIBAL and at GASL. The flow configuration has been idealized in both theory and experiment to correspond to an axisymmetric fuel injection in an essentially infinite oxidizing stream. In a practical combustor the presence of walls, of other asymmetries and of non-uniformities in the oxidizing stream, e.g, due to gradients in stagnation pressure, will complicate the flow so that only a general but essential understanding of the phenomena can be expected from the study of idealized configurations such as are considered herein.

2. THEORETICAL ANALYSIS - GENERAL EQUATIONS

Consider first an engineering analysis of a turbulent jet of a fuel such as hydrogen in an air stream; assume that the mean turbulent quantities are described by the equations for laminar flow if the transport coefficients replace their molecular counterparts. Then (cf. references III-1 and -2) for constant pressure flows the following conservation equations are obtained:

Conservation of Momentum

$$\rho u \frac{\partial u}{\partial x} + \rho v \frac{\partial u}{\partial r} = r^{-1} \frac{\partial}{\partial r} (\epsilon \rho r \frac{\partial u}{\partial r}) \qquad \text{(III-2.1)}$$

Conservation of Energy

$$\rho u \frac{\partial H}{\partial x} + \rho v \frac{\partial H}{\partial r} = r^{-1} \frac{\partial}{\partial r} [(\rho \epsilon p_t^{-1} r \frac{\partial H}{\partial r}) + (p_t - 1) \rho \epsilon p_t^{-1} ru \frac{\partial u}{\partial r} + (S_t - 1) \rho \epsilon p_t^{-1} \sum_{i=1}^{N} h_i \frac{\partial Y_i}{\partial r}] \qquad \text{(III-2.2)}$$

Global Conservation of Mass

$$\frac{\partial}{\partial x} (\rho u) + r^{-1} \frac{\partial}{\partial r} (\rho v r) = 0 \qquad \text{(III-2.3)}$$

Species Conservation

$$\rho u \frac{\partial Y_i}{\partial x} + \rho v \frac{\partial Y_i}{\partial r} = r^{-1} \frac{\partial}{\partial r} (\rho \epsilon S_t^{-1} r \frac{\partial Y_i}{\partial r}) + \dot{w}_i \qquad \text{(III-2.4)}$$

$$i = 1, 2. \text{ - N-L}$$

$$\rho u \frac{\partial \tilde{Y}_j}{\partial x} + \rho v \frac{\partial \tilde{Y}_j}{\partial r} = r^{-1} \frac{\partial}{\partial r} (\rho \epsilon S_t^{-1} r \frac{\partial \tilde{Y}_j}{\partial r}) \qquad \text{(III-2.5)}$$

$$j = 1, 2. \text{ -L}$$

Eqs. (III-2.1) through (III-2.5) are derived from the general equations of turbulent motion by introducing the concept of eddy viscosities that permits to determine the contribution of the fluctuating quantities of the flow as a function of the local gradients of the average properties. On this basis the transport properties due to the turbulent motion can be expressed in the same form as the transport properties due to the molecular motion. However, the coefficients of the terms that represent the molecular motion are functions only of local physical properties of the gas, while the coefficients related to the turbulent motion usually are related to gradients of physical properties of the gas. When the contribution due to molecular motion is small and can be neglected, then the eddy viscosities are the same for all the transport properties; this corresponds to the turbulent Prandtl and Schmidt number equal to unity. In the case that the contribution of the molecular transport is important and must be retained, then it is represented in the equations in an average form, by introducing correcting factors to the different transport properties. This is done by assuming that the turbulent Prandtl and Schmidt numbers are different from unity but constant at any given cross section of the flow. On the equations presented, a single turbulent diffusion coefficient D corresponding to a single turbulent Schmidt number $S_t = \frac{\epsilon}{D}$ has been used.

Fundamental to the application of these equations to the problem of a turbulent jet is a requirement to describe, at least approximately the compressible eddy viscosity ϵ. In the past theoretical analyses of turbulent compressible mixing (see references III-3 and -4) have carried over the Prandtl hypothesis generally accepted for incompressible flow; namely, that the eddy viscosity is essentially uniform across the mixing region and varies at most with the streamwise coordinate.

A different analysis for compressible mixing problems has been presented by the second author in reference III-1. In the analytical work presented here the approach presented in reference III-1 will be

followed and the same formal dependence of the eddy viscosity on spatial coordinates introduced in reference III-1 will be used. However, a different expression that relates the eddy viscosity to the physical properties of flow will be introduced. At the same time more general solutions will be obtained and simplifications will be presented. The results of such analyses will be compared with some experimental results.

3. ANALYSIS OF MIXING

Consider a jet of gas exhausting into an infinite stream, in general of foreign composition. Assume that the gases are nonreactive. Now following references III-1 and -5, introduce a stream function $\tilde{\psi}$ so that

$$\rho u r = \rho_j u_j \tilde{\psi} \frac{\partial \tilde{\psi}}{\partial r} \tag{III-3.1}$$

$$\rho v r = - \rho_j u_j \tilde{\psi} \frac{\partial \tilde{\psi}}{\partial x} \tag{III-3.2}$$

and employ the von Mises transformation, i.e., $(x, r) \rightarrow (x, \tilde{\psi})$ then Eq. (III-2.1) becomes without approximation

$$\frac{\partial u}{\partial x} = (u_j \tilde{\psi})^{-1} \frac{\partial}{\partial \tilde{\psi}} \left[\left(\frac{\varepsilon \rho^2 r^2 u}{\rho_j^2 u_j \tilde{\psi}^2} \right) \tilde{\psi} \frac{\partial u}{\partial \tilde{\psi}} \right] \tag{III-3.3}$$

where from Eq. (III-3.1)

$$r^2 = \int_0^{\tilde{\psi}} \left(\frac{2 \rho_j u_j}{\rho u} \right) \psi d\psi \tag{III-3.4}$$

and at the axis or at infinity $\frac{\partial (\rho u)}{\partial \psi} = 0$. Therefore near the axis

$$r^2 = \frac{\rho_j u_j}{\rho u} \tilde{\psi}^2 \qquad \text{(III-3.5)}$$

and

$$\frac{\epsilon \rho^2 r^2 u}{\rho_j^2 u_j \tilde{\psi}^2} = \epsilon\rho \simeq (\epsilon\rho)_c \qquad \text{(III-3.6)}$$

Assume $(\epsilon\rho)_c = f(x)$, then near the axis $\frac{\epsilon \rho^2 r^2 u}{\rho_j^2 u_j \tilde{\psi}^2} = f(x)$ and Eq. (III-3.3) becomes

$$\frac{\partial u}{\partial x} = \frac{(u_j)}{\psi} \frac{(\epsilon\rho)_c}{\rho_j} \frac{\partial}{\partial \tilde{\psi}} \left[\tilde{\psi} \frac{\partial u}{\partial \tilde{\psi}}\right] \qquad \text{(III-3.7)}$$

if $U = u/u_j$ and

$$\xi = \int_o^x \frac{(\epsilon\rho)_c}{\rho_j u_j a} dx \qquad \text{(III-3.8)}$$

then

$$\frac{\partial U}{\partial \xi} = \frac{a}{\tilde{\psi}} \frac{\partial}{\partial \tilde{\psi}} \left(\tilde{\psi} \frac{\partial U}{\partial \tilde{\psi}}\right) \qquad \text{(III-3.9)}$$

The expression (III-3.6) is accurate near and far away from the axis, and is only an approximate expression moving away from the axis. The error introduced is due to the fact that terms of the order $\left(\frac{\partial^2 (\rho u)}{\partial \tilde{\psi}^2}\right) \tilde{\psi}^2$ are neglected with respect to one in Eq. (III-3.5). Indeed

$$\rho u = (\rho u)_c \left[1 + \frac{1}{4} \frac{1}{(\rho u)_c} \left(\frac{\partial^2 (\rho u)}{\partial \tilde{\psi}^2}\right)_c \tilde{\psi}^2 + \cdots\right] \qquad \text{(III-3.10)}$$

Then, if the second term is neglected in Eq. (III-3.5), Eq. (III-3.6) gives

$$\epsilon\rho^2 ur^2 \sim (\epsilon\rho)_c \tilde{\psi}^2 = f(x)\,\tilde{\psi}^2 \qquad \text{(III-3.11)}$$

This expression leads to Eq. (III-3.9). The solution of Eq. (III-3.9) has been indicated in references III-1 and -5, and is independent of the energy equation.

4. EVALUATION OF THE EDDY VISCOSITY

In reference III-1 the suggestion has been made that the expression

$$\rho_c \overline{\epsilon} = k\,(u_{max} - u_{min})\,\rho_c (r_{\frac{1}{2}})_i$$

be used for definition of the eddy viscosity ϵ, where $(r_{\frac{1}{2}})_i$ is the width of the mixing zone in the incompressible plane wherein the velocity changes from u_{max} to $(u_{max} + u_c)\,\frac{1}{2}$. The value suggested for the constant k was 0.025 as given by Prandtl, then

$$\rho_c \overline{\epsilon} = 0.025\, u_e\, |1 - u_c|\, (r_{\frac{1}{2}})_{inc}\, \rho_e \qquad \text{(III-4.1)}$$

This expression indicates that the turbulence would decay when the two jets have the same velocities even if the two streams have different temperature or composition. This is not consistent with the fact that in these cases a dissipative mechanism still exists due to heat conduction or concentration changes that would sustain turbulence. It would also indicate that a sharp decrease of mixing rates would occur for $\frac{u_j}{u_e} \sim 1$ with rapid changes of mixing rates in both sides of the conditions $\frac{u_j}{u_e} \lesssim 1$. A modification of the expression for the eddy viscosity has been suggested by the first author in reference III-6. The expression used here has the form

$$\rho\epsilon = (\rho\epsilon)_c = k r_{\frac{1}{2}}\, |\rho_e u_e - \rho_c u_c| \qquad \text{(III-4.2)}$$

where k is the constant given by Prandtl and is assumed to be equal to 0.025. This expression still follows the basic concept of mixing length of Prandtl and the basic concept of reference III-1 with respect to the dependence of eddy viscosity on spacial coordinates. In this expression the quantity $r_{\frac{1}{2}}$ is the width of the mixing zone in the physical plane, defined as the value where the quantity ρu has an average value between the value at the axis and the value in the outside flow. Therefore

$$(\rho u)_{r_{\frac{1}{2}}} = (\rho_c u_c + \rho_e u_e)\,\frac{1}{2} \qquad \text{(III-4.3)}$$

It has been found that this expression is in better agreement with the experimental results presented here.

5. THE FREE JET IN A QUIESCENT ATMOSPHERE

Consider next the problem of free jet in a quiescent atmosphere. This problem is of interest because it has been investigated experimentally for a large variety of cases. Assume that the boundary layer at the origin of mixing ($x = \xi = 0$), is negligible. Then $U(\xi, \tilde{\psi})$ is to satisfy the conditions

$$\begin{aligned} U(0, \tilde{\psi}) &= 1 \qquad 0 < \tilde{\psi} < a \\ &= u_e/u_j \qquad \tilde{\psi} > a \\ \lim_{\tilde{\psi} \to \infty} U(\xi, \tilde{\psi}) &= u_e/u_j \end{aligned} \qquad \text{(III-5.1)}$$

The solution of the problem specified by Eqs. (III-3.11) and (III-5.1) is a standard one in the theory of heat conduction (cf. references III-7 and -8). The solution is given by the equation

$$\tilde{U} = \frac{[U-(u_e/u_j)]}{[1-(u_e/u_j)]} = (2\xi/a)^{-1} \exp[-\tilde{\psi}/a)^2/4(\xi/a)] \int_0^1 \exp[-r'^2/4(\xi/a)]$$

$$I_o[r'(\tilde{\psi}/a)(2\xi/a)^{-1}]r'\,dr' \qquad \text{(III-5.2)}$$

and has been tabulated by Masters[III-7] in terms of the function P^* where $\tilde{U} = P^*(Z/\gamma, R/\gamma)\tilde{U}_c$ with $Z/\gamma = (2\xi/a)^{-\frac{1}{2}}$, $R/\gamma = (\tilde{\psi}/a)(Z/\gamma)$. Of particular interest in the present discussion is the velocity decay along the axis in terms of ξ; there is obtained from the solution that

$$\tilde{U}_c = 1 - \exp(-a/4\xi) \qquad \text{(III-5.3)}$$

For the case $u_c = 0$,

$$(\epsilon\rho)_c - f(x) = k\rho_c u_c r_{\frac{1}{2}} \qquad \text{(III-5.4)}$$

$$(\rho u)_{r_{\frac{1}{2}}} = \frac{1}{2}\rho_c u_c \qquad \text{(III-5.5)}$$

Then the quantity $r_{\frac{1}{2}}$ is defined by

$$(r_{\frac{1}{2}})^2 = \left[\int_0^{\tilde{\psi}_{\frac{1}{2}}} \frac{2\rho_j u_j}{\rho u}\,\psi'\,d\psi'\right] \qquad \text{(III-5.6)}$$

Asymptotically ($\xi \to \infty$) this expression becomes equal to

$$r_{\frac{1}{2}} \longrightarrow \left(\frac{\rho_j}{\rho_e}\right)^{\frac{1}{2}} \xi \qquad \text{(III-5.7)}$$

The quantity u_c asymptotically becomes

$$u_c \longrightarrow \frac{u_j a}{\xi} \qquad \text{(III-5.8)}$$

and

$$[(\rho\epsilon)_c]_{as} = k \rho_e u_j a \left(\frac{\rho_j}{\rho_e}\right)^{\frac{1}{2}} = \text{constant} \qquad \text{(III-5.9)}$$

Mr. G. Kleinstein has found from the analysis of numerical and experimental data that the quantity $(\epsilon\rho)_c$ remains constant in a large zone of the mixing, and that the asymptotic expression can be used with good approximation also in the region of the flow near the exit of the jet. On the basis of this observation, the evaluation of Eq. (III-3.9) becomes very simple. If the quantity k is assumed to be the constant given by Prandtl, by introducing Eq. (III-5.9) in Eq. (III-3.10) it results

$$\frac{x}{a} = 40\left(\frac{\rho_j}{\rho_e}\right)^{\frac{1}{2}} \frac{\xi}{a} + \text{constant} \qquad \text{(III-5.10)}$$

Denote the constant in this equation as $\frac{x_i}{a}$, then Eq. (III-5.3) becomes

$$u_e = 1 - \exp\left\{-10\left[\frac{x}{a_e} + \frac{x_i}{a_e}\right]^{-1}\right\} \qquad \text{(III-5.11)}$$

where a_e is an effective area of the jet,

$$a_e = a\left(\frac{\rho_j}{\rho_e}\right)^{\frac{1}{2}} \qquad \text{(III-5.12)}$$

This result is in accord with the observation of Thring and Newby[III-9], that a homogeneous compressible jet has the same behavior as an incompressible one provided the actual jet radius a is replaced by an effective radius a_e.

The accuracy of this simple result can be assessed as follows: Consider experiments with $u_e = 0$ yielding the decay of center line velocity $u_c = u_c(x/a)$; compute from Eq. (III-5.3) for each u_c the value of ξ/a and compare the computed values with the measured values plotted in terms of $0.025(\rho_e/\rho_j)^{\frac{1}{2}}(x/a)$. This has been done in Figure III-1; there have been considered data for homogeneous, isothermal (i.e., incompressible) jets (references III-9, -10, -11, and -13), isothermal jets of carbon dioxide (reference III-13), heated homogeneous jets (reference III-11), and high speed homogeneous jets (reference III-10). A density range of $\frac{1}{2} \leq \rho_e/\rho_j \leq 2$ is represented by the data. With the single exception of the high Mach number data of Warren ($M_j = 2.60$) the correlation of the results is as good as can be expected It is noted that a similar discrepancy with respect to these data was found in reference III-1 and remains unexplained, but that for $M_j = 1.51$ the agreement is satisfactory herein.

The results of Figure III-1 imply that the constant in Eq. (III-5.10) is approximately -0.175 independently of the ratio ρ_e/ρ_j; thus the transformation from the ξ, $\tilde{\psi}$ plane to the x, $\tilde{\psi}$ plane is for this case of $u_e = 0$ simply

$$\frac{x}{a} = 40\left(\frac{\rho_j}{\rho_e}\right)^{\frac{1}{2}}\left[\frac{\xi}{a} + 0.175\right] \qquad \text{(III-5.13)}$$

Note that the final transformation from x, $\tilde{\psi}$ to x, r involves application of Eq. (III-3.4) and requires specification of the density distribution at least in terms of ξ and $\tilde{\psi}$.

In Figures III-2, -3, -4, and -5, some comparisons between measured and calculated quantities for the case of heterogeneous jets, investigated experimentally in reference III-13, are shown.

Figures III-2, -3, and -4 give the decay of velocity and concentration along the axis for nitrogen, carbon dioxide, and helium jets. In the case of helium jet the experimental velocity distribution shown

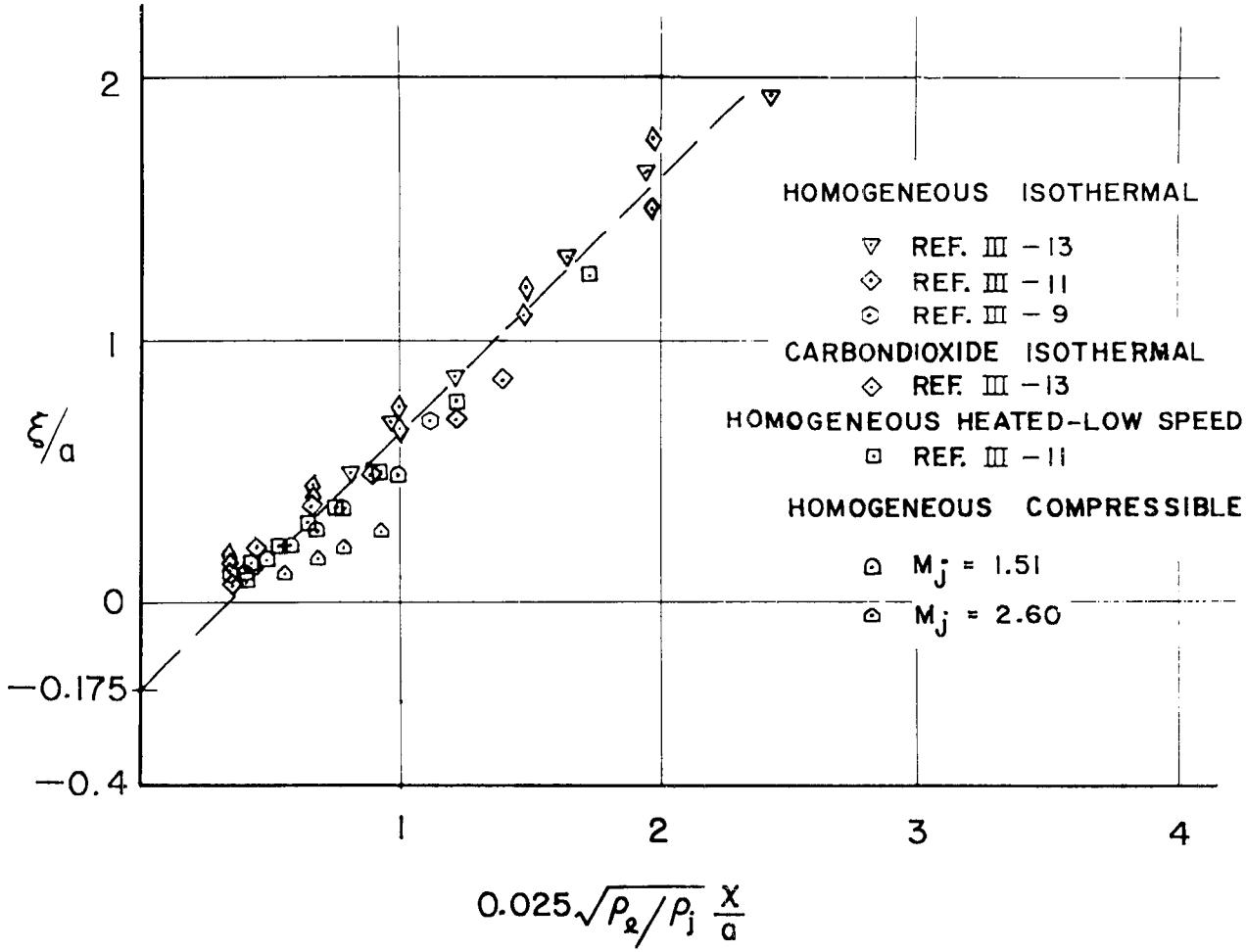

FIG. III-1. Relation Between ξ/a and x/a from Available Experimental Results and Comparison with the Relation Given by the Expression

$$\frac{d\xi}{dx} = 0.025\sqrt{\rho_e/\rho_j}$$

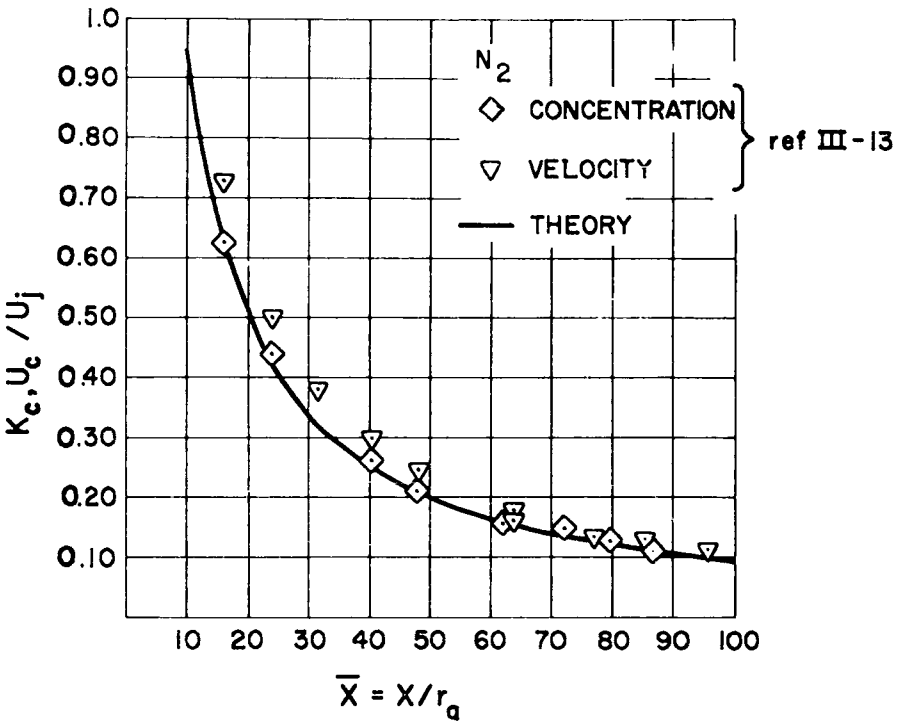

FIG. III-2. Comparison of Theoretical and Experimental Distributions of Center Line Velocity and Concentration for Nitrogen Jet.

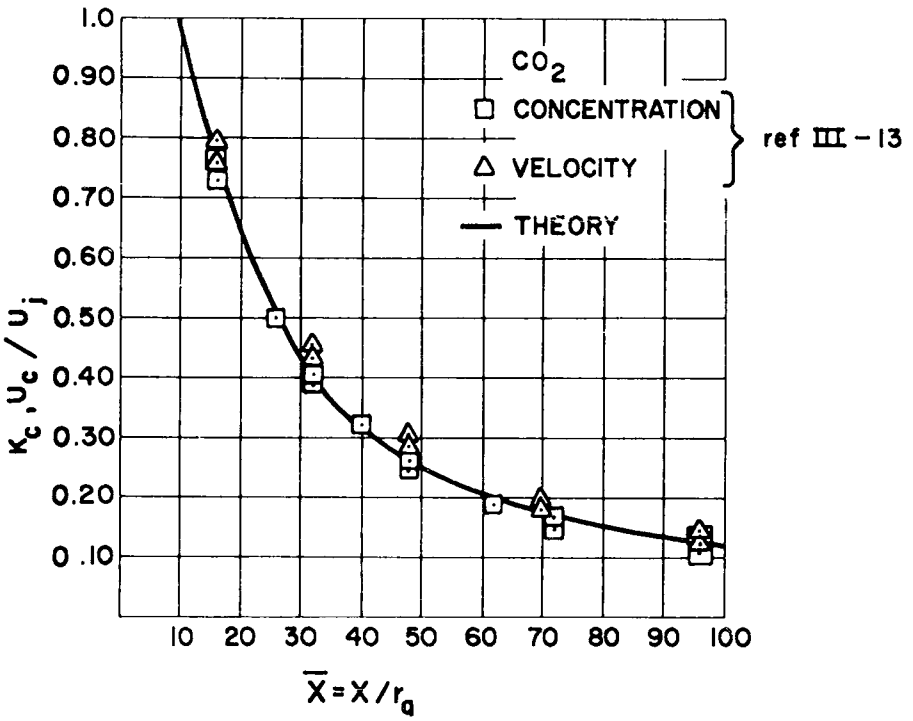

FIG. III-3. Comparison of Theoretical and Experimental Distributions of Center Line Velocity and Concentration for Carbon Dioxide Jet.

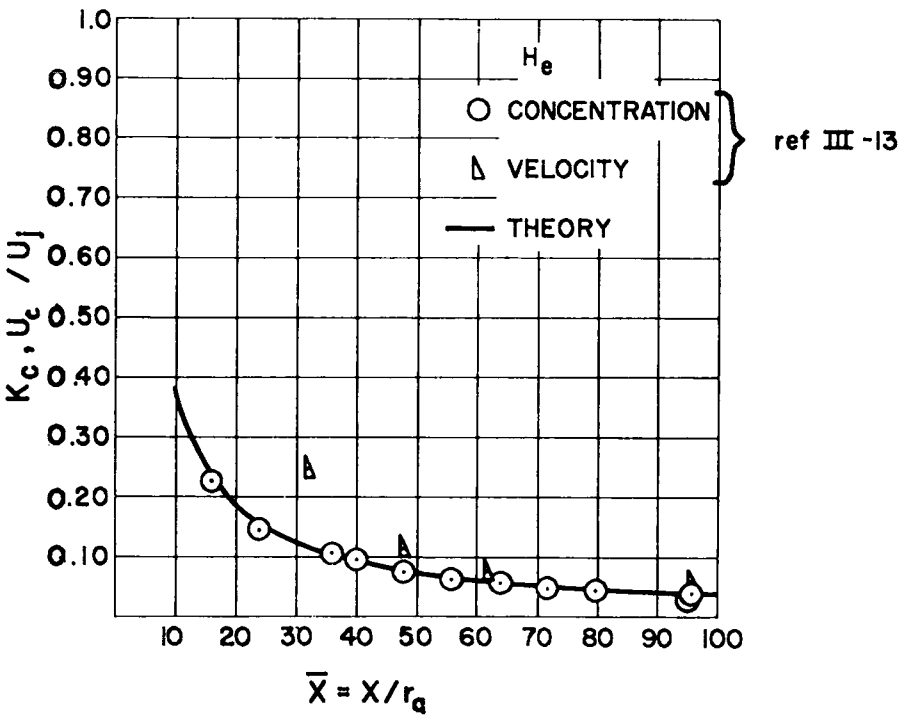

FIG. III-4. Comparison of Theoretical and Experimental Distributions of Center Line Velocity and Concentration for Helium Jet.

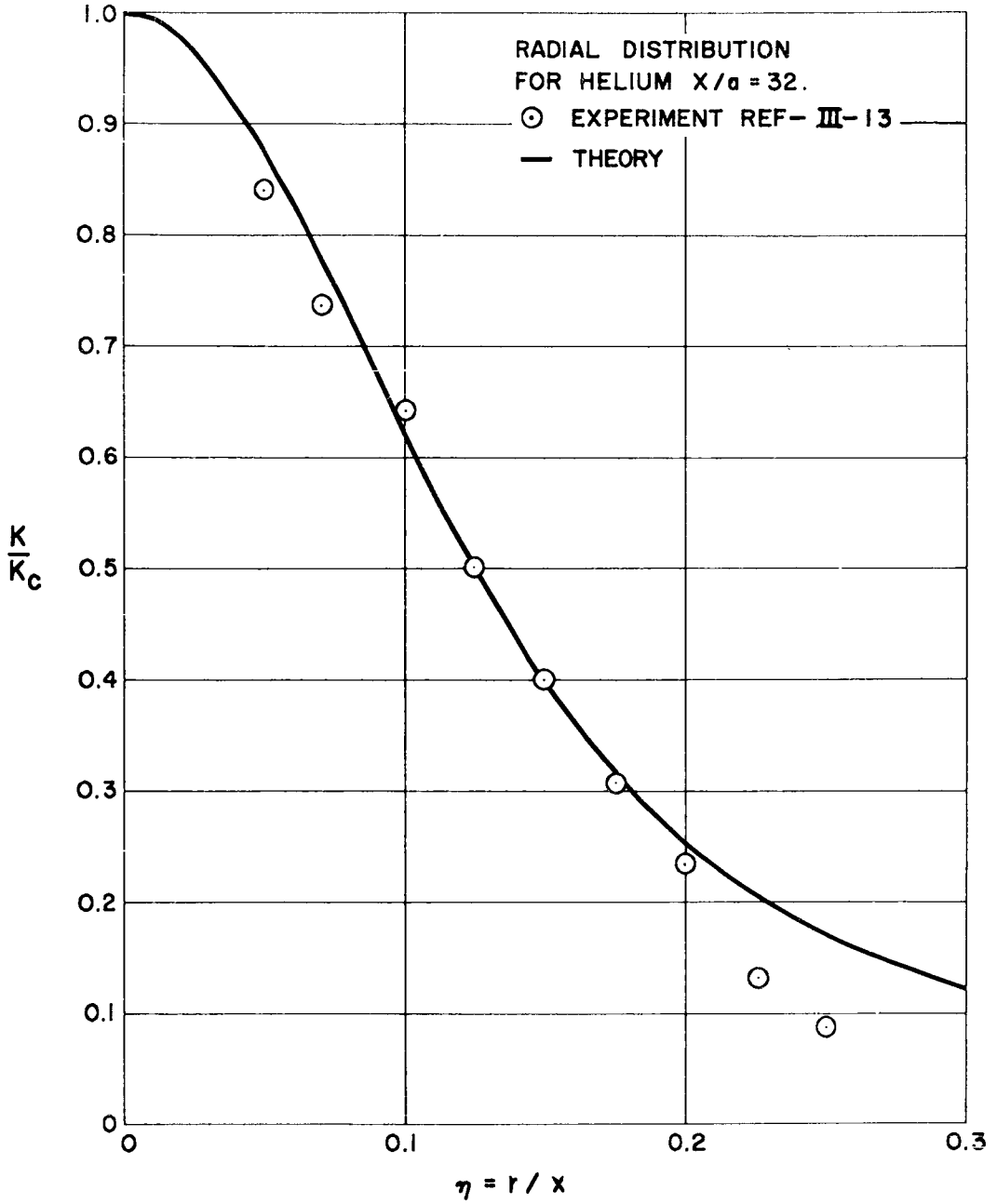

FIG. III-5. Comparison of Theoretical and Experimental Radial Distributions of Concentration for Helium Jet.

does not agree with the analytical value; however, it is stated in reference III-13 that "velocity data could not be obtained for the jet of helium because of the low impact pressures that it produced."

In Figure III-5, a radial profile distribution for the helium experiment is shown. The agreement with the analysis is good.

6. ANALYSIS OF MIXING FOR P_t AND S_t DIFFERENT FROM UNITY

In order to determine concentration and temperature distribution in the flow, Eqs. (III-2.4), (III-2.5), and (III-2.2) must be solved. These equations involve the turbulent Prandtl and Schmidt numbers.

If these numbers are unity, then for jet flows, generalized Crocco relations exist among the velocity stagnation enthalpy and element mass fractions so that the velocity distribution determines the entire flow. If the flow is nonreacting Eqs. (III-2.4) and (III-2.5) are identical, therefore, the same relations are valid also for species mass fractions.

In the case of jets discharging in quiescent atmosphere u_e is zero and if P_t and S_t are unity the ratio $\frac{u}{u_j}$ and K_{cj} (concentration of the constituent of the jet) are exactly the same.

For the case when P_t and S_t are different from unity, solutions of Eqs. (III-2.4) and (III-2.5) can still be carried over directly to obtain concentration and temperature provided P_t and S_t are constant or at most functions of the streamwise coordinate.

Consider a solution to Eq. (III-2.4) applied to one foreign species, i.e., for $Y_i \equiv K$ and for $\dot{w}_i \equiv 0$, i.e., for no chemical reaction. Application of the von Mises transformation and the previous considerations concerning ϵ leads with no further approximation to

$$\frac{\partial K}{\partial x} = \left(\frac{(\epsilon\rho)_c}{\rho_j}\right) \tilde{\psi}^{-1} \frac{\partial}{\partial \tilde{\psi}} \left(S_t^{-1} \tilde{\psi} \frac{\partial K}{\partial \tilde{\psi}}\right) \qquad \text{(III-6.1)}$$

Now the available data on turbulent Schmidt numbers, S_t, for a variety of mixtures indicates that an assumption of a constant value is therefore reasonable (cf. references III-12 and -14). Accordingly, for these jet flows assume S_t to be constant and introduce a new independent variable ξ_1 such that*

$$\xi_1 = S_t^{-1} \int_0^x \frac{(\epsilon\rho)_c}{\rho_j u_j} \frac{dx'}{a} = S_t^{-1} \xi \qquad \text{(III-6.2)}$$

Then Eq. (III-6.1) becomes

$$\frac{\partial K}{\partial \xi_1} = \frac{a}{\psi} \frac{\partial}{\partial \tilde{\psi}} \left(\tilde{\psi} \frac{\partial K}{\partial \tilde{\psi}}\right) \qquad \text{(III-6.3)}$$

Eq. (III-6.3) has the same form as Eq. (III-3.11). For a jet discharging in quiescent atmosphere

$$\begin{aligned} K(0, \tilde{\psi}) &= 1 \qquad 0 < \tilde{\psi} < a \\ &= 0 \qquad \tilde{\psi} > a \qquad \text{(III-6.4)} \\ \lim_{\tilde{\psi} \to \infty} K(\xi_1, \tilde{\psi}) &= 0 \end{aligned}$$

Then the solution for K is the same as that for $\tilde{U}$ given by Eqs. (III-5.2) and (III-5.3) provided ξ is replaced by $\xi_1 = S_t^{-1} \xi$; clearly if $S_t \simeq 1$, $K \simeq \tilde{U}$, i.e., a Crocco relation exists between velocity and concentration of foreign gas. The concentration along the axis is from the solution given by

*Note that with no difficulty S_t could be taken to be a function of x.

$$K_c = 1 - \exp[-S_t/4(\xi/a)] \qquad \text{(III-6.5)}$$

while from reference III-8 the concentration profiles are given as $K/K_c = P^*(Z'/\gamma, R'/\gamma)$, where $Z'/\gamma = (2\xi_1/a)^{-\frac{1}{2}}$, $R/\gamma = (\tilde{\psi}/a)Z'/\gamma$.

For isothermal, isobaric conditions ρW^{-1} = constant or more precisely

$$\rho/\rho_j = [K + (W_j/W_e)(1 - K)]^{-1} \qquad \text{(III-6.6)}$$

Thus from Eqs. (III-6.5) and (III-6.6) evaluated at the center line, Eq. (III-3.5) can be used to carry out the transformation back to the $x - \tilde{\psi}$ plane. Eq. (III-6.2) for $u_e = 0$ and the approximate relation

$$(\rho\epsilon)_c = 0.025\, u_j a \rho_e \left(\frac{\rho_j}{\rho_e}\right)^{\frac{1}{2}}$$

gives

$$\xi_1 = S_t^{-1}\left[0.025 \left(\frac{\rho_e}{\rho_j}\right)^{\frac{1}{2}} x - \text{constant}\right] \qquad \text{(III-6.7)}$$

Therefore, from experimental data of $K_c = K_c(\frac{x}{a})$ it is possible to determine experimentally the value of S_t. The results of these considerations, applied to the jets of helium and carbon dioxide of Figures III-3 and -4, indicate that in this case $S_t \sim 1$. Note that a change in density ratio $\frac{\rho_e}{\rho_j}$ of over an order of magnitude is represented here.

A similar analysis can be performed when the temperature of the jet is different from the temperature of the surrounding flow. In this case

$$\rho/\rho_j = T_j/T$$

so that the temperature field must be computed. For a constant

turbulent Prandtl number, not unity in general, the previous analysis for K can be carried through to yield the temperature field; the dependent variable becomes

$$\theta \equiv (T - T_e)(T_j - T_e)^{-1} \qquad \text{(III-6.9)}$$

while the independent variable becomes

$$\xi_2 \equiv \sigma_t^{-1} \int_0^x (\rho_e/\rho_j)(\bar{\epsilon}/u_j a)\, dx' = \sigma_t^{-1}\, \xi \qquad \text{(III-6.10)}$$

The solution with $\theta \equiv 1$ at $x = \xi_2 = 0$ is again given by Eqs. (III-5.2) and (III-5.3) provided ξ is replaced by ξ_2 and $\tilde{U}$ by θ.

7. EXPERIMENTS CONCERNING HETEROGENEOUS MIXING OF TWO MOVING STREAMS

In order to obtain fundamental data on the mixing processes involved when there is an external flow, a series of experiments concerning the axisymmetric mixing of hydrogen and air have been carried out by Mr. L. Alpinieri at PIBAL in a mixing rig utilizing the supersonic facility at PIBAL; the static temperatures were roughly ambient so that no chemical reaction occurred. Two sets of experiments were performed; in one a subsonic hydrogen jet exhausted into an axisymmetric stream of air with a Mach number of 3.0. The experimental setup is shown in Figure III-6. In the second a subsonic jet of hydrogen exhausted into a subsonic air stream; the experimental rig is shown in Figure III-7. In both sets of tests the distributions of static and total pressures and of hydrogen concentration throughout the mixing region were measured. The pressures were measured by standard techniques while the hydrogen concentration was measured by a thermal conductivity cell which was calibrated against known hydrogen-air mixtures. In the subsonic-supersonic tests the stagnation pressure of the air stream was 1.3 atmospheres. In both sets of tests the stagnation

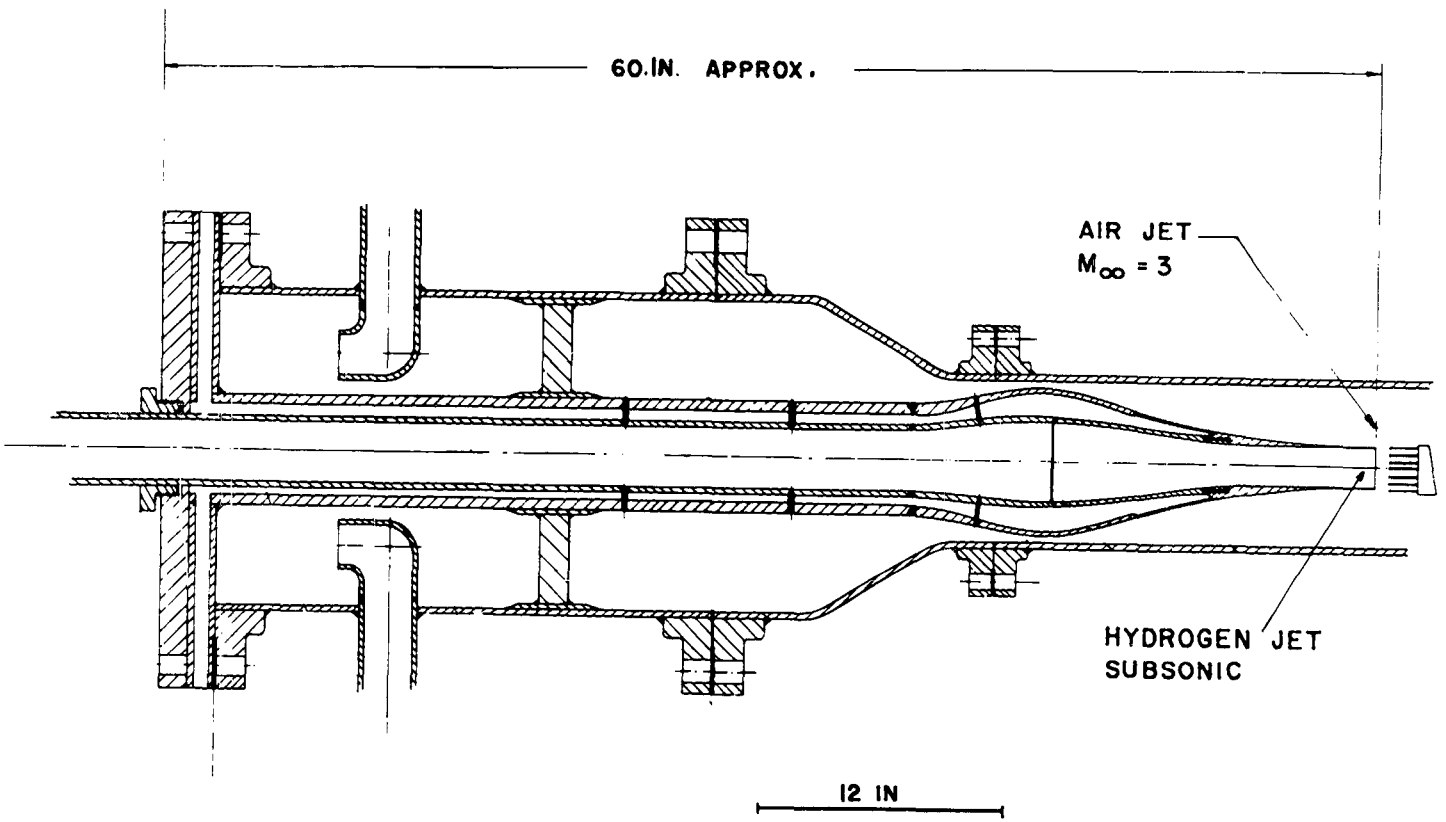

FIG. III-6. Experimental Apparatus for the Investigation of Subsonic-Supersonic Mixing.

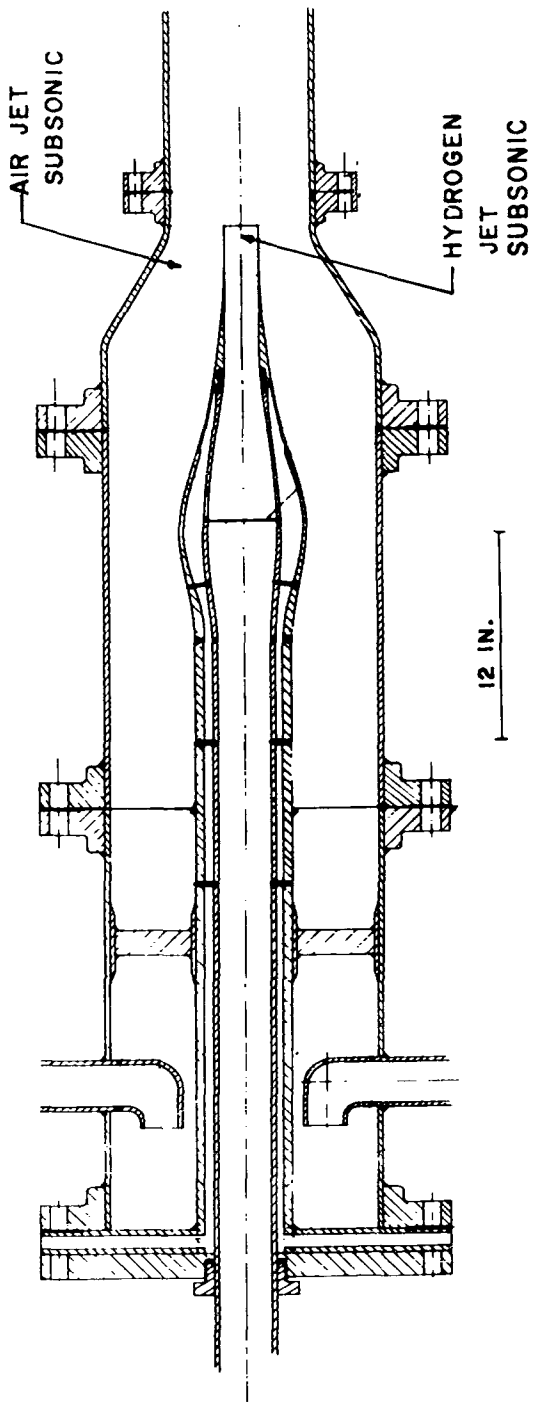

FIG. III-7. Experimental Apparatus for the Investigation of Subsonic-Subsonic Mixing.

temperatures of all streams was approximately 290°K. The experimental results and comparisons with theory will be given later in extenso; for the present only the results indicating some important points will be presented, i.e., those pertaining to the importance of initial boundary layers, to isovelocity mixing, and pressure gradients.

For this purpose consider first the distributions of concentration obtained in the subsonic-supersonic tests; shown in Figure III-8 is the distribution of mass fraction of hydrogen denoted K along the center line for four different values of the velocity ratio, $u_j/u_e \equiv U_j$. Shown in Figure III-9 are the radial distributions of K for the same velocity ratios and for two downstream stations $x/a = 13$ and 32.4. It will be noted first from these figures that the mixing of hydrogen and air is rapid, i.e., K_c drops to 0.1 with a distance corresponding to $x/a \lesssim 12$ for $u_j = 0.36\, u_e$. These results are qualitatively in agreement with the analysis discussed above. For a given u_e, as u_j increases from zero the theory predicts, at a given station $\frac{x}{a}$, an increase in K_c. For the form of the eddy viscosity proposed here the increase of K_c is gradual in the region of $u_j = u_e$, however no changes in sign of the variation of K_c with u_j is predicted. This is not true for the form of the eddy viscosity proposed in reference III-1, which would indicate an increase in K_c until $u_j = u_e$, and then a decrease of K_c for values of $u_j > u_e$.

A direct comparison between these experiments and analysis requires the development of analyses that takes into account the presence of the boundary layer on the air side at the origin of the mixing. These analyses can be derived approximately by extending the present analysis if the thickness of the boundary layer is not too large. The presence of the air boundary layer for the experiments involving mixing of air and hydrogen is very important, because the momentum flux in the air boundary layer is very large with respect to the momentum flux of the hydrogen stream, due to the low density of the hydrogen. In these experiments for the data presented here, the boundary layer is very

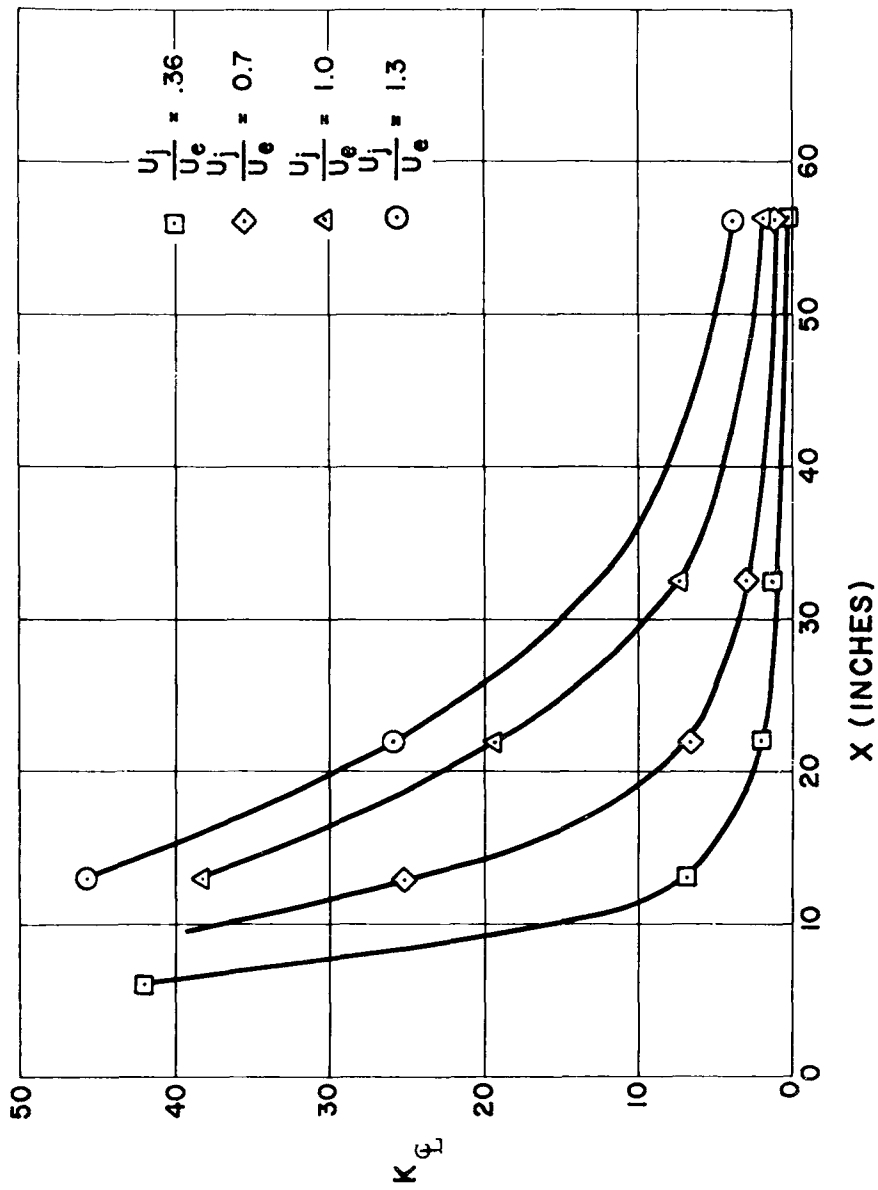

FIG. III-8. Distribution of Center Line Concentration for Various Velocity Ratios; Subsonic - Supersonic - Mixing.

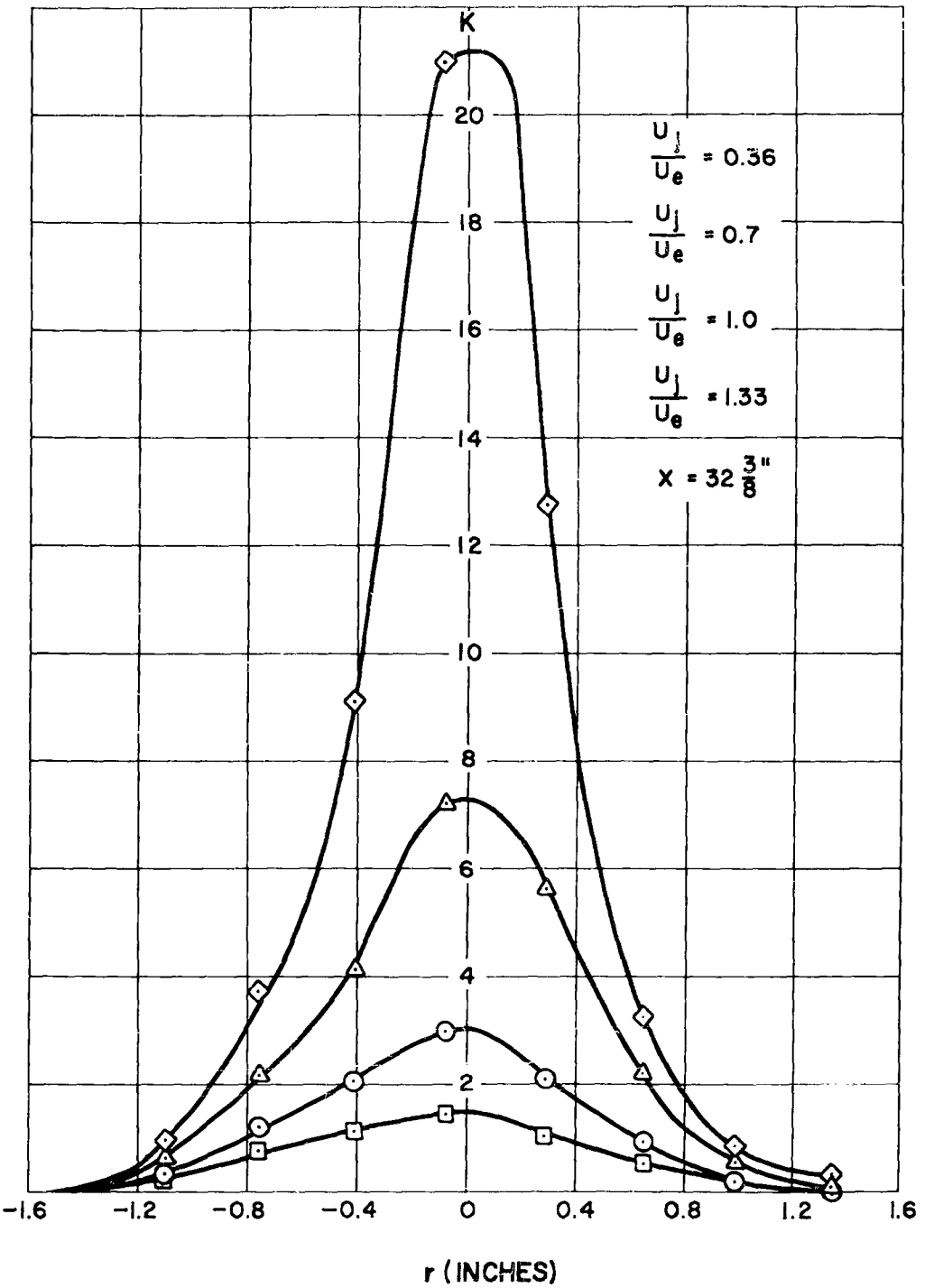

FIG. III-9. Radial Concentration Profiles for Various Velocity Ratios; Subsonic - Supersonic - Mixing x/a = 32.4

large, the thickness is of the order of one-half inch , therefore the momentum flux deficit in the boundary layer is larger than the momentum of the hydrogen. It is difficult to reach even qualitative conclusions from these experiments, and the results shown in Figures III-8 and -9 should not be interpreted in terms of step distributions of velocity at the origin of mixing. Indeed, it is of interest to note the following: The great density difference between hydrogen and air implies that the boundary layer in the air stream at the origin of mixing will generally play an important role in the mixing processes as well, as mentioned previously, in the chemical kinetics under practical conditions of interest in supersonic diffusion flames.

One of the main reasons for setting up the rig for subsonic-subsonic mixing was to reduce significantly the initial boundary layers. Indeed, the results of subsonic-subsonic mixing between hydrogen and air indicate that the qualitative agreement between theory and experiment is not due to the effects of the initial boundary layer. In this case the boundary layer in the air stream at the origin of mixing is thin; consequently, the effect of the initial boundary layers is negligible at a small distance downstream of the origin of the mixing region.

A comparison between experimental and analytical results for axial distributions of concentration of hydrogen for three ratios of jet to free stream velocities is presented in Figure III-10. In Figure III-11 a comparison of radial distributions for a velocity ratio $u_j/u_e = 1$ is shown for values of $x/R = 5$ and 10.5 .

The trend given by the analysis is in agreement with experiments. The concentration at any given station $x = \text{constant}$ increases gradually when u_j changes from 0.7 to 1.3 when the mixing extends to the axis. The concentration initially changes very rapidly with distance and then when small values of concentration are reached changes slowly with distance. Both results indicate that the mixing process is very rapid also for values of $\frac{u_j}{u_e} \sim 1$ and the shape of $\frac{\partial K}{\partial x}$ given by the analysis appear to be in agreement with experiments.

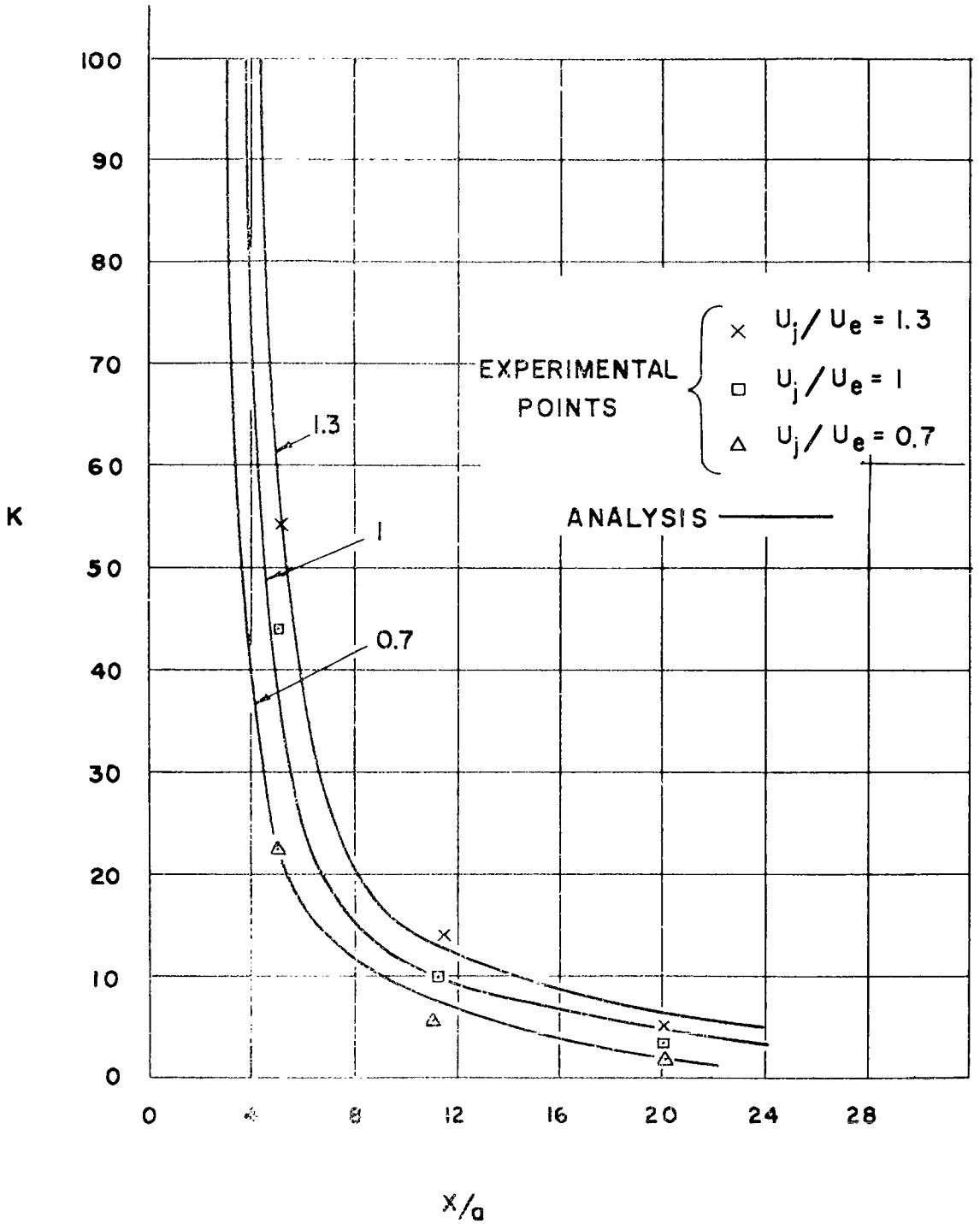

FIG. III-19 Comparison Between Experimental and Analytical Results for Axial Distributions of Concentration of Hydrogen

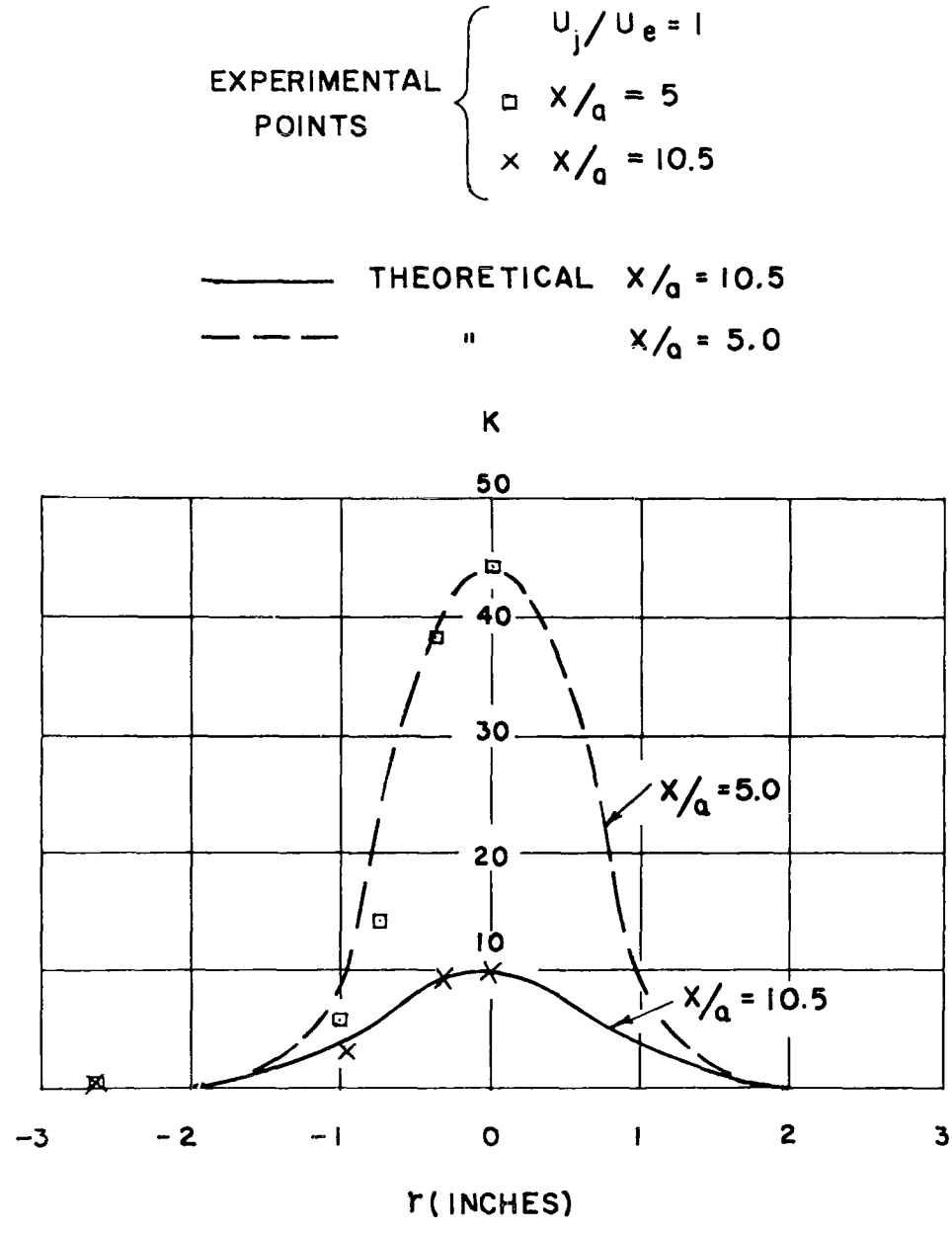

FIG. III-11. Comparison Between Experimental and Analytical Results for Radial Distributions of Concentration of Hydrogen

8. EFFECT OF TURBULENCE ON REACTION RATES

In order to establish properties of mixing, reacting flows, it is necessary to combine mixing analyses of the type described herein with descriptions of the chemical kinetics in turbulent flows. Formally, expressions for the creation terms $\dot{w}_i$ in the species conservation equations are required. It will be recalled that the equations employed here to investigate mixing are in terms of time-averaged quantities so that the desired descriptions are of the time-averaged mass rate of production of each species per unit volume per unit time. While the effect of turbulence in increasing the mixing of fuel and oxidizer is understood from a phenomenological point of view, the effect of turbulence on kinetics is not clear.

The effect of turbulence on the rate of flame propagation has been extensively studied but apparently the fundamentals of the effect are still subject to debate. In reference III-15, Hawthorne, Weddell, and Hottel considered the effect of turbulence to be described by an "unmixed factor" which indicates the degree of inhomogeniety of fuel and oxidizer; they considered, however, that the actual kinetic rates of chemical behavior were infinite so that fuel, oxidizer and products were in equilibrium locally with respect to space and time. Scientific investigation of the chemical kinetics of turbulent flows according to statistical theory has been initiated by turbulence specialists [cf. Corrsin[III-16, -17]] but the idealizations necessary for progress are so drastic as to provide little hope for application to chemical systems of practical interest in the near future.

It is the purpose of this discussion to indicate qualitatively the influence of turbulence on chemical kinetics. For this purpose it is useful to recall the basis for the rate constants employed in the analysis of Section II and shown explicitly in connection with Eqs. (II-3 1). These rate constants have been obtained by theoretical and/or experimental means under the cited assumption that thermodynamic equilibrium roughly prevails and thus that non-equilibrium prevails only with respect to chemical

composition. Therefore, it is assumed that equipartition of energy among particles and internal degrees of freedom exists at least approximately. Now in high speed turbulent flows these assumptions may be open to question; therefore, substituting classical rate expressions into the creation terms interpreted as instantaneous rates and the time averaging thereof in order to obtain time-averaged values for $\dot{w}_i$ may not be valid. However, it appears that the following statements can be made: If at a fixed point in the flow, the absolute velocity squared fluctuations which may arise from either velocity or temperature fluctuations are significant with respect to $2k\bar{T}/m_i$, then these fluctuations influence significantly the collision processes. This appears to be the case for mixing processes of very high velocity streams having very large ratio of static to total enthalpy. In this case the enthalpy connected with the fluctuating process is of the same order of the static enthalpy. Therefore the mechanism of collisions and the number of a given type of collision can be quite different from the values given by statistical mechanics on the basis of thermodynamic equilibrium. The effect of the turbulence on the mechanism of collision can be discussed qualitatively by considering a reaction step following an Arrhenius law. The turbulence effects the value of T on the exponent of the expression and the function of T which multiply the exponential function. Consider, for example, a reaction step following an Arrhenius law [reactions 1-4 to the right or to the left and reactions 5-8 to the left in Eqs. (II-3.1)]. The reaction rate in this case increases greatly with the relative velocity between colliding particles as evidenced by the exponential dependence of the rate constant on temperature. Therefore, it can be expected that a large fluctuation in the absolute velocity squared will increase the reaction rate for reaction steps following an Arrhenius law. On the other hand, for reactions such as reactions 5-8 in Eqs. (II-3.1) proceeding to the right where the rate constant does not have an exponential term it can be expected that turbulence would effect the reaction rates in the sense of increasing the probability of useful collisions. These

statements imply that all of the reactions of interest in the hydrogen-oxygen reaction except the recombination reactions (5-8 to the right) will be accelerated by turbulence.

It would be of fundamental interest to conduct experiments, e.g., in nozzles expanding the products of hydrogen-oxygen combustion with various degrees of turbulence in the stream, to determine the effect of turbulence on reaction rates of practical importance in supersonic combustion.

SECTION IV

EXPERIMENTAL RESULTS OF COMBUSTION

In order to investigate experimentally the process of supersonic combustion controlled by mixing of hydrogen and air, a series of tests is in progress at the Aerodynamics Laboratory of the Polytechnic Institute of Brooklyn. Some of the results of such investigation are presented here.

EXPERIMENTAL APPARATUS

The tests presented here were performed in an axially symmetric jet. The hydrogen was injected axially through subsonic jet at the axis of the air (see Figure IV-1). The air Mach number was chosen equal to 1.54 in order to change sufficiently some of the parameters which are important for chemical reaction and which affect significantly the reaction time. The maximum air stagnation temperature available in the facility was roughly 1660°K; therefore, the maximum static temperature of the air could be changed for M = 1.54 between room temperature and 1110°K. With this Mach number it was possible to change the static pressure in the mixing region from values of the order of 1/20 atm to several atms. However, for safety reasons the maximum

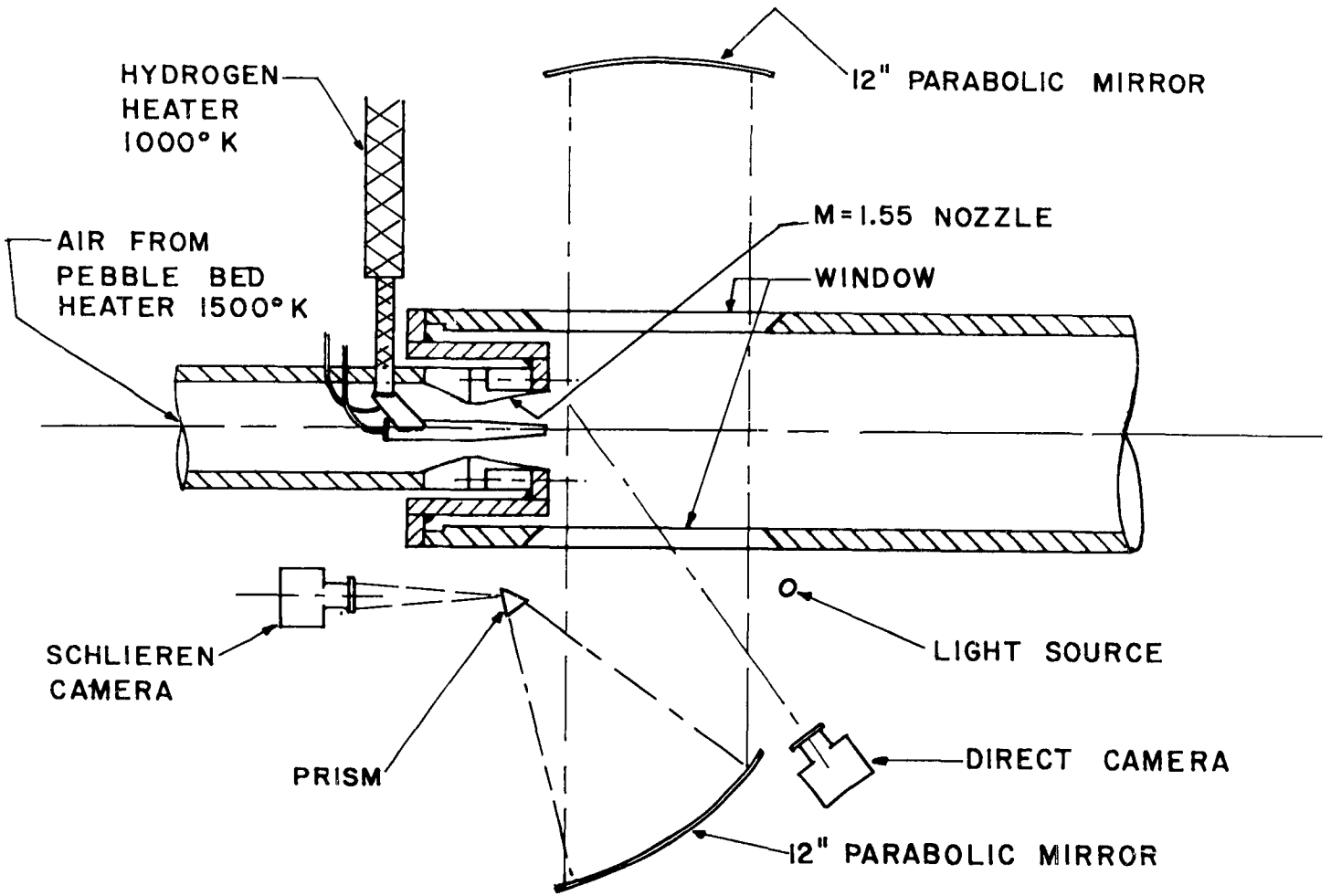

FIG. IV-1. Schematic Representation of Combustion Apparatus; Supersonic-Subsonic Mixing.

pressure, which permits optical observation through the glass windows, was limited to 1.3 atm. The temperature of the hydrogen was also variable between 1110°K and 324°K.

The hydrogen and air jets discharge into a large chamber where the external pressure can be carefully controlled. Therefore, the mixing and combustion process take place in an open jet region, which presents several advantages.

(a) It permits the static pressure along the external part of the jet to be kept constant, independently of the combustion process.

(b) It simplifies the optical observation of the flow.

The measurements made were pressure, velocities and temperature of the two streams. The combustion process was observed by direct photographs and schlieren photographs. Temperature survey was also made. Direct photographs which are important in understanding the processes in the flow were taken by a long time exposure (about 1-7 sec.) of the flame.

The purpose of the tests was to obtain some experimental information on the chemical and mixing process. The mixing process in the tests is complex because of the presence of the boundary layer outside of the hydrogen injector; therefore, initial tests were made in order to determine the effects of the boundary layer on the combustion tests. The presence of the air boundary layer is important for two reasons: (a) it increases the mixing process, and (b) the boundary layer air has regions where the static temperature is higher and the velocity is lower than the static temperature and velocity of the air jet. It must be noted that in all tests the walls of the hydrogen jet are preheated close to the stagnation temperature of the air.

The first part of the test program has been performed at a static pressure of 0.9 atm. For this condition the chemical behavior is described by the data of Figure IV-2, which gives the induction and

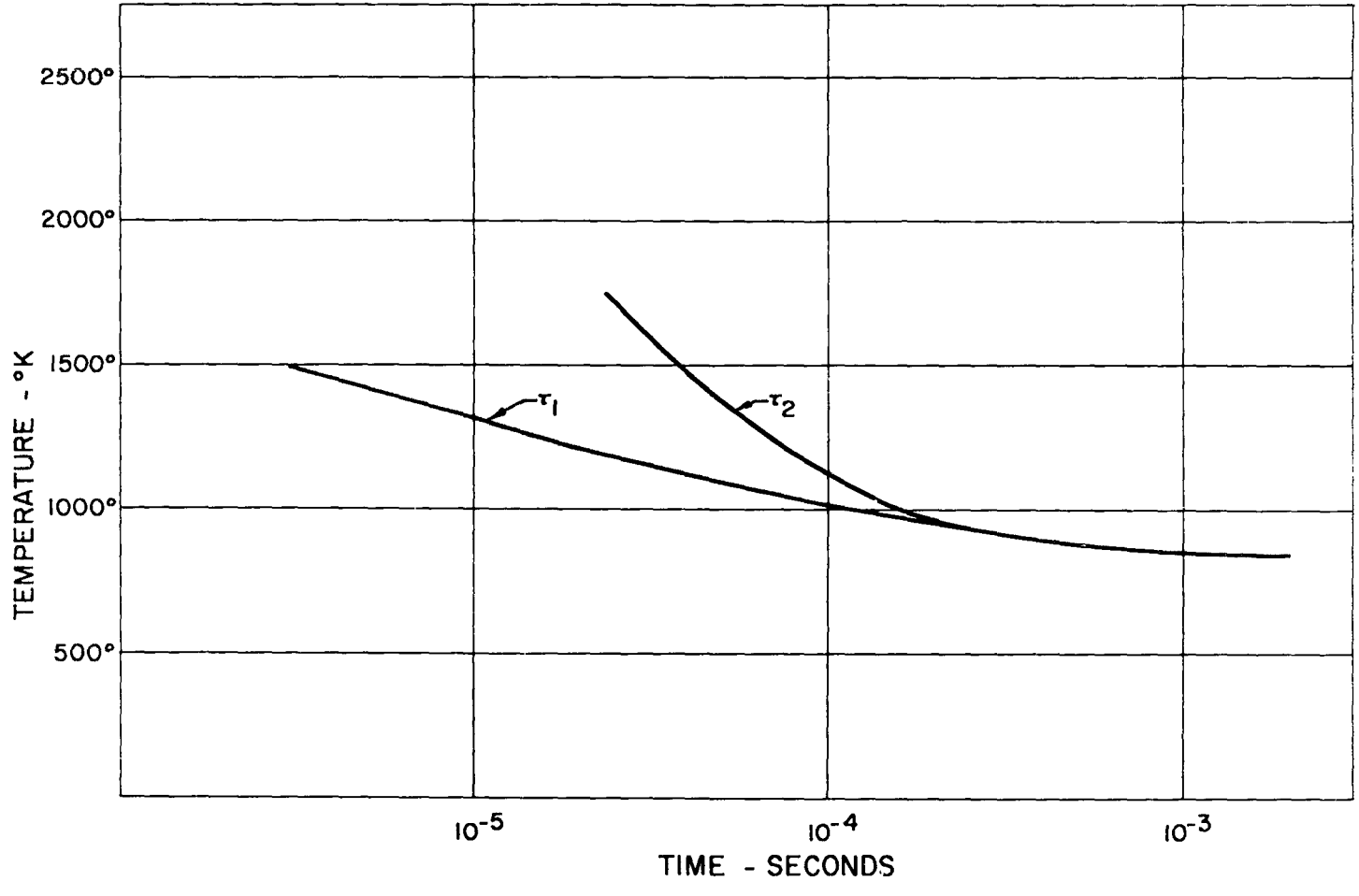

FIG. IV-2. Reaction Times as a Function of Initial Temperature for Stochiometric Mixtures.

energy release times as functions of local temperature. In the range of temperatures, and for the pressure chosen for the tests, these times are practically independent of the chemical composition of the mixture (value of η); therefore, it is possible to obtain indications on the process of mixing and reaction also, if the air and hydrogen concentrations of the mixture are not constant and are not exactly known along any given streamline of the flow. Figure IV-2 also shows that the energy release time is very short, and the induction time represents the larger portion of the total combustion time. Rapid changes of reaction time take place in the range between 800° and 900°K. For example, a variation of temperature between 940°K and 830°K changes the reaction time between 2.0×10^{-4} to 10×10^{-4}, which corresponds to variations of distance in the flow of several inches. This large variation of travel length permits an interpretation of the data obtained from photographic observations.

Several series of tests were performed for the cited air Mach number of 1.54 and for hydrogen Mach number variable but less than one. In each series of tests the stagnation temperature of the air and of the hydrogen were kept constant, and the velocity of the hydrogen u_j was changed.

Several series of tests were performed corresponding to different combinations of stagnation temperature of the air and of the hydrogen.

The mixing analysis does not permit accurate determination of the mixing process; however, it does permit obtaining some relation between velocity stagnation temperature and static temperature as function of concentration. If ρ_e and ρ_j are the partial mass densities of air and hydrogen at a given position where the mass density is ρ, then the average velocity and stagnation temperature can be expressed as

$$\rho u = \rho_e u_e + \rho_j u_j \qquad \text{(IV-1)}$$

where u_e and u_j are the initial velocities of air and hydrogen stream and the effects of viscous losses are neglected. This approximation is

satisfactory in view of the fact that the exchange of momentum between the air and hydrogen stream represents only a small percentage of the momentum of the air stream, and therefore the viscous losses related to this exchange, that depends on the momentum exchanged can be neglected, and

$$H_o = c_p T_o = \rho_e c_{p_e} T_{s_e} + \rho_j c_{p_j} T_{s_j} \qquad \text{(IV-2)}$$

As it has been discussed in Section III, these expressions are consistent with the concept of the mixing length introduced by Prandtl when molecular transport phenomena can be neglected. Therefore, if $K = \frac{\rho_j}{\rho}$,

$$T_o = \frac{H_e + K(H_j - H_e)}{c_{p_e} + (c_{p_j} - c_{p_e})K} \qquad \text{(IV-3)}$$

$$u = u_e + (u_j - u_e)K \qquad \text{(IV-4)}$$

and

$$T = \frac{c_{p_e} T_{s_e} + K(c_{p_j} T_{s_j} - c_{p_e} T_{s_e}) - \frac{1}{2} u^2}{(c_{p_j} - c_{p_e})K + c_{p_e}} \qquad \text{(IV-5)}$$

From these relations and from the relation between reaction time and static temperature T the effect of the variation of H_j and H_e and of the concentration on the flame front can be investigated.

In the first series of tests the stagnation temperature of the air was chosen to be 1170°K corresponding to an air velocity of 2870 ft/sec and to a static temperature of 834°K. The stagnation temperature of the hydrogen was chosen equal to 985°K. The Mach number of the hydrogen stream is low, and the static temperature

changes only slightly when u_j changes, and is close to the stagnation temperature; therefore, in this series of tests the static temperature of the hydrogen is larger than the static temperature of the air. For these conditions the reaction time was expected to be of the order of 10^{-4}. During this time the air in the boundary layer has time to travel several inches and, therefore, because of the small boundary layer thickness, it could be expected that the boundary layer would be mixed with the main flow before combustion starts. Some of the results of such series of tests are presented in the next figures.

Figure IV-3a presents a direct photograph of the process of combustion for low velocity ratio, $\frac{u_j}{u_e} = 0.3$. A drawing of the flame front for the same condition is given in Figure IV-3b. For this condition the velocity of the hydrogen jet is equal to 860 ft/sec. The flame starts at the axis at a distance of 3.5" downstream of the exit of the hydrogen injector; it propagates rapidly across the central region of the mixing zone and then slows down sharply when the flame reaches the outside region of the jet. For a short period the flame width increases very slowly. At a distance of the order of 7" from the exit of the ejector the slope of the flame front changes, and the velocity of propagation in a direction normal to the jet increases again. Downstream of this point the flame width grows approximately at a constant rate, and the flame front is inclined at an angle of approximately 7^{o}-8^{o} with respect to the axis of the jet.

The shape of the flame is consistent with what could be expected from the results of an analysis. In Figure IV-4 the flow travel required for combustion is given as a function of local average concentration for the conditions of this test. This flow travel has been calculated by means of Eqs. (IV-4) and (IV-5) on the basis of the data of Figure IV-2, and does not take into account the effect of the boundary layer.

At the center of the flame the hydrogen concentration is very high; therefore, the static temperature is high and the velocity is low. The flow travel for combustion given by Figure IV-4 here is of the

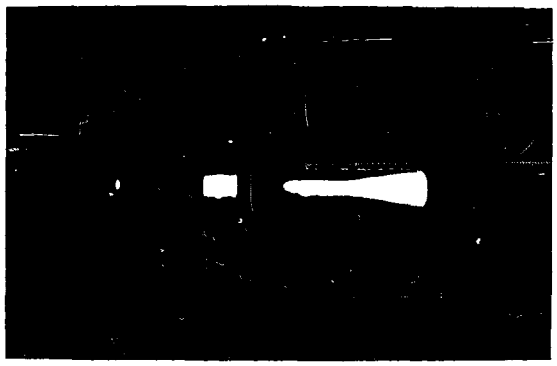

FIG. IV-3a. Direct Photograph of Air Hydrogen Combustion
$T_{s_e} = 1170^{\circ}K$; $T_{s_j} = 985^{\circ}K$; $u_j/u_e = 0.3$

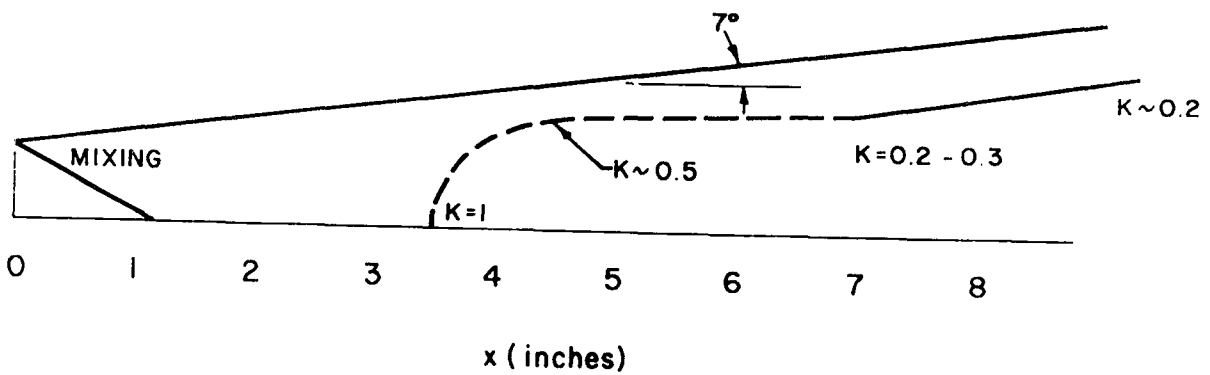

FIG. IV-3b. Schematic Representation of Mixing versus Length.

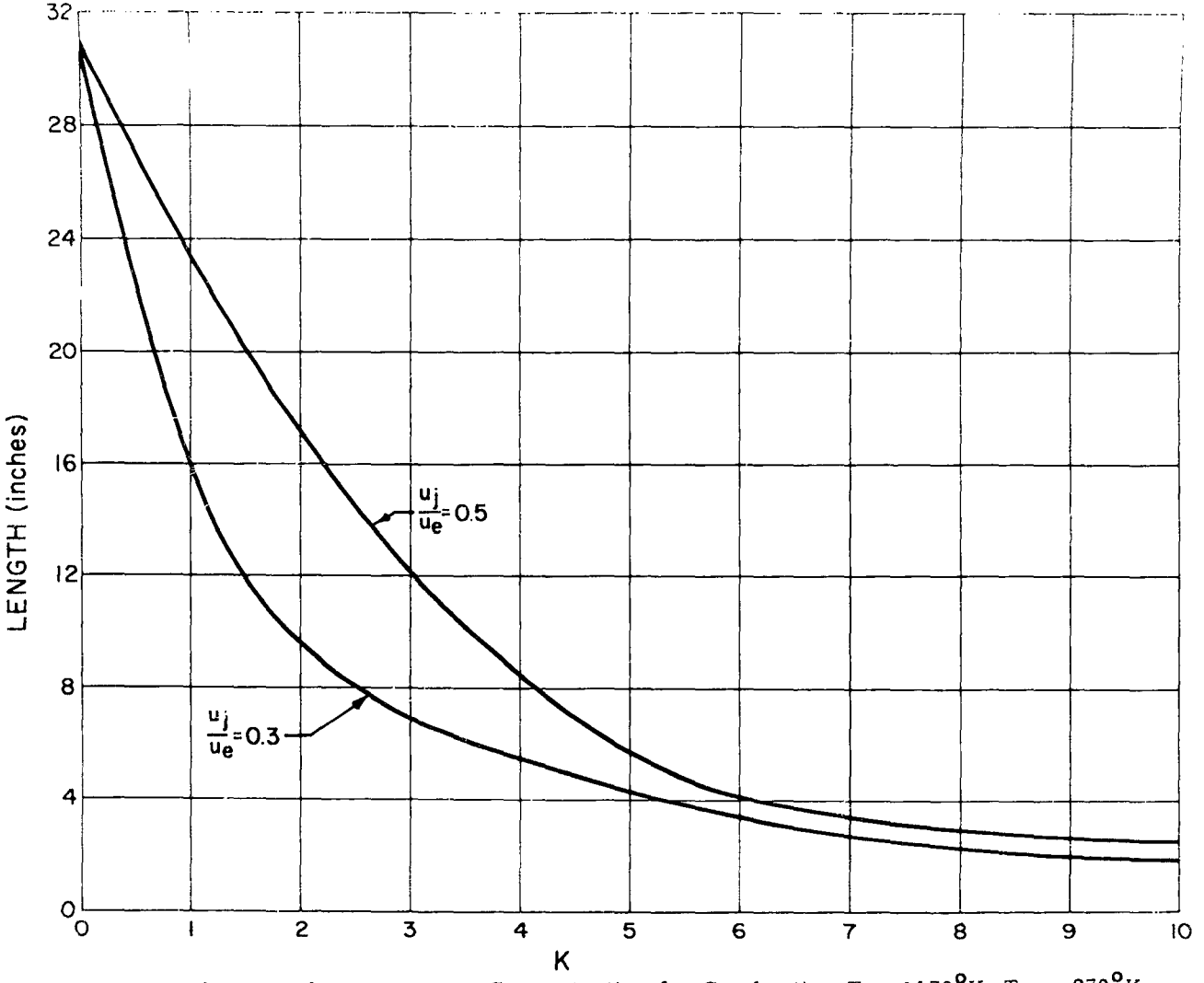

FIG. IV-4. Length versus Mass Concentration for Combustion T_{s_e}=1170°K; T_{s_j} = 970°K

order of 1.9". Therefore, about 1.6" of flow travel are required before some air reaches the center of the jet. When the concentration decreases, the flow travel required for combustion increases; however, the mixing length decreases. Hydrogen concentrations of the order of .50 or lower are reached almost immediately downstream of the injector at the outer edge of the mixing region; therefore, for those conditions the total flow travel between the end of the ejector and the flame front corresponds roughly to the flow travel required for combustion. The flow travel required for combustion for K = 0.50 corresponds to 4.4". This explains the shape of the flame in the central region of the mixing. When the concentration decreases the flow travel for combustion becomes very large; therefore, the velocity of propagation of the flame across the jet decreases very rapidly.

The region of the flame, where the width of the flame remains practically constant, can be attributed to the presence of the boundary layer in the air stream, generated along the external surface of the injector. The air boundary layer near the wall of the injector has larger static temperature and lower velocity than the flow outside of the boundary layer. As a consequence, in the region where the mixture contains boundary layer air, combustion times and flow velocities are smaller; therefore, flow travels for combustion are much smaller. Then the flame front propagates fast into regions of low concentrations. When the air velocity increases and static temperature decreases, the flow travel for combustion for a given value of concentration increases and, therefore, the flame front moves into regions of higher concentrations than for the case of a mixture having boundary layer air. As a consequence, the transversal dimension of the flame increases very slowly because the hydrogen concentration must increase along the flame front. When the flame reaches a region where the air has free stream conditions, the flame front propagates along a line of roughly constant concentration. On this basis the flame front permits information to be obtained on the mixing process. Mixing analysis indicates that the mixing for these conditions propagates at angles of the order of 7^{o}.

When the velocity of the jet increases, then the flame changes shape, as shown in Figure IV-5. The flame moves downstream of the injector and then propagates in similar fashion as before. Again the shape of the flame, the distance from the discharge section of the injector, is consistent with the mixing process and the calculated reaction rates.

In the photograph shown the velocity of the hydrogen u_j is equal to 1430 ft/sec and $\frac{u_j}{u_e} = 0.5$. The stagnation temperature of the air is 1190°K, and of the hydrogen is 970°K. The relation between flow travel for combustion and concentration for these conditions is given also in Figure IV-4. The flame starts at the axis of the mixing zone at a distance of roughly 7.5". There the travel for combustion corresponds approximately to 4.5"; therefore, the mixing travel is equal to 3". If u_j continues to increase, the flame moves gradually downstream of the exit of the injector. For high $\frac{u_j}{u_e}$ the mixing process becomes slower and the combustion starts at the outer edge of the mixing region.

In Figure IV-6 the distance x in inches measured from the discharge section of the injector is plotted as a function of $\frac{u_j}{u_e}$. For the case of $u_j = u_e$ the velocity of the hydrogen is 2820 ft/sec, and the static temperature of the hydrogen is 890°K. For these conditions the temperature of the mixing is also of the order of 872°K, and the combustion will occur after 4.5×10^{-4} sec. Then the distance would be of the order of 13". This value does not agree exactly with the experimental results shown in Figure IV-6 which gives a distance of the order of 10". The difference is due to the presence of the boundary layer that slightly increases locally the static temperature and decreases the velocity of the mixture.

If the velocity u_j increases to a value of $2u_e$, then the static temperature of the hydrogen becomes equal to 834°K and the reaction time becomes of the order of 6.7×10^{-4}; therefore, the length must become of the order of 24". The experimental data agree approximately with the values of the distances given by the analysis.

FIG. IV-5. Direct Photograph of Air Hydrogen Combustion
$T_{s_e} = 1190^{\circ}K$; $T_{s_j} = 970^{\circ}K$; $u_j/u_e = 0.5$

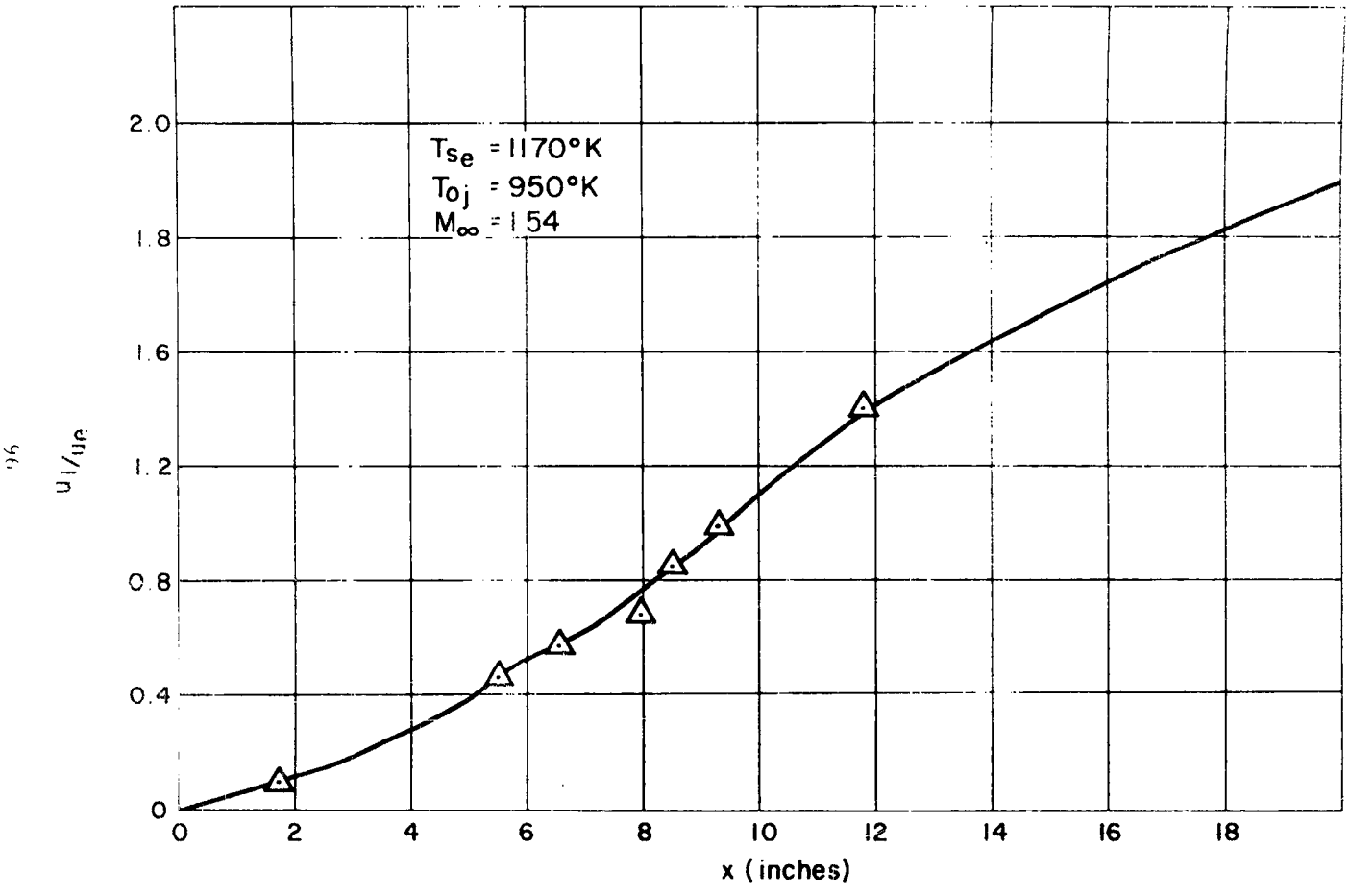

FIG. IV-6. Initiation of Combustion Mixing Region for Various Values of u_j/u_e; T_{s_e} = 1170°K; T_{s_j} = 950°K.

In order to understand the interplay between mixing and combustion phenomena of hydrogen and air, it can be useful to discuss two other series of tests having different stagnation conditions. In the second series the stagnation temperature of the hydrogen is the same as the static temperature of the air, and this temperature is somewhat higher than in the first series; therefore, the reaction rates are faster. In the third series of tests the stagnation temperature of the hydrogen is much lower than the static temperature of the air.

$T_{s_e} = 1320^{\circ}K \quad T_{s_j} = 954^{\circ}K - 1000^{\circ}K$ series 2

$T_{s_e} = 1320^{\circ}K \quad T_{s_j} = 362^{\circ}K$ series 3

For the second series, because the static temperature of the hydrogen and of the air are about the same. The reaction rate is constant and of the order of 1.7×10^{-4} independent of concentration. Photographs for values of $u_j = 0.28$, 0.92, 1.21 u_e are shown in Figures IV-7, -8, and -9, respectively.

For low values of u_j the combustion starts first at the center, Figure IV-7. The distance is roughly 2.6" from the exit of the jet. In this test the hydrogen temperature is equal to 1000°K, and the reaction time at the axis is 1.0×10^{-4}. The velocity is 860 ft/sec; therefore, the reaction length is of the order of 1"; and the mixing length is of the order of 1.6", that is, equal to the value determined in the preceding test for about the same value of u_j/u_e. The flame shape is as shown schematically in Figure IV-10. The flame propagates rapidly across the jet. The flame front depends only from the velocity distribution because the temperature of the mixture is approximately constant everywhere. The velocity outside is 3100 ft/sec, therefore the flame reaches the outside of the mixing at a distance of the order of about 6", which corresponds to a reaction time of 1.7×10^{-4}. This

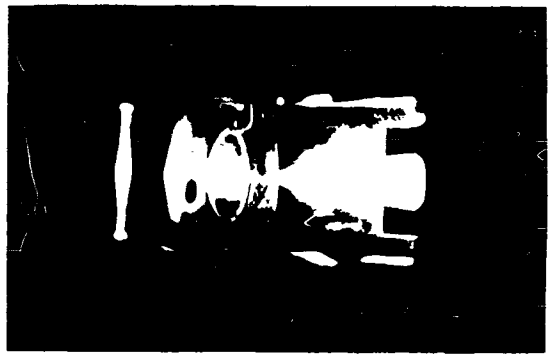

FIG. IV-7. Direct Photograph of Air Hydrogen Combustion
$T_{s_e} = 1300^{\circ}K$; $T_{s_j} = 970^{\circ}K$; $u_j/u_e = 0.28$

FIG. IV-8. Direct Photograph of Air Hydrogen Combustion
$T_{s_e} = 1300^{\circ}K$; $T_{s_j} = 970^{\circ}K$; $u_j/u_e = 0.92$

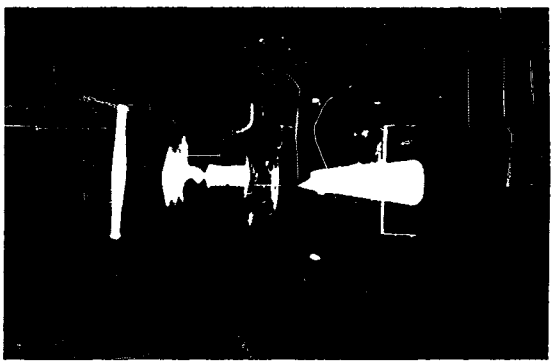

FIG. IV-9. Direct Photograph of Air Hydrogen Combustion
$T_{s_e} = 1300^{\circ}K$; $T_{s_j} = 960^{\circ}K$; $u_j/u_e = 1.21$

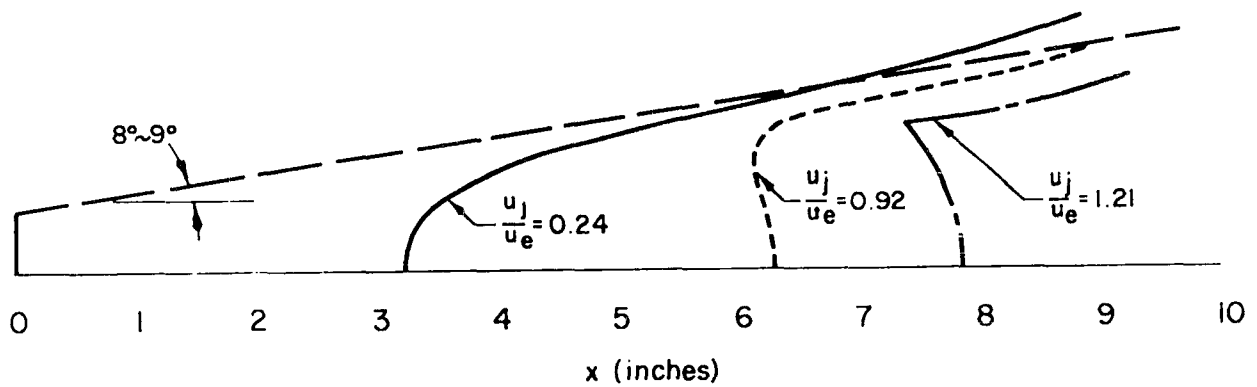

FIG. V-10. Schematic Representation of Combustion for Various Values of u_j/u_e.

agrees with the measured value. The shape of the flame downstream of this point gives the measure of the velocity of turbulent diffusion of the hydrogen normally to the stream.

If the velocity u_j increases, then the time required for initiation of the combustion at the axis increases; however, the outside conditions do not change. This is shown from photographs in Figures IV-8 and -9. If $u_j = 0.92\ u_e$, the static temperature, and therefore, the reaction time are about the same as before; however, the reaction length at the center is larger because of the increase in velocity. The combustion starts at a distance of the order of 6". The flame outside has the same shape as before.

For the condition $u_j = 1.21\ u_e$ the hydrogen temperature is slightly lower. The flame has the same general configuration as for $u_j = 0.92\ u_e$; however, it starts slightly downstream of the preceding case. The difference is of the order of 1". This would indicate a variation or mixing length of the order of 13%; this is in qualitative agreement with the mixing tests. All the photographs indicate that the velocity of propagation of the flame normal to the stream increases moving downstream with the flow. This can be attributed to a gradual axial pressure rise connected with the heat release due to combustion. These tests indicate that the reaction time calculated is in agreement with experiments. It also confirms the results of the mixing experiments which indicate that the mixing is fast when $u_j < u_e$, and decreases only gradually when u_j increases without any significant changes at $u_j = u_e$.

In all the tests presented before the process of heat release is relatively slow, and therefore the local pressure rise due to combustion is small and gradual. The schlieren pictures for such flows indicate that the compression generated by combustion waves does not form an envelope, and shocks are not found in the flow. However, the absence of shock is directly dependent on the mechanism of heat release and on the dimensions and type of boundary of the air jet. Shocks can be produced either by changing the geometry of the air jet or by

accelerating and increasing the mechanism of heat release. Photographs in Figures IV-11 and -12 are proof of such possibilities. Both photographs are a composition obtained by superimposing a schlieren photograph to a flame photograph taken from the same experiment.

The windows for the two photographs are not of the same dimensions and the schlieren axis is perpendicular to the axis of the flow, while the flame photograph is inclined with respect to the axis of the flow as shown in Figure IV-1. Therefore a difference of angle exists for the two data. However the superposition is qualitatively correct and gives a correct impression of the relation between heat release and shock formation.

Two different tests have been performed in order to indicate the effect of the two parameters, mechanism of heat release and boundary conditions.

The photograph of Figure IV-11 corresponds to stagnation conditions $T_{s_e} = 1440^{o}K$, $T_{s_j} = 935^{o}K$, and $u_j = 0.28\ u_e$. For these conditions the reaction rate is about twice as fast as for the case of Figure IV-7 and therefore the heat release is faster. At the same time, the mixing rate increases when combustion takes place because of the pressure rise due to heat release; therefore, as soon as the combustion rate increases the mixing rate also increases, and consequently the heat release becomes much faster. The faster rate of heat release produces stronger pressure rise and, therefore, produces shocks. For the case shown in Figure IV-12 the stagnation temperature of the air is equal to $1170^{o}K$ and the hydrogen temperature to $362^{o}K$, therefore, the combustion rate for a given concentration is lower. However in this test the mixing process has been strongly augmented by creating a positive pressure gradient along the axis of the mixing stream.

The hydrogen jet at the exit of the injector is subsonic, while the air jet is supersonic, therefore, for a short length the central part of the mixing region is subsonic. If a pressure rise is produced in the flow, in some region not too far from the exit of the injector,

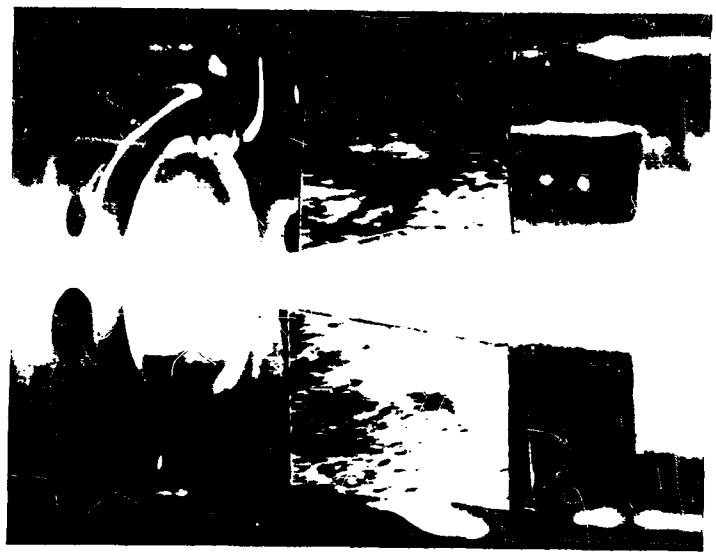

FIG. IV-11. Direct and Schlieren Photographs of Air Hydrogen Combustion
$T_{s_e} = 1440^{\circ}K$; $T_{s_j} = 935^{\circ}K$; $u_j/u_e = 0.28$

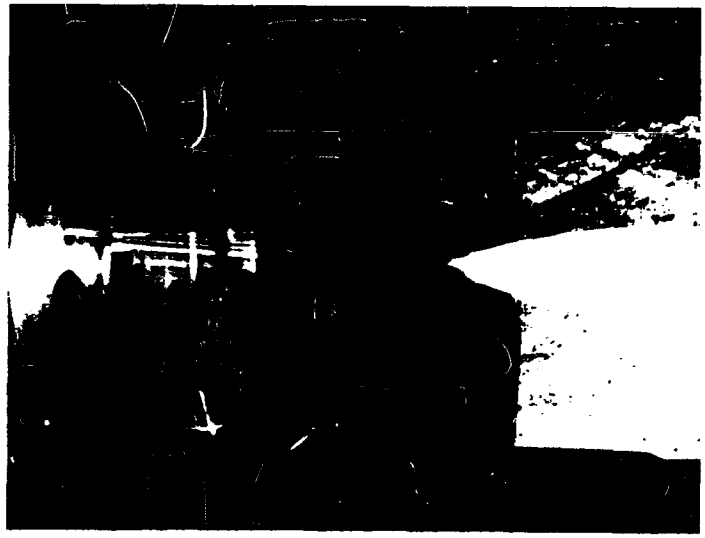

FIG. IV-12. Direct and Schlieren Photographs of Air Hydrogen Combustion
$T_{s_e} = 1280^{\circ}K$; $T_{s_j} = 380^{\circ}K$; $u_j/u_e = 0.27$; $p_a/p_b = 1.4$

this disturbance can travel upstream through the subsonic central part and from the center propagates into the supersonic region. Then the velocity of the central part of the mixing tends to decrease because of the pressure rise, while the mixing tends to produce the opposite effect. As a consequence the mixing is strongly increased, specifically if the velocity at the center is low. In the present test, the static pressure rise has been produced by increasing the static pressure in the discharge chamber to a value of 1.4 the static pressure of the air stream at the exit of the nozzle. Then a shock is produced at the end of the nozzle that travels toward the axis and reaches the axis somewhat downstream of the region where combustion starts. The shock produces a pressure rise in the central part of the mixing where the stream is still subsonic. The pressure rise decreases the velocity and the mixing sharply increases the heat release. While shocks would not be formed in this region in absence of combustion, the rapid combustion process produces sufficient changes in density and pressure to create shocks as shown by the photograph.

Consider now test series 3. For this series the hydrogen is cold, therefore, combustion can occur only when the concentration is low. The flow travel for combustion as function of concentration increases very rapidly for values of concentrations between 0 and 0.1, because this change corresponds to a temperature change between 942°K and 600°K for $u_j = 0.1\ u_e$ and between 942°K and 560°K for $u_j = 0.78\ u_e$. Therefore combustion can take place only in regions where the concentration is somewhat less than 0.10. The velocity of the jet for K = 0.1 changes from 2667 ft/sec to 2983 ft/sec when u_j changes from 0.1 to 0.78 u_a. This change of u is small and therefore it can be assumed that the jet velocity at $K < 0.1$ is about the same independently of the value of u_j. Figures IV-12, -14, and -15 show the flame shape for $\frac{u_j}{u_e} = 0.78,\ 0.525$ and 0.1 respectively. For high velocity of the hydrogen jet ($u_j/u_e = 0.78$ and 0.525) the concentration below 0.1 is reached first in the outside region of the mixing zone, and the flame initiates there. For the temperatures and velocities of the

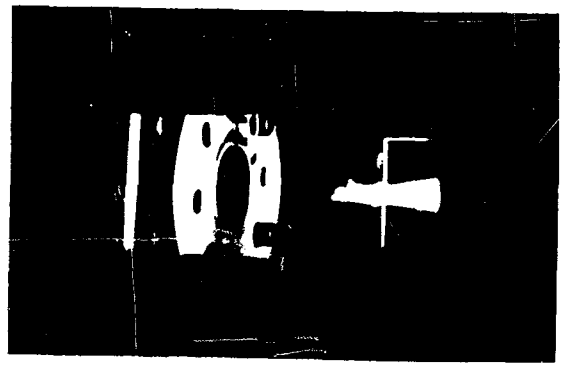

FIG. IV-13. Direct Photograph of Air Hydrogen Combustion
$T_{s_e} = 1320^{o}K$; $T_{s_j} = 330^{o}K$; $u_j/u_e = 0.78$

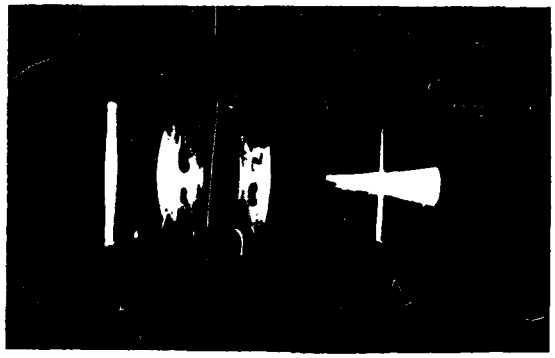

FIG. IV-14. Direct Photograph of Air Hydrogen Combustion
$T_{s_e} = 1320^{\circ}K$; $T_{s_j} = 340^{\circ}K$; $u_j/u_e = 0.525$

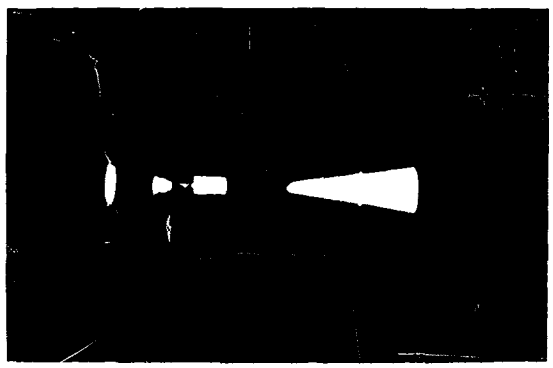

FIG. IV-15. Direct Photograph of Air Hydrogen Combustion
$T_{s_e} = 1320^{\circ}K$; $T_{s_j} = 380^{\circ}K$; $u_j/u_e = 0.1$

experiments the flow travel for combustion for $K < 0.1$, determined on the basis of the calculated reaction rates, is equal to 6.5". The photographs of Figures IV-13 and -14 give for this distance a value of 5.5". The smaller value of flow travel for combustion given by the experiments is justified by the presence of the boundary layer.

For very low values of u_j, $\frac{u_j}{u_e} = 0.1$, the combustion starts at the center. This indicates that a very short flow travel is required to completely mix hydrogen and air when the velocity of the hydrogen is small, so that very low hydrogen concentration is obtained at the axis. Again this rapid mixing can be attributed to the presence of the boundary layer in the air stream. For very low u_j the mass of the hydrogen jet is of the same order of the mass of the air boundary layer, then the mixing is fast and the travel is short, because of the lower velocity of the boundary layer air.

The last experimental investigation on combustion presented here is related to the study of effects of pressure variation on reaction rates. For this series of tests the values of u_j/u_e and the stagnation temperatures of hydrogen and air have been kept constant while the static pressure has been changed. The mixing process is only slightly effected by the pressure changes because the flow is turbulent, therefore, the variation of flame position can be attributed to the effect of the variation of the static pressure on the reaction rate. In Section II an approximate equation has been derived for the ignition delay as function of temperature [Eq. (II-5.1)]. This equation relates the induction time to the values of the static pressure and temperature. The relation is a function of the values of the chemical reaction rates. The experiments permit measuring the distance between the exit of the jet and the initiation of the flame; therefore it permits checking the approximation of such an equation and of the reaction rates used. In order to have an accurate indication of the mixing length, the tests were performed with air at 1440°K and hydrogen cold, 380°K, so that the combustion will start only for very low values of concentration

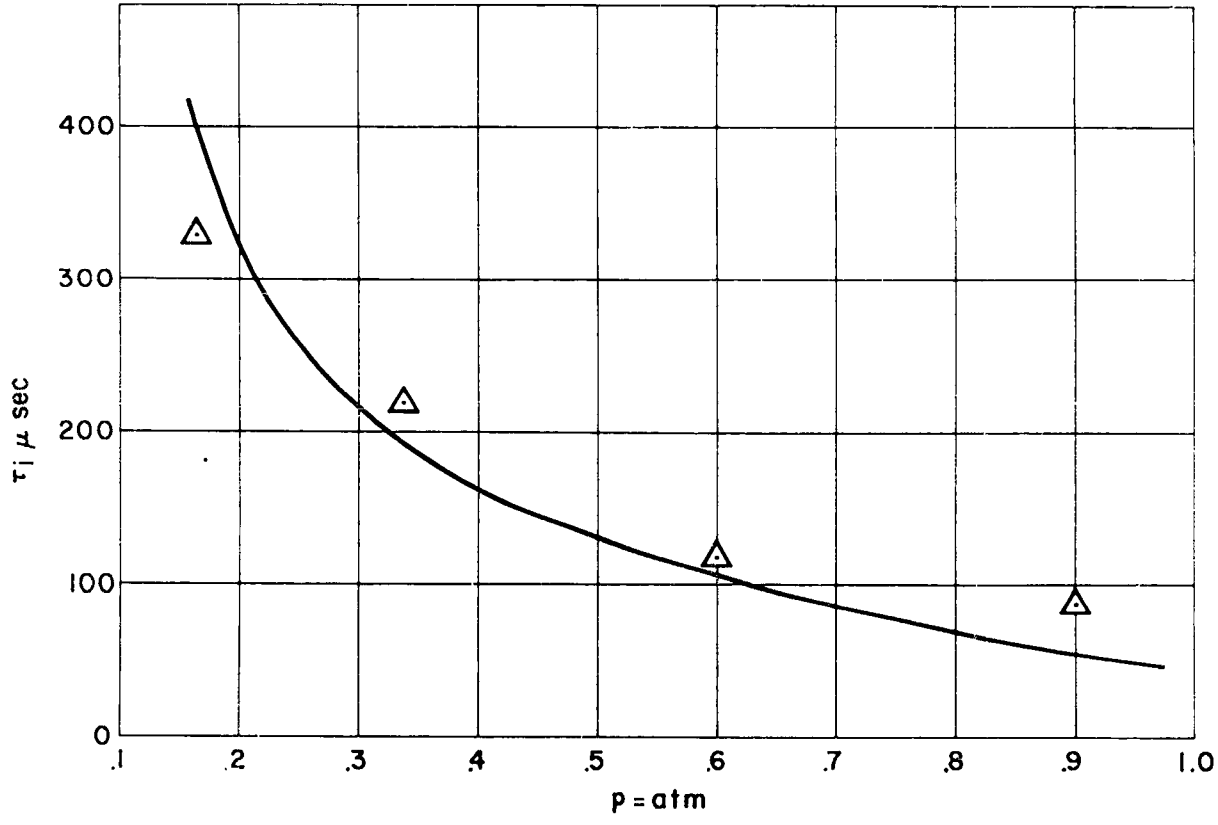

FIG. IV-16. Comparison of Theoretical and Experimental Induction Times.

(below K = 0.05). For such conditions the velocity of the mixture is equal to the velocity of the air, and the travel required for mixing is negligible, because of the rapid mixing process and of the low values of concentration required for combustion.

An analysis of the photographs indicates that the flame front has a discontinuity. This discontinuity is due to the presence of the boundary layer in the air stream. As it has been explained before, the small amount of combustion that occurs before the discontinuity is due to the low velocity part of the boundary layer. The distance used for the determination of the reaction time is the distance between the end section of the hydrogen injector and the discontinuity on the flame front which corresponds to a mixture having a velocity equal to the free stream velocity of the air. Figure IV-16 shows a comparison between the analytical results and the combustion times determined from the distances given by the experiments. The comparison indicates that the analysis is in good agreement with the experimental results.

SECTION V

CONCLUSIONS

The theoretical and experimental investigation reported herein indicates that for the range of conditions investigated the analysis of chemical reactions between hydrogen and air is sufficiently accurate to permit fluid dynamic analysis of the flow field and interpretation of experimental data connected with supersonic diffusion flames. The fluid dynamic problem is complex and requires a better quantitative understanding of mixing problems.

The experimental results indicated that turbulent mixing of hydrogen air stream is fast and at present can be predicted, at least qualitatively, by analyses; however, variations to the incompressible

type of expression of eddy viscosity must be introduced. Such modifications seem called on for physical ground. The presence of air boundary layer strongly affects the mixing and must be taken into account.

On the basis of these results it appears that additional work along the lines indicated in the report is required to improve the analysis of the fluid dynamic aspects of supersonic diffusion flames; the chemical aspects of the problem are well understood for the range of parameters investigated in the experiments reported here and in related work elsewhere. The question of the effect of turbulence on the chemical kinetics is still open.

REFERENCES

SECTION I

I-1. Gross, R. A. and Chinitz, W.: A Study of Supersonic Combustion. J. Aero. Sci., 27, 7, pp. 517-524, July 1960.

I-2. Nicholls, J. A.: Stabilized Gaseous Detonation Waves. ARS J., 29, 8, pp. 607-608, August 1959; also available in modified form as Ph.D. thesis, Univ. of Michigan, 1960, through Univ. Microfilms, Inc., Ann Arbor, Michigan.

I-3. Rhodes, R. D. and Chriss, D. E.: A Preliminary Study of Stationary Shock Induced Combustion with Hydrogen-Air Mixture. AEDC TN 61-36, July 1961.

I-4. Rhodes, R. P., Rubins, P. M., and Chriss, D. E.: The Effect of Heat Release on the Flow Parameters in Shock-Deduced Combustion. AEDC TDR-62-78, May 1962.

I-5. Oppenheim, A. K.: Development and Structure of Plane Detonation Waves. Fourth AGARD Combustion and Propulsion Colloquium, Pergamon Press Ltd., London, England, pp. 186-258, 1960.

I-6. Burke, S. P. and Schumann, T. E. W.: Diffusion Flames. Ind. Eng. Chem., 20, pp. 998-1004, 1928.

I-7. Penner, S. S.: Chemistry Problems in Jet Propulsion, Pergamon Press Ltd., London, England, pp. 267-276, 1957.

I-8. Roy, M.: Propulsion Supersonique par Turboriacetuers et par Statoriacteurs. Advances in Aeronautical Sciences, Pergamon Press Ltd., London, England, 1, pp. 79-112, 1959.

I-9. Ferri, A.: Possible Directions of Future Research in Air-Breathing Engines. AGARD Combustion and Propulsion Colloquium, Pergamon Press Ltd., London, England, pp. 3-15, 1960.

I-10. Nucci, L. M. and Zipkin, M. A.: Composite Air-Breathing Systems. Fourth AGARD Combustion and Propulsion Colloquium, Pergamon Press Ltd., London, England, pp. 16-36, 1961.

I-11. Dugger, G. L.: Comparison of Hypersonic Ramjet Engines with Subsonic and Supersonic Combustion. Fourth AGARD Combustion and Propulsion Colloquium, Pergamon Press Ltd., London, England, pp. 84-119, 1961.

REFERENCES

SECTION II

II-1. Olson, W. T.: Recombination and Condensation Processes in High Area Ratio Nozzles. ARS J., 32, 5, pp. 672-680, May 1962.

II-2. Duff, R. W.: Calculation of Reaction Profiles Behind Steady State Shock Waves. I. Application to Detonation Waves. J. Chem. Phys., 28, 6. pp. 1193-1197, June 1958.

II-3. Schott, G. L.: Kinetic Studies of Hydroxyl Radicals in Shock Waves. III. The OH Concentration Maximum in the Hydrogen-Oxygen Reaction. J. Chem. Phys., 32, 2, pp. 710-716, March 1960.

II-4. Schott, G. L. and Kinsey, J. L.: Kinetic Studies of Hydroxyl Radicals in Shock Waves. II. Induction Times in the Hydrogen-Oxygen Reaction. J. Chem. Phys., 29, 5, pp. 1177-1182, November 1958.

II-5. Libby, P. A., Pergament, H., and Bloom, M. H.: A Theoretical Investigation of Hydrogen-Air Reactions. Part I - Behavior with Elaborate Chemistry. GASL TR 250, AFOSR 1378, August 1962.

II-6. Westenberg, A. A. and Favin, S.: Complex Chemical Kinetics in Supersonic Nozzle Flow. Paper presented at the Ninth International Symposium on Combustion, Cornell Univ., Ithaca, New York, August 1962.

II-7. Momtchiloff, I. N., Taback, E. D., and Buswell, R. F.: An Analytical Method of Computing Reaction Rates for Hydrogen-Air Mixtures. Paper presented at the Ninth International Symposium on Combustion, Cornell Univ., Ithaca, New York, August 1962.

II-8. Bloom, M. H. and Steiger, M. H.: Inviscid Flow with Non-equilibrium Molecular Dissociation for Pressure Distributions Encountered in Hypersonic Flight. J. Aero. Sci., 27, 11, pp. 821-840, November 1960.

II-9. Bloom, M. H. and Ting, L.: On Near-Equilibrium and Near-Frozen Behavior of One-Dimensional Flow. Polytechnic Institute of Brooklyn, PIBAL Report No. 525, AEDC TN 60-156, July 1960.

II-10. Hall, J. G. and Russo, A. L.: Studies of Chemical Nonequilibrium in Hypersonic Nozzle Flows. Cornell Aero. Lab., Report No. AD-1118-A-6, Contr. No. AF 18(603)-141, 1959.

II-11. Vincenti, W. G.: Calculations of the One-Dimensional Non-equilibrium Flow of Air Through a Hypersonic Nozzle - Interim Report. AEDC TN-61-65, Contr. No. AF 40(600)-731, 1961.

II-12. Emanuel, G. and Vincenti, W. G.: Method of Calculation of the One-Dimensional Non- equilibrium Flow of a General Gas-Mixture Through a Hypersonic Nozzle. AEDC-TDR-62-131, June 1962.

II-13. Eschenroeder, A. Q., Boyer, D. W., and Hall, J. G.: Non-equilibrium Expansion of Air with Coupled Chemical Reactions. Phys. Fluids, 5, 5, pp. 615-624, May 1962.

II-14. Nicholls, J. A.: Stabilized Gaseious Detonation Waves. ARS J., 29, 8, pp. 607-608, August 1959; also available in modified form as Ph.D. thesis, Univ. Microfilms, Inc., Ann Arbor, Michigan.

II-15. Fine, B.: Kinetics of Hydrogen Oxidation Downstream of Lean Propane and Hydrogen Flames. J. Phys. Chem., 65, pp. 414-417, March 1961.

II-16. Lezberg, E. A. and Lancashire, R. B.: Recombination of Hydrogen-Air Combustion Products in an Exhaust Nozzle. NASA TN D-1052, August 1961.

II-17. Penner, S. S.: Chemistry Problems in Jet Propulsion. Pergamon Press Ltd., London, England, pp. 267-276, 1957.

II-18. Zinman, W. and Romano, M.: A Simplified Kinetic Model for Multi-component Mixtures. Western State Section of the Combustion Institute, 62-5, 1962.

II-19. Libby, P. A.: Treatment of Partial Equilibrium in Chemical Reacting Flows. ARS J., 32, 7, pp. 1090-1091, July 1962.

II-20. Chu, B. T.: Wave Propagation and the Method of Characteristics in Reacting Gas Mixtures with Application to Hypersonic Flow. WADC TN 57-213, AD 118 350, 1957.

II-21. Wood, W. W. and Parker, F. R.: Structure of a Centered Rarefaction Having a Relaxing Gas. Phys. Fluids, 1, 3, pp. 230-241, May-June 1958

II-22. Sedney, R., South, J. C., and Gerber, N. C.: Characteristic Calculation of Non-equilibrium Flows. Paper presented at AGARD Meeting on "High Temperature Aspects of Hypersonic Flow," Brussels, Belgium, April 3-6, 1962; to be published by Pergamon Press Ltd., London, England.

II-23. Li, T. Y.: Recent Advances in Non-equilibrium Dissociating Gas Dynamics. ARS J., 31, 2, pp. 170-178, February 1961.

II-24. Ferri, A.: The Method of Characteristics. Princeton Series, VI, Section G, "High Speed Aerodynamics and Jet Propulsion," Princeton Univ. Press, Princeton, New Jersey, pp. 583-669, 1954.

II-25. Hayes, W. D. and Probstein, R. F.: Hypersonic Flow Theory. Academic Press, New York, pp. 253-264, 1959

REFERENCES

SECTION III

III-1. Libby, P. A.: Theoretical Analysis of Turbulent Mixing of Reactive Gases with Application to Supersonic Combustion of Hydrogen. ARS J., 32, 3, pp. 388-396, March 1962.

III-2. Vaglio-Laurin, R. and Bloom, M. H.: Chemical Effects in Hypersonic Flows. Polytechnic Institute of Brooklyn, PIBAL Report No. 640, AFOSR 12373, August 1961; also paper presented at the ARS International Hypersonics Conference, Massachusetts Institute of Technology, Cambridge, Massachusetts, August 16-18, 1961.

III-3. Crane, L. J. and Pack, D. C.: The Laminar and Turbulent Mixing of Jets of Compressible Fluid. I. Flow Far from the Orifice. J. Fluid Mech., 2, 5, pp. 449-455, July 1957.

III-4. Napolitano, L. G., Libby, P. A., and Ferri, A.: Recent Work on Mixing at the Polytechnic Institute of Brooklyn. Combustion and Propulsion Third AGARD Colloquium, Pergamon Press, Inc., New York, pp. 118-152, 1958.

III-5. Kleinstein, G.: An Approximate Solution for the Axisymmetric Jet of a Laminar Compressible Fluid. Polytechnic Institute of Brooklyn, PIBAL Report No. 648, ARL 51, AD 257 808, April 1961; also Quart. App. Math., 20, 1, pp. 49-54, April 1962.

III-6. Ting, L. and Libby, P. A.: Remarks on the Eddy Viscosity in Compressible Mixing Flows. J. Aero. Sci., 27, 10, p. 797, October 1960.

III-7. Masters, J. I.: Some Applications in Physics of the P Function. J. Chem. Phys., 23, 10, pp. 1965-1974, October 1955.

III-8. Carslaw, H. S. and Jaeger, J. C.: Conduction of Heat in Solids. Oxford University Press, New York, 2nd ed., pp. 53-56, 260, 1959.

III-9. Thring, M. W. and Newby, M. P.: Combustion Length of Enclosed Turbulent Jet Flames. Fourth Symposium on Combustion, Combustion and Detonation Waves, Williams and Wilkins Co., Baltimore, Maryland, pp. 789-796, 1953.

III-10. Warren, W. R.: An Analytical and Experimental Study of Compressible Free Jets. Princeton Univ. Aeronaut. Eng. Lab. Report No. 381, 1957.

III-11. Corrsin, S. and Uberoi, M. S.: Further Experiments on the Flow and Heat Transfer in a Heated Turbulent Air Jet. NACA TR 998, 1950.

III-12. Schubauer, G. B. and Tchen, C. M.: Turbulent Flow. Princeton Series, V. Section B, "Turbulent Flows and Heat Transfer," Princeton Univ. Press, Princeton, New Jersey, pp. 75-195, 1959.

III-13. Keagy, W. R. and Weller, A. E.: A Study of Freely Expanding Inhomogeneous Jets. Proc. Heat Transfer and Fluid Mechanics Institute, Amer. Soc. Mech. Engrs., New York, pp. 89-98, 1949.

III-14. Schlichting, H.: Boundary Layer Theory. McGraw-Hill Book Co., Inc., New York, pp. 483-506, 1955.

III-15. Hawthorne, W. R., Weddell, D. S., and Hottel, H. C. Mixing and Combustion in Turbulent Gas Jets. Third Symposium on Combustion, Flame and Explosion Phenomena, Williams and Wilkins Co., Baltimore, Maryland, pp. 267-300, 1949.

III-16. Corrsin, S.: Statistical Behavior of a Reacting Mixture in Isotropic Turbulence. Phys. Fluids, 1, 1, pp. 42-47, January-February, 1958.

III-17. Corrsin, S.: The Reactant Concentration Spectrum in Turbulent Mixing with a First-Order Reaction. J. Fluid Mech., 11, 3, pp. 407-416, November 1961.

UNCLASSIFIED